Signalling of Cyclin O complexes through eIF2alpha phosphorylation

Laura Ortet Cortada

TESI DOCTORAL UPF / 2010

DIRECTOR DE LA TESI

Dr. Gabriel Gil Gómez

Programa de Recerca en Càncer IMIM-Hospital del Mar

Als meus pares

ACKNOLEGMENTS/ AGRAÏMENTS

Després del transcurs d'aquests quatre anys, acompanyats de bons i no tant bons moments, per fi ha arribat el final. El final d'una etapa on moltes persones s'han creuat pel meu camí, unes simplement donant-me un somriure al passar per davant d'elles i altres animant-me i aconsellant-me en els moments més difícils. M'agradaria agrair a totes les persones que d'alguna o altra manera han contribuït a que finalment l'escriptura d'aquesta tesis fos possible.

En primer lloc, vull donar les gràcies al Dr. Gabriel Gil Gómez per haver-me acollit al seu grup i per haver confiat en mi, per haver-me deixat fer experiments amb els seus diners, per haver-me ensenyat, aconsellat i rectificat durant aquests quatre anys. Vull agrair a la Pura Muñoz tot el seu suport. També agrair a les persones que han format part del comitè de tesis i que molt amablement una vegada a l'any han intentat aconsellar-me en el meu projecte. I finalment, agrair a tots els membres del tribunal per haver acceptat la invitació de llegir i jutjar aquesta tesis amb tot l'esforç que això comporta.

Aquesta tesis ha rebut el suport econòmic del Fons Social Europeu i del Departament d'Universitats, Recerca i Societat de la Informació de la Generalitat de Catalunya. Agraeixo doncs a la Generalitat de Catalunya la financiació que m'ha donat amb la beca predoctoral FI durant aquests quatre anys. Agraeixo també a la Universitat Pompeu Fabra pel contracte laboral d'aquests últims mesos. Així mateix els agraeixo per avançat l'ajuda que proporciona la Universitat Pompeu Fabra, la Fundació IMIM i la Generalitat de Catalunya per a la publicació de tesis doctorals.

Vull agrair molt especialment a tota la meva família per haver estat sempre al meu costat, especialment als meus pares. Sense ells no hauria arribat mai aquí. Gràcies per haver-me donat una carrera, per haver-me pagat els primers anys de pis i per donar-me sempre el que he necessitat, per sempre animar-me i intentar entendre el que feia i per fer que mai tires la tovallola.

Agraeixo també a tots els membres del meu grup que han contribuït a que poc a poc sapiguem més coses de la nostra Ciclina O. Al Maurici, per ser ell qui va clonar la Ciclina, per haver treballat tant amb ella i per haver tingut l'oportunitat de conèixer-lo com a persona. A la Laia, per tota l'ajuda i companyerisme que em va donar durant el temps que va estar amb nosaltres. A l'Andrea, pels seus clons, gràcies a ells hem descobert moltes coses. Al Ramon, per haver estat la persona que durant els primers anys de la tesis ha estat al meu costat, per sempre haver estat disponible per ajudar-me i per transmetre'm sempre el seu optimisme, tant necessari en molts moments. A la Marta G, per haver estat i estar sempre allí, per totes les immunos fetes per

ella i per l'ajuda i suport que sempre m'ha donat. A la Marta M, per haver estat al costat de la meva "poiata" durant sis mesos i per poder encara ara comptar amb ella. A l'Àlex, per continuar la feina deixada per tots nosaltres i per ajudar-me en els últims moments d'aquesta tesis.

Agraeixo a tots els membres de la ex-UBCM per haver format part d'aquest gran grup. Vull agrair especialment a totes aquelles persones que van formar part de la UBCM durant els meus primers anys de tesis i que ara ja han marxat, gràcies pels bons records i bons moments que m'heu deixat. Gràcies per totes les birres, festes, sopars, viatges i escapades d'aquests anys. Agraeixo a tota la gent dels laboratoris 1, 2, 3 i 4 per formar part de la quotidianitat d'aquests anys. Gràcies al laboratori 1. A l'Elena, per ser una de les primeres persones que vaig conèixer quan vaig arribar a l'IMIM i per estar encara ara sempre disponible pel que faci falta. Gràcies al David, la Neus, el Carles i l'Almu, per totes les bones estones passades. Gràcies a tots els membres de Snail per les seves converses a la sala de cultius, per les anècdotes explicades, pels consells i per deixar-me aquell enzim o anticòs que se m'havia acabat. Gràcies al nou grup vingut a l'IMIM, per ser els meus nous veïns de laboratori i per transmetre'm sempre el bon ambient de treball. Quan formes part d'un grup petit la gent del teu voltant és molt important. Per això finalment agraeixo a tota aquella gent que ha estat o està al laboratori 4, per la seva companyia i consells diaris, pels seus dinars i per les seves quedades fora de la feina. Gràcies Raquel, Marta, Lara i Mercè. També vull agrair a totes aquelles persones situades a l'altra banda de passadís, per haver-se creuat a la meva vida i formar part també d'aquesta tesis.

També vull agrair a totes aquelles persones que m'han ajudat amb els aspectes tècnics dels meus experiments. A l'Òscar Fornàs per tota la seva ajuda en els experiments de citometria, al Xavier SanJuan del servei de Microscòpia Confocal de la UPF i a la Raquel García i a l'Arrate Mallabiabarrera de l'Unitat de Microscòpia Òptica Avançada del CRG per tota la seva ajuda en l'adquisició d'imatges a través del microscopi confocal.

Gràcies a tots els meus amics biòlegs, per haver tingut l'oportunitat de conèixer-vos durant la carrera i després de gairebé 10 anys considerar-vos bons amics. Gràcies als que s'han quedat pel PRBB, per sempre tenir un moment per fer un cafè enmig d'un experiment, per donar-te una altra visió de les coses i per animar-te en aquells moments més desesperants. Gràcies Ana, Jaume,Vero i Neus. Gràcies a l'Esther i a la Ingrid, per intentar sempre trobar un forat per poder quedar i ajudar-me en tot moment.

Gràcies a les meves vallenques, per haver compartit durant tants anys la meva vida barcelonina al pis de Provença, pels milers de bons moments passats, per les confidències, pels sopars i per fer-te sentir sempre com a casa. Gràcies Mireia, Cris, Andrea i Núria.

Gràcies també a tots els miralcampins, per conèixer-vos des de que érem ben petits i perquè, tot i no poder-vos veure tant i com voldria, sempre estar disponibles quan vinc a Miralcamp. Gràcies pels cafès del dissabte a la tarda, pels sopars a cala Alícia, per totes les festes i per tots els bons moments que hem passat. Gràcies Maite, Pau, Alícia ,Òscar, Mònica i Albert.

I finalment només em queda donar-te les gràcies a tu, gràcies Dani per compartir la meva vida diària, per compartir les meves alegries i per curar-me les meves tristeses. Per tot el que ens queda per viure.

Moltes gràcies a tots!!

ASTRACT

We have identified a novel Cyclin, called Cyclin O, which is able to bind and activate Cdk2 in response to intrinsic apoptotic stimuli. We have focused on the study of Cyclin Oα and Cyclin Oβ, alternatively spliced products of the gene. Upon treatment with different stress stimuli, transfected Cyclin Oα accumulates in dense aggregations in the cytoplasm compatible with being Stress Granules (SGs). Furthermore, we have seen that Cyclin Oβ and a point mutant of the N-terminal part of the protein constitutively localize to the SGs. Although both alpha and beta isoforms are proapoptotic, only Cyclin Oα can bind and activate Cdk2. On the other hand, we have demonstrated that Cyclin O is upregulated by Endoplasmic Reticulum (ER) stress and is necessary for ER stress-induced apoptosis. Cyclin O activates specifically the PERK pathway and interacts with the PERK inhibitor protein $p58^{IPK}$. Moreover, Cyclin O participates in the activation of other eIF2α kinases. We have also observed that a pool of Cyclin O is located in active mitochondria, suggesting a function of the protein linked to oxidative metabolism.

RESUMEN

Hemos identificado una nueva Ciclina, llamada Ciclina O, que es capaz de unirse y activar Cdk2 en respuesta a estímulos apoptóticos intrínsecos. Nos hemos centrado en el estudio de la Ciclina Oα y la Ciclina Oβ, productos de splicing alternativo del gen. En respuesta a diferentes tipos de estrés, la Ciclina Oα se acumula en agregaciones citoplásmicas densas que podrían corresponder a Gránulos de Estrés (SGs). Además, hemos visto que la Ciclina Oβ y un mutante puntual de la parte N-terminal de la proteína se localizan constitutivamente en los SGs. Aunque las dos isoformas alfa y beta son proapoptóticas, solo la Ciclina Oα es capaz de unirse y activar Cdk2. Por otro lado, hemos demostrado que los niveles de Ciclina O se incrementan en respuesta al estrés de Retículo Endoplásmico (RE) y que esta proteína es necesaria para la inducción de apoptosis dependiente de estrés de RE. La Ciclina O activa específicamente la vía de PERK e interacciona con la proteína inhibidora de PERK $p58^{IPK}$. Además, la Ciclina O participa en la activación de otras quinasas de eIF2α. La Ciclina O se localiza en mitocondrias activas, lo que sugiere una función de la proteína ligada al metabolismo oxidativo.

ABBREVIATIONS

Apaf-1: Apoptosis Protease-Activating Factor-1
ATF4: Activating Transcription Factor 4
Bak: Bcl-2 homologous antagonist killer
Bax: Bcl-2 associated X
Bcl-2: B-cell lymphoma-2
Bim: BCL2-interacting mediator of cell death
BiP/GRP78: Binding immunoglobulin Protein/ Glucose-Regulated Protein
BSA: Bovine Serum Albumin
β-Trcp: Beta-Transducin repeats-containing protein
CA6: Carbonic Anhydrase 6
CAK: Cdk-Activating Kinase
Cdk: Cyclin-dependent kinases
CHOP: CAAT/enhancer-binding-protein-Homologous Protein
CRG: Centre for Genomic Regulation
Cy2: Cyanine 2
Cy3: Cyanine 3
DAPI: 4',6-diamino-2-phenylindole dihydrochloride
DED: Death Effector Domain
DISC: Death-Inducing Signalling Complex
DMEM: Dulbecco's Modified Eagle's Medium
DR5: Death Receptor 5
dsRNA: double-stranded RNA
DTT: Ditriothreitol
ECL: Enhanced Chemiluminescence
EDTA: Ethylenediaminetetraacetic Acid
EGFP: Enhanced Green Fluorescent Protein
eIF: eukaryotic Initiation Factor
ELISA: Enzyme-Linked ImmunoSorbent Assay
ER: Endoplasmic Reticulum
ERAD: ER Associated Degradation
ERSE: ER-Stress Response Element
FACS: Fluorescent Activated Cell Sorting
FADD: Fas Associated Death Domain
FCCP: Carbonyl cyanide-p-trifluoromethoxyphenylhydrazone
FITC: Fluorescein Isothiocyanate
FLIP: FLICE-like Inhibitory Protein
GADD134: Growth Arrest and DNA-damage-inducible protein-34
GCN2: General Control Non-derepressible-2
GFP: Green Fluorescent Protein
GSK3β: Glycogen Synthase Kinase-3
GST: Glutathione-S-Transferase
HA: Hemagglutinin
hCyclin O: human Cyclin O
HEK: Human Embryonic Kidney
HEPES: 4-(2-hydroxyethyl)-1-piperazineethanesulfonic acid

HPRT: Hypoxanthine Guanine Phosphoribosyl Transferase
HRI: Heme-Regulated Inhibitor
HRP: Horse Radish Peroxidase
IF: Immunofluorescence
IHC: Immunohistochemistry
IPTG: Isopropyl-beta-D-thiogalactopyranoside
IRE1: Inositol-Requiring transmembrane kinase/Endonuclease 1
IRES: Internal Ribosomal Entry Site
JNK: Jun N-terminal Kinase
MEFs: Mouse Embryonic Fibroblasts
mCyclin O: mouse Cyclin O
MOI: Multiplicity Of Infection
MOMP: Mitochondrial Outer Membrane Permeabilization
MRFP: Monomeric Red Fluorescent Protein
MW: Molecular Weight
NA: Numerical Aperture
NES: Nuclear Export Signal
NLS: Nuclear Localization Signal
NO: Nitric Oxide
NOS: Nitric Oxide Synthase
ORF: Open Reading Frame
PBs: Processing Bodies
PBS: Phosphate Buffered Saline
PCR: Polymerase Chain Reaction
PDI: Protein Disulfide Isomerase
PEI: Polyethylimine
PERK: PKR-like Endoplasmic Reticulum Kinase
PEI: Polyethylenimine
PKR: Protein Kinase RNA
qRT-PCR: quantitative Reverse Transcriptase-Polymerase Chain Reaction
RFP: Red Fluorescent Protein
RIPA: Radio-Immunoprecipitation Assay
ROS: Reactive Oxigen Species
RT: Room Temperature
RT-PCR: Reverse Transcriptase-Polymerase Chain Reaction
SDS: Sodium Dodecyl Sulfate
SDS-PAGE: Sodium Dodecyl Sulfate Polyacrilamide Gel Electrophoresis
SEM: Standard Error of the Mean
shRNA: short hairpin RNA
SGs: Stress Granules
TBS: Tris Buffered Saline
TBS-T: Tris Buffered Saline Tween-20
TIA-1: T-cell Internal Antigen-1
TRADD: TNF Receptor Associated Death Domain
TRB3: Tribbles Related Protein 3

Tris: Tris-hydroxymethyl-aminomethane
TTP: Tristetraprolin
UPF: Universitat Pompeu Fabra
UPR: Unfolded Protein Response
UV: Ultraviolet
WB: Western Blot
XBP1: X-box Binding Protein 1

INTRODUCTION

1. Cell death

Cell death can be classified according to four distinct criteria: according to its morphological appearance, which may be apoptotic, necrotic or autophagic; according to its zymological criteria, with or without the involvement of nucleases or of distinct classes of proteases, such as Caspases, Calpains, Cathepsins and Transglutaminases; according to its functional aspects, which can be programmed or accidental, physiological or pathological; and finally, according to its immunological characteristics, which can be immunogenic or non-immunogenic[1]. The Nomenclature Committee on Cell Death (NCDD) reported updated guidelines to unify the criteria for the definition of cell death.

Three distinct types of cell death can be defined according to morphological criteria: apoptosis, autophagy and necrosis. The expression 'apoptosis' is the original term introduced by Kerr *et al.*[2] to define a type of cell death with specific morphological features. Apoptosis is characterised by rounding-up of the cell, retraction of pseudopodes, reduction of cellular volume (pyknosis), chromatin condensation, nuclear fragmentation (karyorrhexis), classically little or no ultrastructural modifications of cytoplasmic organelles, plasma membrane blebbing (but maintenance of its integrity until the final stages of the process) and engulfment by resident phagocytes *in vivo*. It is not correct to assume that programmed cell death and apoptosis are synonyms because cell death, as it occurs during physiological development, can manifest non-apoptotic features[3]. In addition to this, the presence of proteolytically active Caspases or of cleavage products of their substrates is not sufficient to define apoptosis. So apoptosis is not a synonym of programmed cell death or Caspase activation. However, it may be acceptable, if the irreversibility of these phenomena is demonstrated, to

measure Caspase activation and/or DNA fragmentation to identify apoptotic cell death *in vivo*[4].

The process of autophagy is morphologically defined as a type of cell death that occurs in the absence of chromatic condensation but accompanied by massive autophagic vacuolization of the cytoplasm. In contrast to apoptotic cells, cells have little or no association with phagocytes[5].

The process of necrosis is morphologically characterised by a gain in cell volume (oncosis), swelling of organelles, plasma membrane rupture and subsequent loss of intracellular contents. In the absence of a common biochemical denominator, necrosis is identified in a negative fashion as a cell death lacking the features of apoptosis or autophagy[6]. The necrotic cell death is regulated by a set of signal transduction pathways and catabolic mechanisms, such as death domain receptors and Toll-like receptors[7].

It is argued that it can not be classified the different cell death modalities based only on morphological criteria. One solution is replacing morphological aspects with biochemical/functional criteria. But unfortunately, there is not a clear equivalence between morphological and biochemical criteria, suggesting that the ancient morphological terms are destined to disappear and to be replaced by biochemical definitions[4].

1.1. Apoptosis

Apoptosis is a ubiquitous physiological process used to eliminate damaged or unwanted cells in multicellular organisms. It is a genetically conserved pathway in all metazoans essential for the generation of multicellular tissues during embryonic development as well as the maintenance of cellular homeostasis[8].

Deregulation of apoptosis is now widely believed to be involved in the pathogenesis of many human diseases. Suppression of the apoptotic machinery causes autoimmune diseases and is a hallmark of cancer[9,10]. For example, the BH3-only protein Bim (BCL2-interacting mediator of cell death) deficiency causes a systemic lupus erythematosus (SLE)-like autoimmune disease[11] and may predispose to lymphomagenesis. In contrast, the apoptosis-inhibiting protein Bcl-2 is overexpressed in several cancers[12]. On the other hand, abnormal upregulation of apoptosis is associated with neurodegenerative disorders[13] and AIDS[14].

Intensive effort has been made to explore the molecular mechanisms of the apoptotic signalling pathways including the initiation, mediation, execution, and regulation of apoptosis. The molecular understanding of cell death started with genetic studies in the nematode *Caenorhabditis elegans*. This nematode has an invariant pattern of cell death during development: every nematode eliminates the same 131 cells out of 1090 that form the immature organism. H. R. Horvitz had the insight to mutagenize *C.elegans*, in order to identify genes regulating all 131 cell deaths[15]. These genes are named and listed *ced* from -1 to -10. Ced-3, -4 and -9 regulate the executing phase of apoptosis and the rest are involved in the process of elimination by apoptotic cell phagocytosis. The cloning of *ced-3*, *ced-4* and *ced-9* genes revealed a high degree of conservation during evolution and the mammalian homologs were identified (*caspase-1*, *apaf-1* and *bcl-2*, respectively). In higher organisms, activation and regulation of apoptosis is much more complex. In mammals, a wide array of external signals may trigger two major apoptotic signalling pathways, namely the extrinsic pathway (death receptor pathway) or the intrinsic (the mitochondrial) pathway within a cell (Figure 3). The extrinsic pathway is activated by apoptotic stimuli such as binding of death inducing ligands to cell surface receptors. On the other hand, the intrinsic pathway is initiated by signals including DNA damage caused by irradiation or

genotoxic chemicals, growth factor deprivation, Endoplasmic Reticulum (ER) stress, loss of adhesion, etc. Each pathway diverges from the other in the initial steps, being the executioner phase common in the activation of effector Caspases[8].

1.1.1. Caspases

Caspases are cysteinyl aspartate proteinases (cysteine-aspartic proteases), which contain a cysteine residue in the catalytic site which cleave their substrates after an aspartate residue. The first known member of the Caspase family was Caspase-1, initially known as Interleukin-1β-Converting Enzyme (ICE), an enzyme required for the maturation of IL1β[16]. In 1993, Horvitz and Yuan found that the protein encoded by the *C. elegans* gene *ced-3* had similar properties to the ICE[17], lately known as Caspase-1. Up to now, about 14 mammalian Caspases have been identified, which are involved either in inflammation or in apoptosis. Although the first mammalian Caspase cloned, Caspase-1, was identified to be an important regulator of inflammatory response, at least 8 of the 14 Caspases play important roles during apoptosis[18]. Caspases are synthesised as inactive zymogens containing a prodomain followed by a p20 (large) and p10 (small) subunits. These zymogens can be cleaved to form active enzymes following the induction of apoptosis.

Based on their function, the Caspases can be classified into three groups: inflammatory Caspases, Apoptotic initiator Caspases and Apoptotic effector Caspases (Figure 1). Inflammatory Caspases are encoded by three main genes in humans: *caspase-1*, *caspase-4* and *caspase-5*, three main genes in mouse: *caspase-1*, *caspase-11* and *caspase-12* and one gene in cow *caspase-13*. Although human and mouse Caspase-1 are likely orthologues, sequence analysis suggests that human Caspase-4 and Caspase-5 have originated from a duplication of Caspase-11[19]. Caspase-1 is involved in cytokine maturation,

and it has been shown to activate interleukin-18 and interleukin-33[20]. Caspase-12 activates inflammatory cytokines such as interleukin-1 and interleukin-18[21] and is also involved in mediating apoptosis following ER stress (see section 6.1). The function of Caspase-4 is not fully understood, but it is believed to be an inflammatory Caspase, along with Caspase-1, Caspase-5 and the murine homolog Caspase-11, with a role in the immune system[22]. Apoptotic initiator Caspases possess long prodomains containing either a Death Effector Domain (DED) (Caspase-8 and -10) or a Caspase Activation and Recruitment Domain (CARD) (Caspase-2 and -9), which mediate the interaction with upstream adaptor molecules. Finally, Apoptotic effector Caspases, which includes Caspase-3, -6 and -7, are characterised by the presence of a short prodomain. They are typically processed and activated by upstream Caspases and perform the downstream execution steps of apoptosis by cleaving multiple cellular substrates[23]. The mechanism of activation of the initiator Caspases depends critically on the engagement and activation of recruitment platforms such as the Death Inducing Signaling Complex (DISC)[24] for Caspase-8 and Caspase-10, the PIDDosome[25] for Caspase-2 and the apoptosome[26] for Caspase-9. These recruitment platforms integrate cellular signals, promote oligomerization of initiator Caspases and induce their activation. On the other hand, Caspase-14 is not involved in apoptosis or inflammation, but instead it is involved in skin cell development[27].

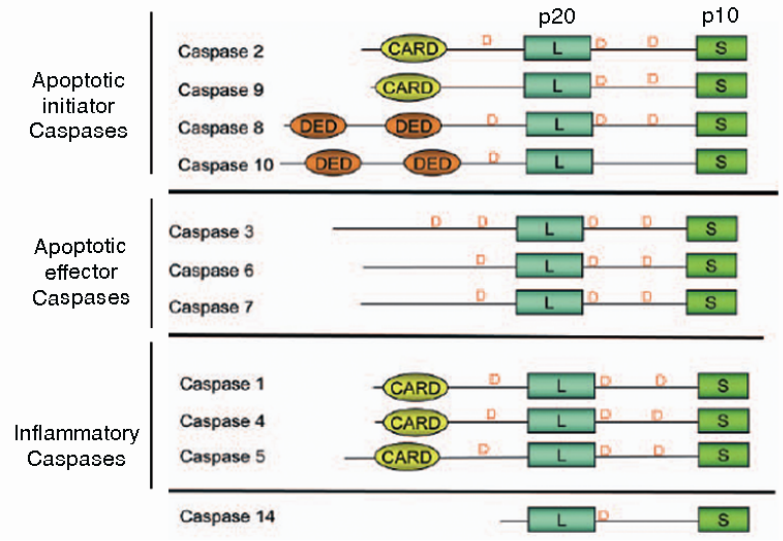

Figure 1. Classification of mammalian Caspases. The Caspases can be classified into three groups: Apoptotic initiator Caspases, Apoptotic effector Caspases and Inflammatory Caspases (Adapted from Jin *et al.*, 2005[28]).

The key step for Caspase activation is the formation of the apical Caspase activation platforms: DISC, PIDDsome and apoptosome (for apoptotic Caspases), and inflammosome (for inflammatory Caspases). However, there are also other mechanisms of regulation including transcriptional regulation, posttranslational regulation and protein degradation. In addition to this, the enzymatic activity of Caspases can be inhibited by IAPs (Inhibitors of Apoptosis). IAP proteins were first identified in baculoviruses based on their ability to suppress apoptosis in insect cells[29]. Mammalian IAPs include XIAP (X-linked IAP), cIAP-1, cIAP-2, NAIP (Neuronal Apoptosis Inhibitory Protein), Survivin and Livin. IAPs are regulated by two proteins released from mitochondria. One is SMAC/Diablo (Second Mitochondrial Activator of Caspases / Direct IAP Binding Protein with Low pI), and the other is Omi/HtrA2 (High Temperature Requirement Protein 2). SMAC/Diablo and Omi/HtrA2 promote Caspase activation by the removal of IAP inhibition[30].

1.1.2. Bcl-2 family of proteins

The Bcl-2 family of proteins regulates the mitochondrial outer membrane permeabilization (MOMP). Bcl-2 (B-cell lymphoma-2) was the founder member of this family and was first identified as an oncogene that instead of promoting cell proliferation, blocked cell death[31]. The members of the Bcl-2 family are characterised by having at least one Bcl-2 homology (BH) domain and are divided in three groups based on their structure and their role in apoptosis. The anti-apoptotic Bcl-2-like proteins contain all of them, the BH1, BH2, BH3 and BH4 domains. The pro-apoptotic Bcl-2-like proteins are subdivided in the multidomain proteins, such as Bax (Bcl-2 associated X) and Bak (Bcl-2 homologous antagonist killer) and the BH3-only proteins which only have the short and proapoptotic BH3 domain[32] (Figure 2).

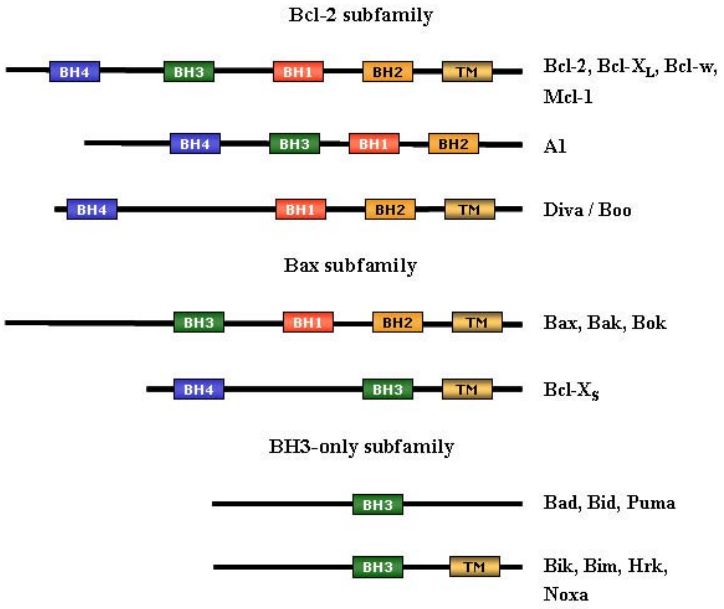

Figure 2. The Bcl-2 family of proteins. The Bcl-2 family of proteins can be classified in three groups: Bcl-2 subfamily (anti-apoptotic proteins), all containing multiple BH domains; Bax subfamily (multidomain containing, proapoptotic proteins) and BH3-only subfamily (pro-apoptotic members containing only a single BH3 domain)[33].

The mechanism by which the Bcl-2 family of proteins controls MOMP is still controversial. Current debate focuses on which interactions within the family are crucial to initiate MOMP. Bax and Bak induce the MOMP either alone or with the collaboration of BH3-only proteins. Bcl-2-like proteins interact with Bax and Bak and keep them inactive. Two models have been proposed to explain the role of the BH3-only proteins: the classical or direct model and the hierarchy or indirect model[33,34]. The indirect model proposes that BH3-only proteins bind to the anti-apoptotic Bcl-2 proteins, which in turn leads to the release of the proapoptotic members Bax and Bak. The direct model proposes the classification of the BH3-only proteins into activators and inactivators. The inactivators, which bind to the Bcl-2-like proteins as in the indirect model, and the activators, which bind to Bax and Bak and work together in the MOMP[33].

1.1.3. Intrinsic pathway

Intrinsic cell death signals generally converge within the cell at the outer membrane of mitochondria (Figure 3). They result in the loss of mitochondrial membrane integrity and the subsequent activation of downstream apoptotic pathways. So, a crucial event in the mitochondrial pathway is MOMP. MOMP is mainly mediated and controlled by Bcl-2 family members. Once MOMP occurs, Cytochrome c is released into the cytoplasm. Upon release, cytosolic Cytochrome c binds to Apoptosis Protease-Activating Factor 1 (Apaf-1) and Procaspase-9, generating an intracellular DISC-like complex known as apoptosome. Within the apoptosome, Caspase-9 is activated, leading to processing of the effector Caspases-3, -6 and -7, which in turn cleave hundreds of cellular components and result in irreversible cell death[26].

In addition to Cytochrome c, other mitochondrial factors are released during the MOMP process. These apoptogenic factors can augment apoptosis by a

variety of different mechanisms. For example, Smac/Diablo inactivates the inhibitors of Caspase activation, Apoptosis-Inducing Factor translocates to the nucleus and induces chromatin condensation, and Endonuclease G assists in nucleosomal DNA fragmentation (reviewed in Saelens *et al.*, 2004 [35]).

1.1.4. Extrinsic pathway

The extrinsic pathway is activated by the engagement of a specialized cell-surface receptor called death receptor by a protein ligand (Figure 3). The death receptors belong to the Tumour Necrosis Factor Receptor (TNFR) gene superfamily, which contain a Death Domain (DD) in their cytoplasmic tails[36]. Death receptors family includes, among others, Fas/CD95/Apo1, TNF-αR (Tumour Necrosis Factor-alpha Receptor) and two receptors for TRAIL (TNF-α Related Apoptosis-Inducing Ligand): DR4 and DR5. Ligation of death receptors with ligands results in the formation of DISC which recruits other DD-containing adaptor proteins through homotypic interactions. There are two major DD-containing adaptor proteins involved in death receptor signalling: Fas Associated Death Domain (FADD) protein and TNF Receptor Associated Death Domain (TRADD) protein[37,38]. FADD binds to Fas, TRAIL-R1 and TRAIL-R2, while TRADD preferentially binds to TNFR1, DR3 and DR6 [39-42].

The better characterised receptor of this family is probably Fas/CD95/Apo1. After FasL binding to Fas, the DD domain in the cytoplasmic tail of Fas recruits the adaptor protein FADD. FADD is a cytosolic adaptor protein composed of two functional domains: an N-terminal Death Effector Domain (DED) and a C-terminal Death Domain (DD). After the DD domain of FADD binds to Fas, the DED domain of FADD recruits Procaspase-8 leading to activation of Caspase-8[43,44]. Recruitment of Procaspase-8 to the DISC juxtaposes multiple Procaspase-8

molecules, resulting in dimerization, cleavage of the prodomain, and activation of Caspase-8. How Caspase-8 transducers the apoptotic signal depends on the cell type and on the quantity of active Caspase-8 produced in the DISC[45]. Cells can be divided into type I and type II based on the requirement of the mitochondrial pathway for apoptosis induced by death receptors. In type I cells, a high production of active Caspase-8 can directly process the effector Caspase-3, leading to its activation and ultimately to apoptosis. In type II cells, however, only a small amount of FADD and Caspase-8 are recruited to DISC, so insufficient activation of Caspase-8 requires involvement of mitochondria to finally induce apoptosis. So apoptosis in these cells is dependent, at least in part, on the cleavage of the BH3-only protein Bid, resulting in the generation of a proapoptotic fragment termed tBid (truncated Bid). tBid induces mitochondrial permeabilization and thus activation of effector Caspases through the apoptosome[46,47]. Although the apoptotic mitochondrial events occur in both types of cells, only the apoptosis in type II cells is abrogated if the mitochondrial pathway is blocked by overexpression of Bcl-2 protein[8].

Other proteins have been found associated with the DISC, such as Caspase-10 and c-FLIP (FLICE-like Inhibitory Protein). Caspase-10 is highly homologous to Caspase-8 at both sequence and function level. However, there is no murine homolog for Caspase-10. c-FLIP is a protein similar to Caspase-8 but with a mutated catalytic site, thus not having caspase activity and functions as a competitive inhibitor of Caspase-8[48]. Two isoforms of c-FLIP have been described at the protein level: c-FLIP$_L$ and c-FLIP$_S$, which can inhibit Procaspase-8 activation[49]. On the other hand, other studies have reported that c-FLIP is able to heterodimerize with Caspase-8 producing active complexes, thus acting as a pro-apoptotic protein[50]. So, the role of FLIP in death receptor-mediated apoptosis is still controversial and not well

established, since knockout mice show embryonic lethality due to failure in heart development[51].

Genetic evidence from knockout mice and mutagenized cell lines supports the idea that all death receptors investigated so far, critically depend on the death domain-containing adaptor protein FADD and Caspase-8 to induce cell death[52].

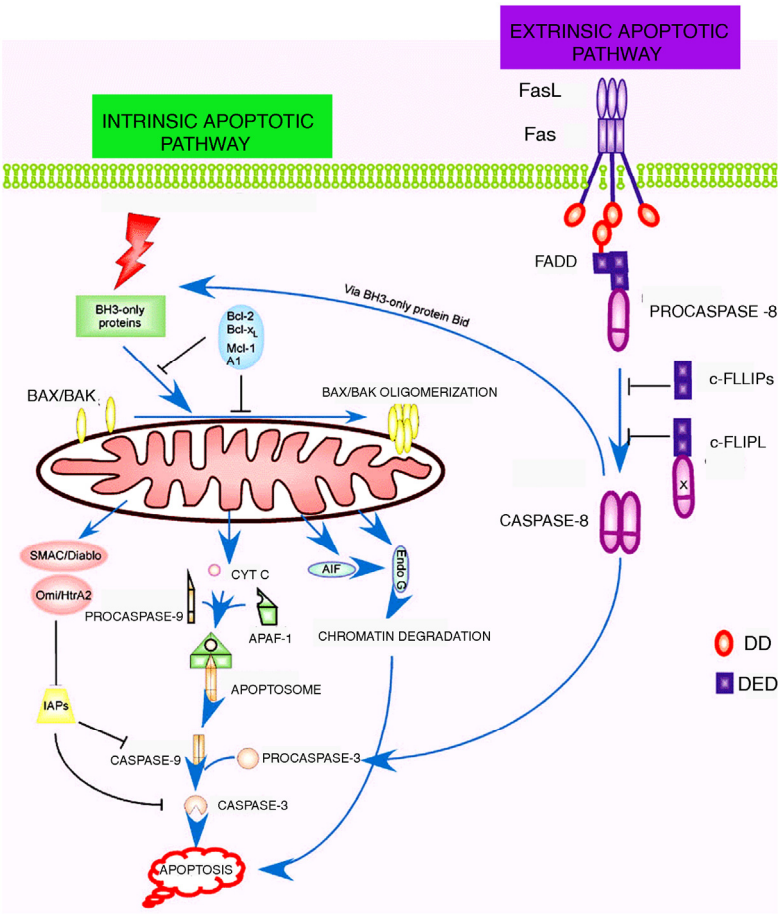

Figure 3. Apoptotic pathways. Two major pathways lead to apoptosis: the intrinsic apoptotic pathway mediated by the mitochondria and the extrinsic apoptotic pathway controlled by the death receptor signalling (Adapted from Zhang *et al.*, 2005[53]).

2. Cytoplasmic bodies

Cytoplasmic RNA granules were originally described in 1865 as dark staining granules at one pole within fruit fly larvae. Later studies found different analogous structures that contained different cytoplasmic granules. These granules are called polar granules in *Drosophila*, dense bodies or germinal granules in *Xenopus*, and P granules in *C. elegans,* that collectively are called germ cell granules[54]. These germ cell granules contain proteins involved in translation initiation, translational control and mRNA decay. Also the germ cell granules have been implicated in the regulation of the timing of maternal mRNA translation to promote germ cell development in the early embryo and establish the germ line for the next generation. Different cytoplasmic RNA granules have also been found in somatic cells, including Stress Granules (SGs), Processing Bodies (PBs), and Neuronal Granules. In general, the cytoplasmic RNA granules have an important role in the posttranscriptional regulation of gene expression[55].

Neuronal Granules, found exclusively in neurons, regulate the translation of selected mRNA transcripts. These transcripts are packaged into the RNA granules and transported to dentritic synapses, where their proteins products are required, and only then are released and translated[56].

2.1. Stress granules (SGs)

SGs were originally described 20 years ago as transient microscopic foci found in heat-stressed Peruvian tomato cells[57]. Lately similar SGs were found in the cytoplasm of mammalian cells treated with different environmental stresses such as heat shock, oxidative conditions, UV irradiation or hypoxia. Many different types of stress reduce global translation by triggering the phosphorylation of the α-subunit of eukaryotic initiation factor eIF2 at residue Ser51. The phosphorylation of eIF2α reduces

the translation of most mRNAs. However eIF2α phosphorylation specifically enhances the translation of a few selected mRNAs, which encode proteins that function in the adaptation to stress and in the recovery of translation[58]. This phosphorylation is produced by a family of four serine/threonine kinases, which include Protein Kinase RNA (PKR), PKR-like Endoplasmic Reticulum Kinase (PERK), General Control Non-derepressible-2 (GCN2) and Heme-Regulated Inhibitor (HRI). It is known that phosphorylation of Ser51 of eIF2α is critical for the assembly of SGs.

Phosphorylation of the eIF2α allows TIA-1 (T-cell Internal Antigen-1) to promote the assembly of untranslated, non-canonical 48S preinitiation complexes that are the core constituents of SGs. SGs also contain other proteins that vary with cell type and with the nature and duration of the stress involved, such as transcription factors, RNA helicases, exonucleases, scaffold proteins and many RNA-binding proteins including HuR, Staufen, Smaug, TTP (tristetraprolin), G3BP, CPEB and SMN, among others. On the other hand, SGs contain proteins that regulate diverse cell signalling pathways, such as TRAF2, which functional significance has to be determined[59]. More recently, SGs have been shown to contain the Argonaute proteins, microRNAs, mRNA-editing enzymes and proteins required for transposon activity[60].

SGs are heterogeneous in size and shape with about 0.1 to 2.0 μm in size, not surrounded by membrane, and associated with the endoplasmic reticulum. Five to thirty SGs can be found per cell (Figure 4B). The function of the SGs is to protect RNAs from harmful conditions and function as a decision point for unstranslated mRNAs. So the formation of SGs determines whether individual mRNAs can be stored, degraded or re-initiated. SGs are not sites of long-term mRNP storage, where the half-life of stress-granule-associated RNA binding proteins is very brief, on the order of

seconds to minutes[61]. There is a dynamic equilibrium between polysomes and SGs. While drugs that stall initiation can cause SG assembly, drugs that inhibit translational elongation, such as cycloheximide, prevent SG assembly and force the disassembly of pre-formed SGs[61].

TIA-1 is a RNA-binding protein that possesses three RNA recognition motifs (RRM) at their N-terminal part and a glutamine-rich domain at their C-terminal part. The amino acid sequence of TIA-1 is 80% identical to the TIA-1 related protein, TIAR (TIA-1 Related Protein). TIA-1 and TIAR normally predominate in the nucleus, where they have been shown to act as selective regulators of alternative mRNA splicing[62,63]. But these proteins shuttle continuously between the nucleus and the cytoplasm. In the cytoplasm, TIA-1 and TIA1R have shown to regulate the translation of various mRNAs by binding to AU-rich elements (AREs) located in these mRNAs 3' unstranslated regions (3' UTRs), such as the mRNAs encoding TNF-α[64]or Cyclooxygenase-2 (Cox-2)[65], among others. In addition to the translational silencing of selected cytoplasmic transcripts, TIA and TIAR participate in the assembly of the SGs. In response to environmental stresses, TIA-1 and TIA1R accumulate in the cytoplasm, where they aggregate at the SGs. So TIA-1 and TIAR act downstream of the stress induced phosphorylation of eIF2α to drive mRNA from polysomes to SGs[66].

2.2. Processing Bodies (PBs)

The PBs are small cytoplasmic foci that contain components of the RNA decay machinery including deadenylases, the decapping enzymes Dcp1/Dcp2, the 5'-3' exonuclease Xrn1 and scaffolding proteins such as GW182 or Hedls/Ge-1. Since mRNA decay intermediates accumulate in PBs after inhibition of the RNA decay machinery, PBs are believed to be the actual sites where deadenylation, decapping and 5'-3' mRNA decay occurs[67].

PBs also contain ARE-binding proteins such as TTP, BRF1 and BRF2 and participate in ARE-mediated mRNA decay (AMD)[68]. PBs are not a terminal end-point for mRNAs, on the contrary, a mRNA in a PB can return to the actively translated pool of mRNAs if an appropriate stimulus is received. In addition, mRNAs translationally silenced by micro-RNAs are also recruited to PBs[69]. So PBs have a dual role as sites of translational suppression and mRNA decay.

PBs often associate with SGs. Contrary to SGs, PBs are uniform spheroid particles that increase in size (between 0.1-1.0 μM) and number in response to stress[70]. We can found between one to thirty PBs per cell (Figure 4A). Both SGs and PBs contain mRNA, eIF4E, microRNAs and argonaute proteins, and various regulators of mRNA stability and translation (TTP, RCK/p54, and CPEB). Although SGs and PBs share some protein and mRNA components, they are structurally, compositionally and functionally distinct and have markers specifics of each structure. For example, PBs lack ribosomal subunits or translation initiation factors. In mammalian cells, SG formation requires eIF2α phosphorylation whereas stress-induced PB formation does not[70] .

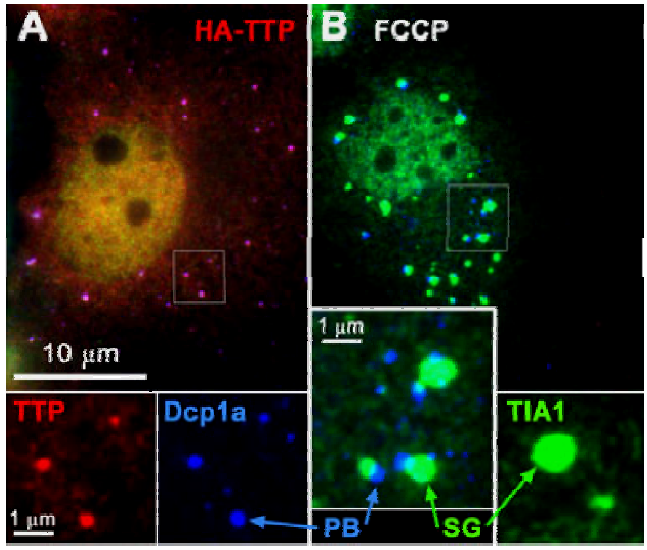

Figure 4. In **(A)** it is shown Processing Bodies (PBs) marked in blue by Dcp1A (deccaping enzyme) which colocalizes with TTP (tristetraprolin) in red. In **(B)** it is shown Stress Granules (SGs) marked in green by TIA-1 (T-cell Internal Antigen-1) induced after stress treatment with the mitochondrial inhibitor FCCP. SGs appear juxtaposed to PBs.

3. Translational response to stress

3.1. Translation initiation

Protein translation is regulated at the level of initiation, elongation and termination, although the translation initiation process is the main regulation point[71]. Eukaryotic translational initiation begins when the 43S preinitiation complex composed of the small ribosomal subunit 40S, eukaryotic initiation factors (eIFs) 3,1,1A and 5 and the ternary complex (eIF2/GTP/methyionyl initiator tRNA (Met-tRNA$_i^{met}$) bind to the capped mRNA in association with the eIF4G scaffold protein, the eIF4A RNA helicase, and the eIF4E cap-binding protein. The resulting 48S preinitiation complex scans along the 5-UTR until it reaches and identifies the initiation codon that is recognized by the anticodon tRNA$_i^{met}$. Recognition of the initiation codon triggers hydrolysis of eIF2-associated GTP catalyzed by eIF5. Then, the early initiation factors dissociate from the 40S subunit, and the 60S subunit is recruited to form the catalytically competent 80S ribosome. The complete ribosome (80S) then initiates translation elongation, during which the sequence between the "start" and "stop" codons is translated from mRNA into an amino acid sequence (Figure 5)[72].

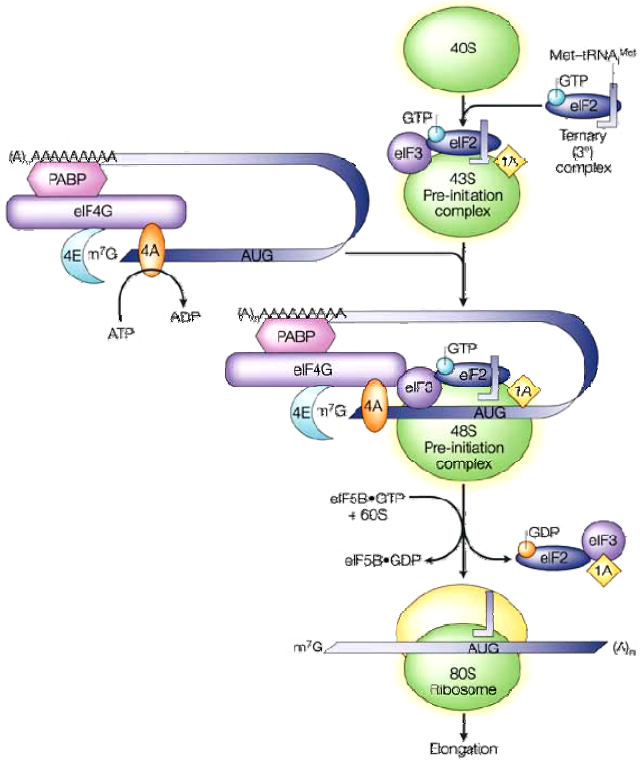

Figure 5. Initiation of translation. The translation of eukaryotic mRNA involves the recognition and recruitment of mRNAs by the translation-initiation machinery, and the assembly of the 80S ribosome on the mRNA. This process is mediated by proteins that are known as eukaryotic Initiation Factors (eIFs)[73] .

eIF2 is part of the ternary complex and is composed of three subunits: α, β and γ. Exchange of GDP for GTP on eIF2 is catalysed by eIF2B, a GDP /GTP exchange factor also known as GEF (Guanine Nucleotide Exchange Factor), and is required to reconstitute a functional ternary complex for a new round of translation initiation. Under different environmental stress conditions, the α subunit of the eIF2 is phosphorylated at residue Ser51. This phosphorylation blocks the GTP-exchange reaction by reducing the dissociation rate of eIF2 from eIF2B. In effect, this sequesters eIF2B and, as a consequence, GDP-GTP exchange no longer occurs, the ternary complex is not formed and the translation is inhibited[74-76].

3.2. eIF2α kinases

We have seen before that the phosphorylation of eIF2α is mediated by four distinct serine/threonine protein kinases (GCN2, HRI, PKR and PERK). These kinases share homology in their catalytic domains, but their effector domains are distinct and are subjected to different regulatory mechanisms (Figure 6). Phosphorylation of eIF2α decreases the translation of mRNAs encoding housekeeping proteins, whereas the translation of mRNAs encoding molecular chaperones and enzymes involved in damage repair, such as GCN4 in yeast or ATF4 in mammals, is maintained or enhanced. The term "integrated stress response" refers to the process mediated by the four eIF2α kinases that respond to different stress signals and converges in the phosphorylation of eIF2α, which activates a common set of target genes (Figure 7).

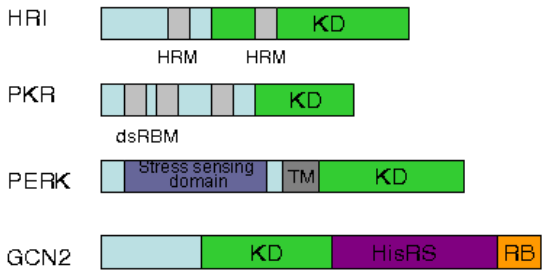

Figure 6. Schematic representation of eIF2α kinases: HRI, PKR, PERK and GCN2. The blue boxes denote the N-terminal part and the green boxes the kinase domain (KD) of the C-terminal part. The structure of HRI includes two HRMs (Heme-Regulatory Motif). The structure of PKR includes two dsRBMs (dsRNA Binding Motif) in its N-terminal part. The structure of PERK includes a TM (Transmembrane Domain) and a lumenal stress-sensing domain in its N-terminal part. The structure of GCN2 includes a HisRS-like (Histidyl-tRNA Synthetase) domain and a RB (Ribosome Binding) domain in its C-terminal part.

3.2.1. GCN2/EIF2AK4 (General Control Non-Derepressible-2, Eukaryotic Tranlation Initiation Factor 2-Alpha Kinase 4)

GCN2 was originally discovered in *Saccharomyces cerevisiae* as an eIF2α kinase called Gcn2p. Gcn2p is composed by a kinase domain (KD), an amino acid sequence of about 530 amino acids related to Hisdidyl-tRNA Synthetases (HisRS) juxtaposed to this KD and a Ribosome Binding (RB) domain located at the end of the C-terminal part (Figure 6). The HisRS region is required for Gcn2p positively regulatory function *in vivo* and the RB domain is essential for its interaction with the 60S ribosomal subunit[77]. Gcn2p is activated by binding to uncharged tRNAs through the HisRS region, which accumulate in amino acid starved cells. This activation leads to increased translation of the GCN4 mRNA. This gene-specific regulation is mediated by four short upstream Open Reading Frames (ORFs) located in the noncoding portion of the GCN4 mRNA. When cells are not limited for amino acids, the upstream ORFs block translation of the GCN4 coding sequences. In response to amino acid starvation, Gcn2p phosphorylation of eIF2α leads to reduced eIF2-GTP levels, thereby reducing the translation initiation efficiency of the upstream ORFs and allowing for elevated GCN4 translation. The GCN4 transcription factor activates genes involved in amino acid biosynthesis and metabolism[74].

Ggn2 gene is conserved from yeast to mammals. Studies of mammalian and yeast cells suggest that GCN2 is activated by many different cellular stresses, which are not directly linked to amino acid starvation. For example, in yeast phosphorylation of eIF2α by GCN2 can be enhanced by purine or glucose deprivation, exposure to high concentrations of sodium chloride, and treatment with rapamycin or hydroxyurea. GCN2 can be also activated in UV irradiated-cells independently of the activation of JNK or p38 MAP-kinases[78]. It is known that UV-induced activation of NF-κB requires GCN2,

which may act simply by preventing translation of IκB-α to replace pools that have been ubiquitinated and degraded. Then, the reduced levels of IκB-α facilitates NF-κB entry into the nucleus and induction of its target genes[79]. It has been also demonstrated that PERK phosphorylates eIF2α in response to UV irradiation. Recently, it has been identified an upstream regulator, Nitric Oxide Synthase (NOS), which controls the activation of both PERK and GCN2 upon UV irradiation. UV irradiation induces NOS activation and $NO^{\cdot}$ (Nitric Oxide) production, which react with superoxide $O_2^{\cdot -}$ to form peroxynitrite $ONOO^-$ and activate PERK. The $NO^{\cdot}$ production also leads to L-Arg depletion and GCN2 activation[80].

3.2.2. HRI/EIF2AK1 (Heme-Regulated Inhibitor, Eukaryotic Translation Initiation Factor 2-Alpha Kinase 1)

HRI is a serine/treonine kinase present in all vertebrates, which contains two Heme Regulatory Motifs (HRM) located in the N-terminal part and kinase insertion[81] (Figure 6). HRI is expressed predominantly in erythroid cells and is regulated by heme. HRI coordinates the synthesis of globin chains with the availability of heme in reticulocytes. Under heme-deficient conditions, HRI is activated and phosphorylates the α subunit of eIF2, leading to the inhibition of protein synthesis. Both N-terminal part and kinase insertion are involved in the heme binding and the heme regulation of HRI[81]. Activation of HRI in response to heme deficiency requires several steps. HRI is present in unstressed cells as inactive pro-inhibitor. During heme deficiency, HRI is activated to a form that is completely reversible by hemin. Then, HRI is converted into an intermediate form whose activity is partially inhibited by hemin. And finally, HRI progresses to a heme-irreversible form. It has been demonstrated that the Hsp90 chaperone is obligatory for the maturation of newly synthesised HRI into an active heme-regulated kinase[82].

HRI is also activated by various cytoplasmic stresses independent of heme, including arsenite treatment, heat shock and osmotic stress, but not by ER stress or nutrition starvation. HRI is the only eIF2α kinase that is activated by arsenite treatment of erytroid cells, at variance with its activation by osmotic stress or heat shock that can also be mediated by other eIF2α kinases. The mechanism of activation of HRI by arsenite is different from the activation by heat shock or osmotic stress. Arsenite is an oxidative stress inducer and can cause increases of intracellular Reactive Oxygen Species (ROS)[83]. Moreover, HRI activated by arsenite is hyperphosphorylated compared to HRI activated by heat shock or osmotic shock. So it seems that the involvement of HRI and PKR upon different stresses depends on the tissue-expression of these kinases[84].

3.2.3. PKR/EIF2AK2 (Protein Kinase R, Eukaryotic Translation Initiation Factor 2-Alpha Kinase 2)

PKR is a serine-threonine kinase present in mammals, composed by a KD in its C-terminal part, which is conserved in the other eIF2α kinases, and by a cluster of basic amino acids, which play a regulatory role, in its N-terminal part. The N-terminal part contains two basic regions where two divergent copies of a dsRNA Binding Motif (dsRBM) required for RNA binding are located and a third basic region which is dispensable for its function (Figure 6). PKR contributes to a broad variety of cellular responses such as signal transduction, transcriptional control, cell growth and apoptosis[85]. PKR is localized mostly in the cytoplasm in an 80% of the cases, mainly associated with ribosomes, and about a 20% localized in the nucleus. The biological significance of PKR translocation to the nucleus is still unknown, but it seems that it could be involved in stress-induced apoptosis[86].

PKR is activated by double-stranded RNA (dsRNA), the synthesis of which can be caused by viral infection and leads to an inhibition of translation in

virus-infected cells. Binding of dsRNA to the N-terminal dsRBM motif of the protein, triggers a conformational switch of PKR, resulting in PKR dimerization and autophosphorylation. PKR autophosphorylation represents the activation reaction and leads to the phosphorylation of eIF2α, and then to the inhibition of protein synthesis. Besides, PKR is also activated by other activators such as pro-inflammatory stimuli, growth factors, cytokines and oxidative stress. Among many viral proteins, HIV Tat has been shown to generate oxidative stress and induce apoptosis[87]. Oxidative stress induces PKR activation essentially via the cytokine IFN-γ activation signal and causes apoptosis[88]. Furthermore, in the absence of virus infection, other conditions of stress can lead to PKR activation through the PACT (PKR-associated Activator) protein[89].

PKR has a role in signal transduction and transcriptional control through the IkB/NF-kB pathway[90]. In response to dsRNA, PKR through TRAF adapter (TRAF2 or TRAF5), activates the kinase complex IKKα/IKKβσ which leads to the release of the NF–κB transcription factor as a consequence of the phosphorylation of its inhibitor IκBα[91]. PKR is also an activator of signalling cascades involving stress activated protein kinases, and it has been described to mediate JNK and p38 activation in response to different stimuli[92].

PKR can trigger apoptosis, in part through its ability to control protein translation, but it has also been seen that NF-kB, ATF3 and p53 have been implicated in mediating this process[93]. PKR induces apoptosis through interaction with FADD, which activates the Caspase-8 pathway, which in turn can directly cleaves Procaspase-3 and activates the mitochondrial pathway via Bid/Bax interaction, release of Cytochrome c from the mitochondria and finally the formation of the apoptosome[94].

As a result of the effects of PKR on translation, transcription and apoptosis, PKR can function to control cell growth and cell differentiation, and its activity can be controlled by the action of several oncogenes[95]. Despite the implications of PKR in cell growth and differentiation, PKR knockout mice develop normally and are fertile[96]. PKR knockout mice do not develop spontaneous tumours but in response to dsRNA show deficient activation of the NF-κB pathway[97].

The function of PKR can be regulated positively by cellular proteins such as PACT, but it can be also regulated negatively by other proteins such as p58^{IPK}, TRBP, nucleophosmim or Hsp90/Hsp70. P58^{IPK} is a member of the tetratricopeptide repeat (TPR) family of proteins, which interacts directly with PKR and inhibits its kinase activity[98]. Also the chaperones Hsp90/Hsp70, which are initially required for folding and maturation of PKR, can inhibit PKR activating autophosphorylation[99].

3.2.4. PERK/EIF2AK3 (PKR-like Endoplasmic Reticulum Kinase, Eukaryotic Translation Initiation Factor 2-Alpha Kinase 3)

PERK or PEK (Pancreatic eIF2α Kinase) is an ER kinase present in metazoans, that share homology with the other eIF2α kinases in its kinase domain located on the C-terminal part, and has a distinctive N-terminal part (Figure 6). Under ER stress, PERK is autophosphorylated and activated, which induces the phosphorylation of eIF2α[100]. In yeast *S. cerevisiae*, phosphorylation of eIF2α by Gcn2p leads to translational upregulation of the transcription factor GCN4. In mammalian the metazoan homologue of GCN4 is ATF4, which is induced by PERK, and is similarly regulated (see section 5.2)[101].

EIF2α kinases work together with additional stress-sensing pathways. PERK functions in conjunction with IRE1 and ATF6 to control ER stress and elicit a program of gene expression referred to as the Unfolded Protein Response (UPR) (see section 5)[102]. The UPR is a coordinate adaptive programme that is produced by ER stress, which leads to the inhibition of global protein synthesis and the selective transcription and translation of some proteins related to the recovery of the homeostasis of the cell.

Independent of its translational regulatory capacity, PERK-dependent signals induce the activation of the prosurvival transcription factor NF-E2-related-factor-2 (Nrf2) via site-specific phosphorylation. Under basal conditions, Nrf2 is localized in the cytoplasm through the interaction with the protein Keap1 (Kelch-like Ech-associated protein1). PERK-dependent phosphorylation leads to the nuclear accumulation of Nrf2 and increases transcription of Nrf2 target genes[103]. Nfr2 activation provides a protective mechanism by which cells increase glutathione production, which leads to minor accumulation of ROS during the UPR and, as a consequence, attenuates apoptotic induction after ER stress[104].

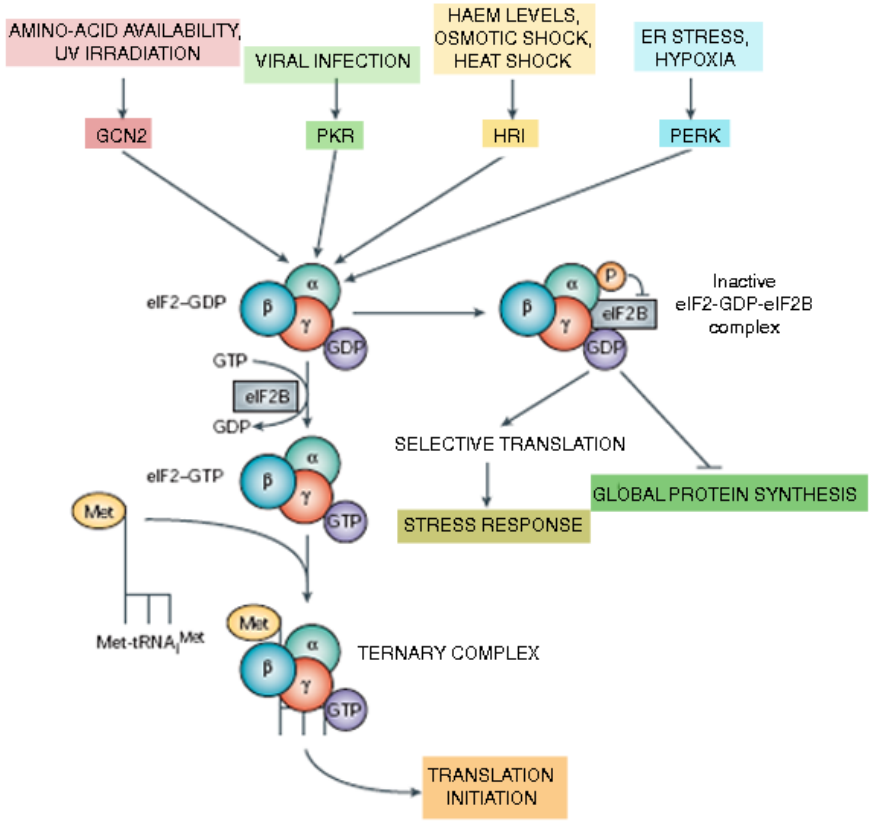

Figure 7. Integrated stress response. Upon different environmental stresses, four different eIF2α kinases (Protein Kinase R (PKR), PKR-like Endoplasmic Reticulum Kinase (PERK), General Control Non-derepressible-2 (GCN2) and Heme-Regulated Inhibitor (HRI)) induce the phosphorylation of the eukaryotic Initiation Factor 2-α (eIF2α). EIF2α is a subunit of eIF2 that is part of the ternary complex (eIF2-GTP-Met-tRNA$_i^{Met}$). Phosphorylation of eIF2α inhibits the exchange of GDP for GTP by reducing the dissociation rate of eIF2B. As a consequence, the ternary complex is not formed and the translation is inhibited. (Adapted from Holcik and Sonenberg, 2005[72]).

4. Protein folding and quality control

The ER is a subcellular organelle composed of a reticular membranous network that extends through the cytoplasm and that can be contiguous with the nuclear envelope. This organelle is responsible for the synthesis and folding of secreted, membrane-bound and some organelle-targeted proteins[105]. The ER is also a site of calcium storage, and steroid, cholesterol and lipid biosynthesis. Correct folding of newly-synthesised proteins is made possible thanks to the existence of the ER "quality control". ER "quality control" suppresses the formation of aggregates by ensuring fidelity of transcription and translation, by chaperoning nascent or unfolded proteins, and by selectively degrading improperly folded polypeptides before they can aggregate[106].

When correct folding is difficult or impossible and degradation by the proteasome is not performed rapidly, proteins interact with other unfolded or partially folded proteins, leading to the formation of aggregates. Cells then destroy protein aggregates through the aggresome pathway, which is a proteasome-independent pathway. So if nascent peptides do not fold correctly, they will coaggregate to form a single aggresomal particle. After their formation, the aggresomal particles are transported towards the Microtubule Organizing Center (MTOC), where they are sequestered into a single large cellular garbage bin-like structure known as the aggresome[107]. Movement of the aggresome particle is an active process and requires intact microtubules and association with motor dynein. HDAC6 acetylates α-tubulin and associates with dynein to facilitate transport of aggregated bodies through the cytosol to lysosomes for degradation. Aggresomes are irregular structures of 60-80 nm, which contain subcellular organelles and filaments, various proteins, including molecular chaperones (Hsc70 and Hsp40), the chaperonin TriC/TCP, centrosome material, proteins of cytoskeleton as well

as of the UPS (Ubiquitin-Proteasome System) and are surrounded by a network of intermediate filament protein vimentin[108]. The aggresome may disappear, through proteasomal and lysosomal degradation of the accumulated protein, if the load of defective proteins is reduced.

The ER "quality control" is composed of several ER chaperone proteins including BiP/GRP78 (Binding immunoglobulin Protein, Glucose-Regulated Protein), Protein Disulfide Isomerase (PDI), ERp57, calnexin, calreticulin, and the peptidylpropyl isomerase family. BiP/GRP78, which is the one of the most abundant and best-characterised ER chaperones, consists of an N-terminal ATPase and a C-terminal substrate-binding domain. This chaperone interacts with the hydrophobic domains of a wide range of proteins. This binding to hydrophobic domains helps preventing misfolding during translocation into the ER in an energy dependent manner[109]. PDI catalyses the formation and breakage of disulfide bonds between cysteine residues within proteins as they fold. This allows proteins to quickly find the correct arrangement of disulfide bonds in their fully-folded state[110]. Calnexin and calreticulin are lectin proteins responsible for glycoprotein quality control. Calnexin is a transmembrane protein and calreticulin is the soluble luminal homolog[111]. Erp57 is a member of the PDI family that interacts specifically with newly synthesised glycoproteins and forms discrete complexes with ER lectins, calnexin and calreticulin[112]. And finally the peptidylpropyl isomerise family proteins that catalyse the *cis–trans* isomerisation of peptide bonds N-terminal to proline residues in polypeptide chains[113].

Perturbations that alter ER homeostasis consequently disrupt protein folding and lead to accumulation of unfolded proteins and protein aggregates that can be injurious to the cell. ER stress can be provoked by various physiological and pathological stresses such as perturbations in the calcium homeostasis, glucose deprivation, ischemia, viral infections, hypoxia or

disruption of intracellular pH. All these perturbations in the ER homeostasis lead to an increased demand on the ER's protein-folding capacity[114]. For example, disturbances in the cellular redox regulation caused by hypoxia, oxidants or reducing agents, interfere with disulphide bonding in the lumen of the ER, leading to protein unfolding and misfolding. When the extent of unfolded proteins in the ER lumen reaches a critical level, the cell trigger an evolutionarily conserved response termed the UPR (Unfolded Protein Response)[102].

5. The UPR (Unfolded Protein Response)

On a cellular level, the adaptive phase of the UPR triggers three types of protective cellular responses. The first response is the upregulation of genes encoding ER chaperone proteins such as BiP/GRP78 or GRP74 and structural components of the ER including Sarcoplasmic ER Ca^{2+}-ATPase 2 (SERCA2) to increase the protein-folding capacity in the ER[115]. It has been seen that some genes involved in amino acid transport, glutathione biosynthesis and protection against oxidative stress are also upregulated[116]. The second response is translation attenuation reducing the load of new protein synthesis and preventing further accumulation of unfolded proteins through eIF2α phosphorylation[117]. And finally the third response is the degradation of misfolded proteins by the proteasome by a process called ER Associated Degradation (ERAD)[118]. These three responses are protective measures to limit protein load and alleviate ER stress. But if the induction of these responses fails and misfolded proteins continue to accumulate in the ER, the UPR activates ER-initiated pathways by activating NFκB, a transcription factor that induces expression of genes encoding mediators of host defense[119] or activating Mitogen-Activated Protein Kinases (MAPKs), Jun N-terminal Kinase (JNK) and p38 MAPK kinases[120]. However if the ER damage is extensive or prolonged, cell death is induced typically by apoptosis[121].

The UPR is an integrated signal transduction pathway that transmits information about protein-folding status in the ER lumen to the nucleus to increase protein folding capacity. The UPR was first characterised in yeast in a screening for mutations blocking UPR-inducible reporter activity. It was found a unique gene named *IRE1p (*Inositol-Requiring Transmembrane Kinase/Endonuclease 1) which encodes a type 1 ER-resident transmembrane protein with a novel lumenal domain and a cytoplasmic

portion that contains a protein kinase domain[122]. In higher eukaryotes, the UPR gained complexity as it is mediated by at least three distinct UPR signalling pathways initiated by the sensors IRE1[120], PERK (PKR-like Endoplasmic Reticulum Kinase)[123] and ATF6 (Activating Transcription Factor 6)[124] (Figure 8). All three sensors are maintained in an inactive state at the ER membrane by binding to the chaperone BiP. Upon accumulation of unfolded proteins, bound BiP dissociates from ATF6, IRE1 and PERK to chaperone the misfolded proteins and allowing the activation of one or more of these transducers[125].

UPR is essential to a range of normal physiological and developmental processes. These include, for example, the regulation of insulin secretion by pancreatic β-islet cells[126] and the differentiation of immunoglobulin-secreting plasma cells[127]. In these cases, the activation of the UPR is crucial to maintain the homeostasis in the cell. On the other hand, it has been demonstrated that accumulation of misfolded proteins and ER stress is associated with a variety of human diseases, such as neurodegenerative diseases, diabetes and cancer. In some neurodegenerative diseases, such as Parkinson's, Alzheimer[128] and Huntington's diseases, the progressive loss of specific types of neurons is caused by the chronic exposure to misfolded proteins and proteins aggregates in the cytoplasm. Diabetes can be produced by mutations in components of the UPR signalling. For instance, PERK mutations were found in patients with a form of type I insulin diabetes, called the Wolcott-Rallison syndrome[129]. In cancer, the activation of the UPR may protect the tumour cell from the increased amount of misfolded proteins caused by the high number of mutations and decreased supply of nutrients and oxygen[130]. Hypoxia, a common occurrence in solid tumours, is a potent activator of PERK and its downstream target ATF4[131,132].

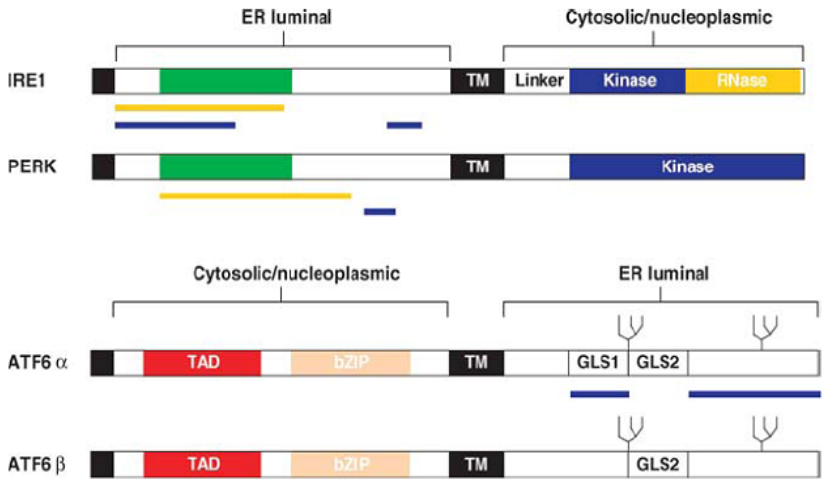

Figure 8. Primary structure of the ER stress sensors: IRE1, PERK and ATF6. Yellow bars represent regions sufficient for signal transduction or oligomerization. Blue bars represent regions interacting with BiP. The black boxes represent the signal peptides, and the green boxes describe the region of limited homology between IRE1 and PERK. bZip: basic-leucine zipper; GLS1 and GLS2: Golgi localization sequences 1 and 2; TAD: transcriptional activation domain and TM: transmembrane domain[109].

5.1. IRE1 (Inositol-Requiring Transmembrane Kinase/Endonuclease 1)

IRE1 is a bifunctional type I transmembrane protein with a lumenal stress-sensing domain and a cytosolic part that contains a serine-threonine kinase domain and an endoribonuclease domain (Figure 8). The binding of BiP to the luminal domain of IRE1 maintains it in an inactive state. The dissociation of BiP from IRE1 due to the presence of misfolded proteins in the ER lumen allows the oligomerization and activation of this protein. Yeast *IRE1p* was the first gene described in the UPR. The activation of IRE1p depends on both the dissociation of BiP and the direct interaction with the unfolded proteins. In contrast, the activation of mammalian IRE1 strongly depends on the dissociation of BiP, rather than on the direct

interaction with unfolded proteins. The different properties of yeast IRE1p and mammalian IRE1 could be as a result of their structural differences which are derived from their sequence characteristics[133]. In 1998 two different mammalian homologs, which were named IRE1α and IRE1β, were independently identified. IRE1α is expressed ubiquitously, with high levels in pancreas and placenta[134], whereas IRE1β is only expressed in the gut epithelial cells[135]. Deletion of mouse IRE1α caused lethality at embryonic days E10.5, whereas IRE1β-deficient mice are viable, but exhibit increased susceptibility to experimentally induced colitis[136].

When IRE1 activates its endoribonuclease activity, the cleavage of the mRNA encoding bZIP (basic-leucine zipper) transcription factor HAC1 in yeast[137] or its functional homologue X-box Binding Protein (XBP)1 in metazous[138] take place (Figure 9).

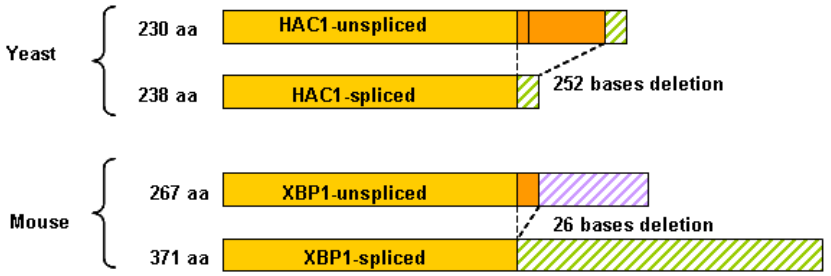

Figure 9. Schematic representation of unspliced and spliced forms of HAC1/XBP1 mRNA. The dark orange boxes of yeast HAC1 or mouse XBP1 represent the sequence removed by splicing. 252 bases are deleted in the splicing of HAC1 and 26 bases in the case of splicing of XBP1.

The unspliced form of the HAC1 mRNA contains a translational attenuation sequence in its intron which is removed by splicing[139]. The splicing reaction cleaves the HAC1 mRNA at two sites, which then are rejoined by the tRNA ligase Rlg1[140]. As a result, splicing of the HAC1 mRNA results in the efficient translation of the HAC1 protein product, which functions as a transcription factor that recognizes the UPR element located in the upstream regions of the UPR target genes. HAC1 pre-mRNA encodes a protein of 230 amino acids (HAC1 unspliced) while HAC1 mature mRNA encodes a protein of 238 amino acids (HAC1 spliced).

XBP1 mRNA has two conserved overlapping ORFs. On activation of the UPR, IRE1 removes a 26-nucleotide intron from unspliced XBP1 mRNA, which leads to a translational frame shift to produce a fusion protein encoded from the two ORFs, similar to what it is described for yeast HAC1. Thus, the unspliced and spliced forms of the XBP1 mRNA differ by a frame shift in the downstream region of the intron sequence and generate protein products that differ in their carboxyl regions. Unlike yeast HAC1 mRNA, XBP1 mRNA is effectively translated even in the absence of splicing by IRE1, generating the translation product called XBP1u (unspliced) protein. However, it is known that XBP1u produced at low levels is rapidly degraded by the proteasome and that only the XBP1s (spliced) protein, which escapes from proteasome-mediated degradation, has been demonstrated to function as a transcription factor binding to the ER Stress Response Element (ERSE) promoter in target genes such as ER chaperones, ERAD factors, factors involved in the ER membrane biogenesis[141,142] and p58^{IPK} [143] (Figure 10). Although XBP1u is not active as a transcription factor, it may act as a negative feedback regulator of IRE1 signalling, by binding and targeting XBP1s for degradation. Thanks to this negative feedback, the cell can shut off the transcription of XBP1 target genes immediately upon the inactivation of IRE1 that occurs when the ER stress is resolved[141]. The

activation of XBP1 target genes is required during normal development, since XBP1 knockout mice are embryonic lethal and have defects during liver formation and plasma cell differentiation[144,145].

In mammals, in addition to catalysing XBP1 mRNA splicing, IRE1 has additional functions in cell signalling. Through its serine-threonine kinase domain, recruits the adaptor protein TNF Receptor-Associated Factor 2 (TRAF2) to the ER membrane. This recruitment is regulated by c-Jun NH_2-Terminal Inhibitory Kinase (JIK), which interacts with both IRE1α and TRAF2. The IRE1/TRAF2 complex recruits Apoptosis Signal-regulating Kinase 1 (ASK1), causing activation of ASK1 and the downstream Jun N-terminal Kinase (JNK) pathway leading to cell death[146]. IRE1 also modulates other "alarm genes" such as the activation of p38, ERK[147] and NF-κB pathways[148], possibly by binding of the SH2/SH3 containing adaptor proteins NcK and a protein complex between IkB Kinase (IKK)/TRAF2, respectively. It has been demonstrated that under basal conditions, ER-associated Nck represses ERK activation and upon ER stress this pool of Nck dissociates from the ER membrane to allow the activation of ERK. It is also known that in response to ER stress, IRE1 binds to the IKK complex and then activates NF-κB by promoting degradation of IκBα. Therefore, it is establishes a novel link between ER stress and the membrane death receptor signalling through IRE1–NF-κB–TNFα–TRAF2, which demonstrates a crosstalk between the ER and the death receptor pathway (extrinsic pathway) to initiate apoptotic signalling. So, to sum up, it has been demonstrated that IRE1 has a dual function in ER stress responses: regulating adaptation to stress and cell survival though the control of XBP1 expression and activation of apoptosis in cells irreversibly damaged by the activation of the JNK/ASK1 pathway.

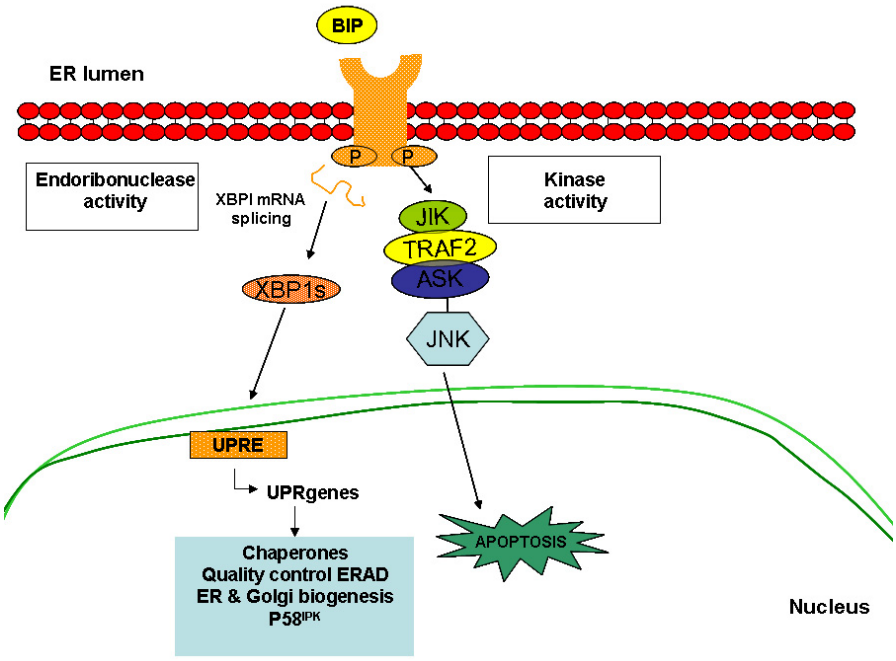

Figure 10. IRE1 pathway. The release of BiP from IRE1, allows for homodimerization and activation of IRE1 through autophosphorylation. IRE1 is a bifunctional transmembrane kinase/endoribonuclease that induces the non-conventional splicing of XBP1 mRNA to produce another b-ZIP transcription activator, XBP1s. XBP1s protein translocates to the nucleus, where it binds to UPR elements (UPRE) and activates many genes. In addition to its endoribonuclease activity, IRE1 also leads to activation of JNK, through TRAF2 and ASK1, which can lead to apoptosis.

5.2. PERK (PKR-like Endoplasmic Reticulum Kinase)

PERK is a type I transmembrane protein with a lumenal stress-sensing domain and a cytosolic domain with kinase activity (Figure 8). IRE1 and PERK have a similar lumenal stress-sensing domain that is experimentally interchangeable[149]. Binding to BiP holds PERK in an inactive monomeric state. Upon ER stress, BiP dissociates allowing cytosolic domain of PERK to autophosphorylate and dimerize, which induces transphosphorylation of other PERK molecules, which promotes PERK oligomerization. Unlike IRE1, for which the only known substrate is itself, PERK phosphorylates

the α-subunit of eIF2 at Ser51. This phosphorylation causes attenuation of translation reducing the load of newly synthesised proteins, a second respond to protect cell against ER stress[123]. However, this attenuation of translation is not absolute; genes carrying certain regulatory sequences in their 5' untranslated regions (for example, an Internal Ribosomal Entry Site (IRES)) can bypass the eIF2α-dependent translational block[109]. The best characterised of these genes is ATF4 (Activating Transcription Factor 4), named GCN4 in yeast, a member of the bZIP family transcription factor which encodes a member of the cAMP response element-binding transcription factors (C/EBP). Thus, phosphorylated eIF2α increases the expression levels of ATF4 by bypassing the inhibitory upstream ORFs in ATF4 mRNA that orderly impair translation under resting conditions[101]. ATF4 increases the transcription of UPR target genes including CHOP (C/EBP Homologous Protein), GADD134 (Growth Arrest and DNA-Damage-Inducible Protein-34), ATF3 and genes encoding proteins involved in amino acid transport, glutathione biosynthesis and resistance to oxidative stress[116] (Figure 11).

Activation of PERK occurs in a reversible manner, allowing to the recovery from translation attenuation after ER stress, which could otherwise cause permanent damage to the cell. Several eIF2α phosphatases have been described, such as GADD134 and CReP (Constitutive Repressor of eIF2α Phosphorylation), which help to this recovery from translational attenuation. CReP is constitutively expressed and contributes to baseline eIF2α phosphorylation[150], whereas GADD134 is induced as part of the gene expression programme activated by ATF4 and acts as a negative feedback mechanism of eIF2α phosphorylation[151]. In addition, PERK is inhibited by binding of the HSP40 co-chaperone $p58^{IPK}$ to its kinase domain. $P58^{IPK}$ expression is induced by IRE1/XBP1 during ER stress[152] or by ATF6 during late phases of the UPR[153].

P58IPK, also known as DnaJC3, was identified originally in the cytosol as a repressor of the kinase activity of PKR (see pag. 38), which is activated posttranscriptionally by stress caused by viral infection[154]. Since the kinase domain of PKR is very similar to the kinase domain of PERK (about a 40%), it was investigated whether p58IPK was also involved in the regulation of PERK activity. It has been shown that p58IPK is induced during the UPR, interacts with PERK, attenuates PERK mediated eIF2α phosphorylation during ER stress, and negatively regulates selective translation of UPR target proteins such as BiP and CHOP[152]. Upregulation of p58IPK is not an immediate event, as its induction occurs only several hours after the phosphorylation of PERK and eIF2α. P58IPK contains a J-domain, found in a large class of co-chaperones, which function together with the Hsp70 family of chaperones. P58IPK was reported to reside also in the ER lumen, where it interacts with BiP in a J-domain-dependent manner and influences protein maturation efficiency[155]. So p58IPK helps to optimize protein folding homeostasis in the ER[156]. It was also determined that p58IPK contains a functional ER targeting signal consisting of 26 hydrophobic amino acids at the N-terminal part, implicating that p58IPK may enter the ER. It seems that slight inefficiencies in the translocation of p58IPK into the ER generate sufficient amounts of cytosolic p58IPK to inhibit PERK and PKR kinase activities. For this reason, up-regulation of p58IPK during the late phase of the UPR could possibly simultaneously improve ER folding capacity (via its abundant ER lumenal form), while mitigating translational attenuation by inhibition of PERK kinase activity in the cytosol[157].

The importance of PERK-initiated signals for protecting cells against ER stress has been documented in studies of PERK (-/-) cells and knock-in cells that express non-phosphorylatable eIF2 α (Ser51Ala), both of which are hypersensitive to ER stress[158]. It has been also seen that deletion of downstream components of PERK signalling, such as ATF4 and CHOP,

impaired or enhanced cell survival in response to protein misfolding depending on the cell type studied[159,160]. It is known that not all cell types are protected from ER stress by preventing eIF2α phosphorylation, indicating that PERK/eIF2α may have subtle cell type-specific roles in translational control. Thus, PERK besides of being involved in the UPR pathway is also essential for the normal function of highly secretory cells in the pancreas and skeletal system, as proved by the observation that PERK, ATF4 and CHOP-deficient animals are viable but have show defects in pancreatic function, metabolism, and skeletal development[161,162]. Like IRE1, PERK can also activate NFκB as a result of inhibition of IκB translation[163].

5.2.1. CHOP/GADD153 (CCAAT/enhancer-binding Protein Homologous Protein, Growth Arrest and DNA Damage-inducible Protein)

CHOP/GADD153, which is a member of the C/EBP family of bZIP transcription factors, was originally identified as part of the response to the DNA damage. But it also plays an important role in ER stress-induced apoptosis because CHOP (-/-) mice exhibit reduced apoptosis in response to ER stress[164]. During ER stress, all three arms of the UPR induce transcription of CHOP, as the CHOP gene promoter contains binding sites for ATF4, ATF6 and XBP1, and various studies have prove its activation[165-167]. However, to upregulate CHOP protein expression the PERK-eIF2α-ATF4 branch is essential. The IRE-1-Ask1-p38 MAPK pathway may also enhance CHOP activity at a posttranscriptional level[168]. So during prolonged stress, the PERK and IRE1 pathways might converge on CHOP activation. Although it is clearly important for ER stress-induced apoptosis in different conditions, it seems that CHOP is not uniformly essential for cell death induced by ER stress, as demonstrated by the observation that PERK (-/-) and eIF2α (Ser51Ala) knock-in-cells are hypersensitive to ER stress-induced apoptosis but fail to induce CHOP gene expression[169]. Although the precise

mechanism by which CHOP mediates apoptosis is unknown, it activates the transcription of several genes that may potentiate apoptosis, including CA6 (Carbonic Anhydrase VI)[170], ERO1α, DR5 (Death Receptor 5), GADD134, TRB3 (Tribbles Related Protein 3) and Bcl-2. Although CHOP mainly induces gene expression, Bcl-2 is an example of a gene that is downregulated by CHOP.

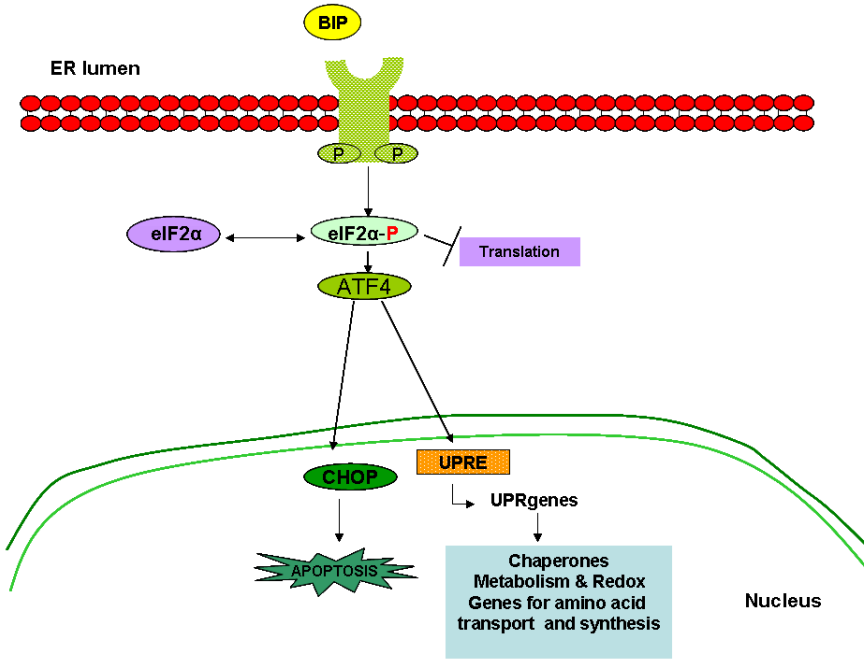

Figure 11. PERK pathway. PERK is activated by dimerization and autophosphorylation following the release of BiP. Once activated, it phosphorylates eIF2α, resulting in translation attenuation. Phosphorylated eIF2α selectively enhances translation of the ATF4 transcription factor. ATF4 translocates to the nucleus, where it activates UPR target genes, including CHOP, which induces apoptosis.

5.3. ATF6 (Activating Transcription Factor 6)

ATF6 is a type II transmembrane protein with a cytosolic domain containing a bZIP motif, a transcription activation domain (TAD) and an ER luminal domain that binds BiP[171]. In mammals two homologous proteins exist, ATF6α and ATF6β, which have quite ubiquitous tissue distribution (Figure 8). ER stress triggers a different mechanism of protein activation for ATF6 proteins compared with PERK and IRE1. Under conditions of ER stress, ATF6α (90 kDa) dissociates from BiP, which uncovers Golgi localization signals present in the transcription factor. Then, ATF6α is transported from the ER to the Golgi apparatus, where it is cleaved by Golgi-resident proteases, first by S1P (Site 1 Protease) and then in an intramembrane region by S2P (Site 2 Protease) to release the cytosolic DNA-binding portion ATF6 fragment (ATF6f) of about 50 kDa, which goes to the nucleus to activate the transcription of target genes[172]. ATF6α stimulates ER genes either as a homodimer or upon heterodimerization with another bZIP transcription factor, such as XBP1. ATF6α induces genes containing an ATF/cAMP Response Element (CRE) or with an ERSE in their promoter, which include ER chaperone proteins such as BiP, GRP94, PDI, CHOP, XBP1 and p58^{IPK}, among others[173] (Figure 12). Binding of ATF6 to the ERSE requires the presence of an additional transcription factor called Nuclear Factor-Y (NF-Y)[174]. ATF6β processing is also activated by ER stress and shows strong similarity to ATF6α in the bZIP domain, conferring similar DNA-binding specificity[175]. But at variance with what happens with ATF6α, ATF6β seems to play a secondary role in the UPR[176]. ATF6β has considerably weaker transcriptional activity compared to ATF6α, which raises the possibility of ATF6β having a dominant-negative role on ATF6α. However, studies in ATF6α and ATF6β knockout cells have not demonstrated such antagonism[177]. Mice that lack either ATF6α or ATF6β develop and grow

normally, and display no obvious gross abnormality; however deletion of both ATF6 genes causes embryonic lethality[178].

Recently it has been found newly identified ATF6 homologs that are modulated by ER stress in specific tissues. All of these ATF6-related bZIP factors are processed at the Golgi in a similar way as ATF6[102]. These include BBF2H7 (also known as CREB3L2), Cyclin AMP Responsive Element Binding Protein 4 (CREB4), CREB H, Luman (also known as CREB3) and Oasis (also known as CREBL1). Oasis protein, for example, is expressed in astrocytes[179] and CREB H is expressed exclusively in liver[180]. The role of these proteins in the UPR is poorly characterised and mores studies are required.

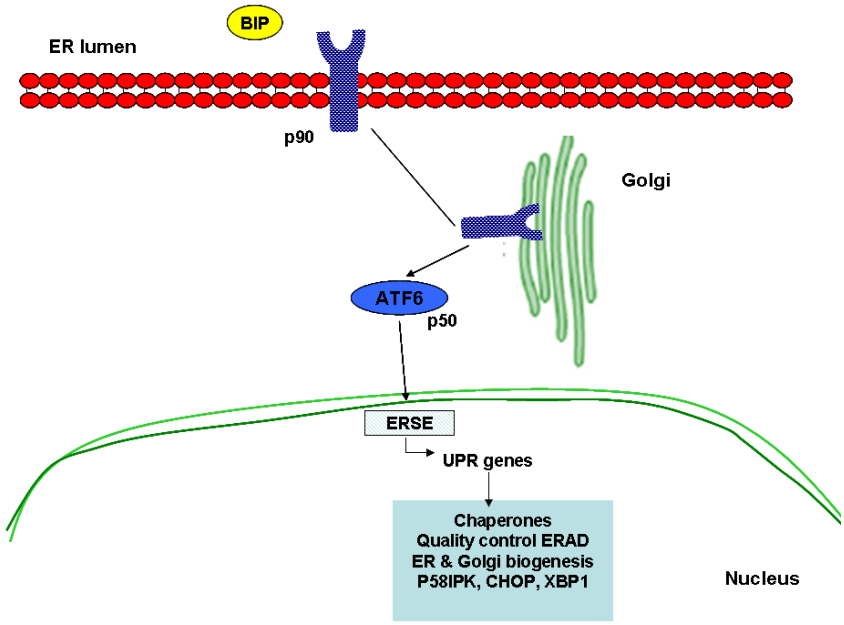

Figure 12. ATF6 pathway. The release of BiP exposes a Golgi-localization sequence within ATF6, targeting the molecule to the Golgi. In the Golgi, ATF6 is sequentially cleaved by the S1P/S2P proteases. This releases the ATF6 fragment (ATF6f) transcription factor, which translocates to the nucleus, binds to ER-Stress Response Elements (ERSEs) and induces transcription of target genes.

5.4. Similarities and differences between the arms of the UPR

Although IRE1, PERK and ATF6 activation proceeds independently in ER-stressed cells, it is well known that the three axes of the UPR form a coordinate response. One example is the crosstalk between ATF6 and IRE1 pathways, as demonstrated with ATF6 which binds to ERSEs and induces transcription of target genes such as BiP and XBP1. It is also known that XBP1u is a negative feedback regulator specific to the ATF6 and IRE1 pathways. In addition to this, XBP1 and ATF6 present strong similarities in their target DNA sequences[171]. Another crosstalk between the different UPR arms is observed in the case of $p58^{IPK}$, which is induced by IRE1/XBP1 or by ATF6 and negatively regulates PERK activity.

Upon ER stress, all three arms of the UPR are activated but the behaviour of each arm depends on the timing after the beginning of the stress. The different time courses of the individual UPR arms influence the cell's ultimate fate. The UPR can induce cytoprotective functions that re-establish homeostasis or cell destructive functions that promote apoptosis. IRE1, PERK and ATF6 activation result in cytoprotective outputs such as reduced translation, enhanced ER protein folding capacity and clearance of misfolded ER proteins. But if these steps fail to re-establish homeostasis, IRE1 signalling and lately ATF6 signalling are attenuated. In contrast, PERK signalling persisted much longer in the presence of prolonged ER stress [181,182] (Figure 13).

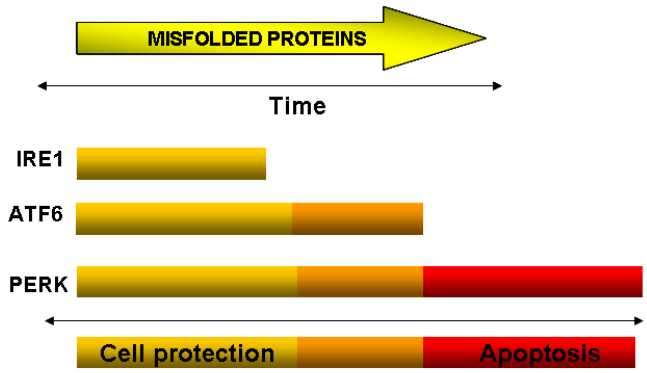

Figure 13. Different time courses of the arms of UPR. Accumulation of misfolded proteins triggers both cell protective and cell death responses, but with different time courses. Under prolonged stress, IRE1 and lately ATF6 responses are attenuated, but PERK response persists (Adapted from Lin *et al.*, 2007[181]).

.

6. ER and apoptosis

All three UPR pathways contribute to induce apoptosis when the cell protective changes mediated by the UPR fail to restore folding capacity. CHOP, the Bcl-2 family of proteins, the JNK kinase cascade and the Caspases are candidates to contribute to mediate apoptotic signalling in response to ER stress (Figure 14).

6.1. Caspases

In mice, Caspase-12 was the first to be characterised as a key mediator of ER stress-induced apoptosis[183]. Procaspase-12 is localized on the cytoplasmic side of the ER and upon ER stress is cleaved and activated. Procaspase-12 is activated by Calpains, a family of Ca^{+2}-dependent cysteine proteases. Once it is activated, Caspase-12 cleaves Procaspase-9 leading to the activation of effector Caspases such as Caspase-3. However, the role of Caspase-12 in human cells is not clear, since the gene has been silenced by several mutations[184]. Caspase-4 has been proposed to perform the function of Caspase-12 in humans, but this has not been fully demonstrated. In addition to this, Caspase-7, which upon ER stress translocates from the cytosol to the cytoplasmic side of the ER membrane, has been reported to interact with Caspase-12 leading to its activation[185].

6.2. CHOP and Bcl-2 family of proteins

CHOP expression increases ROS, which likely contributes to ER stress-associated cell death[186]. CHOP upregulates ERO1α expression, a thiol oxidase that mediates disulfide bond formation to promote folding in the ER, but this action also generates ROS. On the other hand, CHOP downregulates the expression of the anti-apoptotic protein Bcl-2[187] and upregulates the BH3-only protein Bim[188].

Several studies have shown that the Bcl-2 family proteins have a role in mediating ER stress-induced apoptosis. Cells derived from Bax and Bak double knockout mice are resistant to proapoptotic agents that induce the UPR response[189] and have a similar phenotype to the IRE1α-deficient cells. Two pathways have been proposed by which Bax and Bak may promote apoptosis in response to ER stress[190]. During ER stress, Bax and Bak undergo conformational changes and oligomerization in the ER membrane, which cause the release of Ca^{2+} from the ER stores to the cytoplasm. The increase in Ca^{2+} concentration in the cytosol activates Calpains, which cleave and activate Procaspase-12. The second pathway involves cytosolic Ca^{2+} being taken up by mitochondria, causing depolarization of mitochondrial inner membrane and Cytochrome c release which leads to apoptosis. Interestingly, Bax and Bak also bind to the cytosolic domain of IRE1 and are required for efficient splicing of XBP1 mRNA during ER stress[191]. Thus, Bax and Bak function at the ER membrane to activate IRE1 signalling and to provide a physical link between members of the core apoptotic pathway and the UPR.

The signalling events that connect ER stress with the mitochondrial apoptotic machinery are still unclear. Recently, it has found that the BH3-only protein Bid may be involved in the crosstalk between these two organelles, although is not the only protein involved, since Bid (-/-) cells are not completely resistant to ER stress-induced apoptosis. Moreover, it has been identified Caspase-2 as the premitochondrial protease that cleaves Bid in response to ER stress[192]. However, it is still not clear how Caspase-2 is activated by ER stress or if it is downstream of one or more of the three stress pathways of the UPR. The BH3-only protein Bim[188], PUMA (P53 Upregulated Modulator of Apoptosis) and NOXA (Neutrophil NADPH Oxidase Factor)[193], have been proposed as being candidates in the ER stress machinery. However, although both PUMA and NOXA play a role in the

ER stress-induced apoptosis, a direct molecular relationship linking them to components of the UPR has yet to be identified[194].

6.3. JNK kinase cascade

As it is shown before, JNK is activated by the IRE1-TRAF2-ASK1 branch of the UPR. JNK is a proapoptotic kinase that targets several Bcl-2 family proteins and modulates their activity via phosphorylation. For instance, it has seen that it can phosphorylate Bcl-2[195] and the BH3-only protein Bim[188]. It has also been demonstrated that TRAF2 plays an essential role in the activation of Caspase-12. In unstressed cells, TRAF2 formed a stable complex with Procaspase-12. The stimuli that induce ER stress led to the dissociation of Procaspase-12 from TRAF2, and simultaneously dimerization of Procaspase-12 was promoted[196].

.

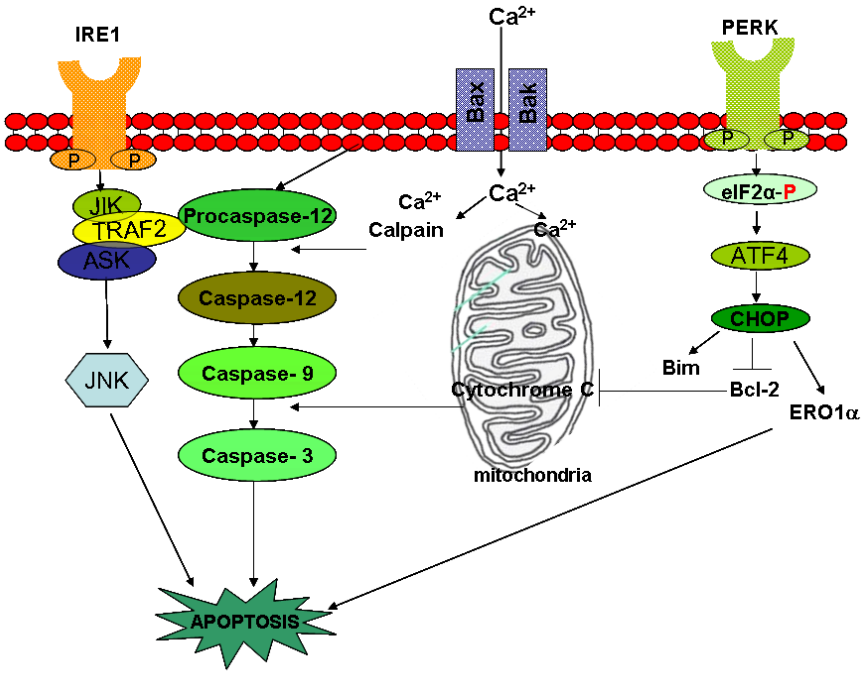

Figure 14. Mechanisms of induction of apoptosis by ER stress. IRE1/TRAF2/ASK activate JNK signalling that induces apoptosis. The recruitment of TRAF2 to IRE1 permits TRAF2 to dissociate from Procaspase-12, allowing to its activation. During ER stress, Bax and Bak in the ER membrane oligomerize and allow the release of Ca^{2+} from the ER to the cytosol, which activates Calpains. The direct activation of Caspase-12 by Calpains activates the Caspase-9, Caspase-3 cascade. In addition, Ca^{2+} released from the ER is taken up by the mitochondria, causing the release of Cytochrome c. Activation of CHOP by the PERK pathway leads to the upregulation of pro-apoptotic and downregulation of anti-apoptotic Bcl-2 family proteins. CHOP also induces ERO1α, which induces apoptosis.

7. Cyclin-dependent kinases and Cyclins

The Cyclin-dependent kinases (Cdks) are a family of serine/threonine protein kinases that share a high degree of homology at the amino acid level (40%) and have a similar size (~ 35-40 kDa). The members of the Cdk family have been implicated in the control of cell-cycle progression, transcription and neuronal function. For example, Cdk1, 2, 4 and 6 are directly involved in cell-cycle control. Cdk7, 8 and 9 are components of the machinery that controls basal gene transcription by RNA polymerase II[197] and Cdk5 controls the differentiation of nerve cells[198]. Based on sequence similarity, the human genome contains 21 genes encoding Cdks and five additional genes encoding a more distant group of proteins known as Cdk-like (CdkL) kinases. According to the current nomenclature for Cdk proteins, there are 11 classical Cdks (Cdk1-11), two newly proposed family members (Cdk12 and 13) and additional proteins whose names are based on the presence of a cyclin-binding element (PFTAIRE and PCTAIRE proteins) or simply based on sequence relationship with the original Cdks, such as CDC2-like kinases (CDC2L) or cell cycle-related kinases (CCRK). The HUGO Gene Nomenclature Committee (HGNC) and the Mouse Genomic Nomenclature Committee (MGNC) agreed on putting the "CDK" prefix in all the 21 human Cdks[199].

Cdks are activated by binding to Cyclin proteins and by phosphorylation/dephosphorylation and are inactivated also by phosphorylation/dephosphorylation and binding to specific inhibitors (Figure 15)[197]. Two families of Cdks Kinase Inhibitors (CKIs) have been described: the INK4 family ($p16^{INK4a}$, $p15^{INK4b}$, $p18^{INK4c}$, $p19^{INK4d}$), and the Cip/Kip family ($p21^{Cip1}$, $p27^{Kip1}$, $p57^{Kip2}$)[200]. INK4 proteins specifically bind to and inhibit monomeric Cdk4 and Cdk6 proteins. Cip and Kip proteins, by contrast, bind to all Cdk-Cyclin complexes[201]. On the other hand, active Cdk-Cyclin complexes need to be phosphorylated in the T-loop of the Cdk

subunit by the Cdk-Activating Kinase (CAK) (Threonine 160 in the case of Cdk2). CAK is responsible for the activating phosphorylation of Cdk1, Cdk2, Cdk4 and Cdk6. CAK is composed of three subunits: Cdk7, Cyclin H and MAT1 (Ménage A Trois)[202]. In contrast, Wee1 and Myt1 kinases inhibit the kinase activity of Cdk-Cyclin complexes by phosphorylating adjacent tyrosine and threonine residues (Tyrosine 15 and Theonine 14) in the Cdk subunit, whereas Cdc25 phosphatases (Cdc25A, Cdc25B and Cdc25C) activate these kinases by dephosphorylating the same amino acid residues[197].

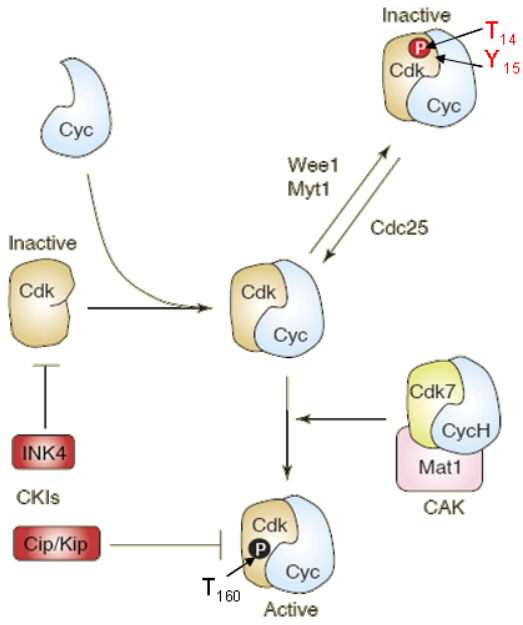

Figure 15. Mechanism of Cdk regulation. Cdks are regulated at different levels. Cdks bind to their activating subunit, the Cyclins. Cdk Kinase Inhibitors (CKIs) block their kinase activity: INK4 proteins bind to Cdks, while Cip/Kip proteins bind to the Cdk-Cyclin complexes. To become active, Cdk-Cyclin complexes have to be phosphorylated in the T-loop of the Cdk subunit by the CAK (Theonine 160 in the case of Cdk2). Myt1 and Wee1 kinases inhibit the kinase activity of Cdk-Cyclin complexes by phosphorylating respectively Theonine 14 and Tyrosine 15 in the Cdk subunit, whereas Cdc25 phosphatases activate the kinases by dephosphorylating the same amino acid residues (Adapted from Malumbres *et al.*, 2005[197]).

Cyclins (Cyclin Box containing proteins) were named because of the cyclic regulation of the founder members of the family (Cyclin B and Cyclin A) which oscilated in a cyclic fashion during the cell cycle. They are synthesised and degraded as needed in order to drive the cell through the different stages of the cell cycle. The Cyclin Box domain is responsible for binding to Cdks. Although the best characterised Cdk/Cyclin complexes are involved in cell-cycle regulation, Cdk/Cyclin complexes are involved in other functions including neuronal development, regulation of transcription or DNA damage repair[203]. For example, Cdk8-Cyclin E, Cdk9-Cyclin T and Cdk9-Cyclin K complexes have a role in transcriptional regulation[204-206]. G-type Cyclins (G1 and G2) are targets of p53 and seem to be involved in the ATM-p53-Mdm2 pathway[207]. Cyclin S seems to be involved in transcriptional changes related to the duration of memory in neurons[208]. Recently, analysis of the human genome has identified at least 29 genes encoding related proteins that contain a Cyclin Box. Not all the Cyclins show cyclic variations in their abundance[197].

In mammals there are several cell cycle related Cdks and Cyclins, each one associated with a specific function during cell cycle progression (Figure 16). Cyclin Ds, which are the first Cyclins produced in the cell cycle in response to extracellular signals such as growth factors, associate with Cdk4 and Cdk6. Cdk4-Cyclin Ds and Cdk6-Cyclin Ds regulate the Go-G1 transition (in quiescent cells) and the early phases of G1 (in proliferating cells) by phosphorylating the retinoblastoma protein (pRb). PRb dissociates from the E2F/DP1/Rb complex, activating E2F. Activation of E2F results in transcription of various genes like Cyclin E, Cyclin A, DNA polymerase, thymidine kinase, among others. The Cdk2-Cyclin E complex promotes the G1-S transition[209]. Then, Cdk2 associates with Cyclin A driving progression through S phase. Finally, Cdk1 participates in the S-G2 and G2-M transitions by sequential binding to Cyclin A and Cyclin B[210]. Cdk1-Cyclin B complex

activation causes breakdown of nuclear envelope by phosphorylating nuclear Lamins[211], initiation of prophase and subsequently, its deactivation causes the cell to exit mitosis.

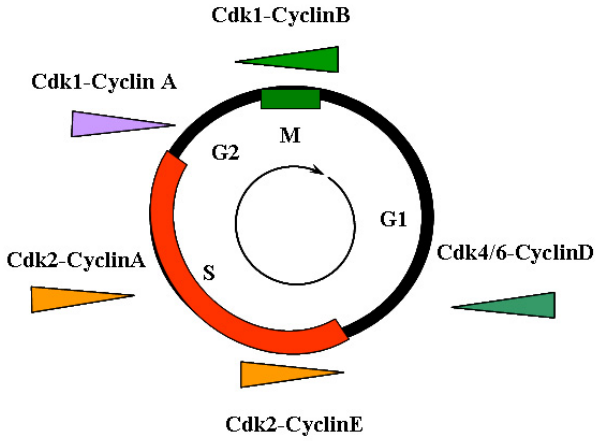

Figure 16. Cell cycle regulation by Cyclin-dependent kinases (Cdks). Cyclin Ds associated with Cdk4 and Cdk6 regulate G1-phase progression. Entry into S-phase is regulated by Cdk2-Cyclin E complex and S and G2-phase progression by Cdk2-Cyclin A and Cdk1-Cyclin A complexes. Finally, mitosis is regulated by Cdk1-Cyclin B complex.

8. Cell cycle and apoptosis

The connection between cell cycle and apoptosis is not well defined, due to the lack of genetic evidence. The data which suggest the link between cell cycle and apoptosis comes from unscheduled overexpression of otherwise normal components of the cell cycle[212] or expression of cell cycle regulators in arrested cells in the presence of mitogens to force the cell to re-enter proliferation[213]. Most of these experiments have been performed in proliferating cell lines, which makes difficult to separate the activation of a given cell cycle regulator acting in apoptosis from its normal role in cell cycle. A good model to study the relationships between apoptosis and cell cycle are thymocytes, since 90 % of these cells are quiescent and they do not progress through the cell cycle *in vitro*[214]. In thymocytes, activation of Cdk2 has been shown to take place during antigen-mediated negative selection[215] and during dexamethasone or γ-radiation induced apoptosis[216]. Its relevance has been proven by the fact that chemical inhibition of Cdk2 completely blocks apoptosis[216,217].

We and others have demonstrated that overexpression of the proteins Bax and Bcl-2 in T cells of transgenic mice leads to perturbations in the dividing population of thymocytes. The effect of the *bax* transgene is to increase the number of cycling thymocytes whereas the *bcl-2* transgene has the opposite effect. Given these data, we examined whether Bax and Bcl-2 could modulate Cdk2 activity during thymocyte apoptosis. We demonstrated a linear relationship between $p27^{Kip1}$ degradation, Cdk2 activation and thymocyte apoptosis which is modulated by p53, Bax and Bcl-2. These results show that Cdk2 activation during apoptosis is a highly regulated process under the control of known apoptosis regulators such as Bax and Bcl-2[216]. Our laboratory has also proven that the activation of Cdk2 is a very early step that precedes both the loss of plasma membrane asymmetry and the activation of apical Caspases[217]. This implies that Cdk2 activation must

be upstream of the translocation of the Bcl-2 family members Bax and Bid to the mitochondria and the loss of mitochondrial function that finally results in the release of Cytochrome c into the cytoplasm. We also demonstrated that downstream of Cdk2 activation it is necessary gene transcription to trigger apoptosis[217].

Cdk2 activation needs *de novo* transcription and translation, since both cycloheximide and actinomycin D abolish the increase in Cdk2 activity and can block thymocyte apoptosis in response to both dexamethasone and γ-irradiation. Since Cdk2 activation is not mediated by the canonical Cyclins, Cyclins E and A, which regulate it during cell-cycle progression, our group proposed that it might be mediated by an unknown Apoptosis Related Cdk2 Activator (ARCA). Using *in silico* analysis of the human genome we identified several non-characterised Cyclin-like proteins, from which preliminary results encouraged us to further characterise one of them, located in human chromosome 5 and in mouse chromosome 13, named Cyclin O.

9. Cyclin O

During the last years our group has been studying this novel Cyclin. We have demonstrated that Cyclin O is able to bind and activate Cdk2 in response to intrinsic apoptotic stimuli such as glucocorticoids or DNA damaging agents (Figure 17). We have also observed that the *de novo* synthesis of Cyclin O precedes apoptosis induction. Finally, downregulation of the expression of Cyclin O abrogates DNA damage and glucocorticoid-induced apoptosis, whereas CD95-induced apoptosis (extrinsic pathway) remains intact[218]. This lack of apoptotic response after Cyclin O downregulation is due to a failure in the activation of apical Caspases and is not a consequence of defective signalling in the DNA damage or glucocorticoid pathways. Then, Cyclin O is the most likely candidate to be the ARCA.

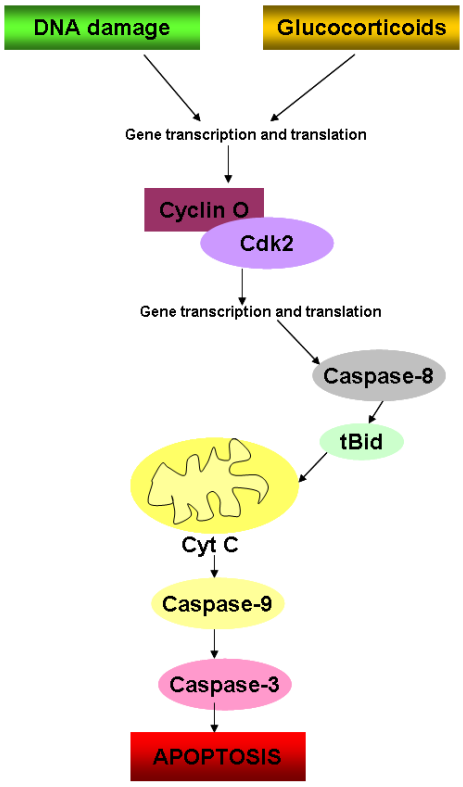

Figure 17. Positioning of Cyclin O in the intrinsic apoptotic pathway. Upon cell treatment with glucocorticoids or DNA damaging agents, Cyclin O is synthesised, binds and activates Cdk2. Activated Cdk2 activates the apical Caspase-8 that cleaves its target, Bid. Then, loss of the plasma membrane asymmetry and activation of apical Caspases take place.

Cyclin O locus encodes four transcripts that arise from the use of two alternative promoters and alternative splicing: Cyclin Oα, Cyclin Oβ, Cyclin Oε and Cyclin Oδ/γ. In the first part of this thesis, we focused on the characterization of Cyclin Oα and the alternatively spliced product Cyclin Oβ. We demonstrated that both Cyclin Oα and Cyclin Oβ are expressed at least at the mRNA level in human and mouse cells[218]. The aim of this thesis is to further characterise the function of Cyclin Oα and Cyclin Oβ. We aim to determine whether both isoforms share the same function and to further characterise their signalling mechanism.

9.1. Structure of Cyclin O

Human Cyclin Oα has 350 amino acids and is encoded by a highly conserved gene present in all the vertebrate genomes sequenced until now. The protein is composed by a highly conserved C-terminal Cyclin Box, sharing about 28% of homology with human Cyclins A2 and B1, and a less conserved N-terminal part composed by the first 100 amino acids (Figure 18). This N-terminal part is rich in basic amino acids and contains several conserved putative regulatory motifs, suggesting a regulatory role. These putative regulatory motifs include an NLS (Nuclear Localization Signal), a Cy motif, motif present in Cdk substrate proteins[219], a GSK3β (Glycogen Synthase Kinase-3) phosphorylation site, a β-Trcp (Beta-Transducin repeats-containing protein) interacting motif, involved in the degradation of the target proteins through the proteasome, an LxxLxL motif that resembles a NES (Nuclear Export Signal) and several putative Cdk and MAPK phosphorylation sites. The Cyclin O 3D structure was modelled by homology with Cyclin A[220,221] in collaboration with the groups of Dr. Baldomero Oliva (UPF, Barcelona) and Dr. Jordi Villà (UPF, Barcelona). The Cyclin Box of Cyclin O is composed by one N-terminal α-helix and two repeats of five α-helixes (N-terminal and C-terminal repeats). Some conserved putative regulatory motifs are found inside the Cyclin Box, such as the LxxLL motif and a second putative NES. The LxxLL motif has been implicated in the binding of Cyclin D1 to SRC-1 (Steroid Receptor Coactivator-1)[222].

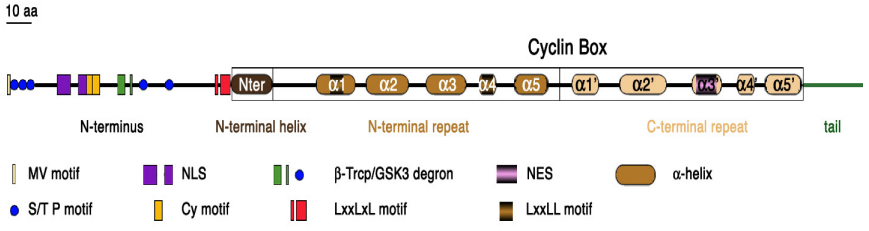

Figure 18. Structure of Cyclin O. Scheme of Cyclin O where are represented the different motifs of the N-terminal part and the Cyclin box.

OBJECTIVES

Our group has characterised a novel cyclin called Cyclin O as the "Apoptotic Related Cdk2 Activator" required for the intrinsic apoptotic pathway in lymphoid cells.

Our **first objective** was to study the expression pattern of the alpha and beta isoforms, their subcellular localization and the putative regulatory motifs of the N-terminal part of this protein.

Our **second objective** was to study the nature of the Cyclin O aggregates that appear in the cytoplasm, which we hypothesize to correspond to Stress Granules.

Our **third objective** was to determine if Cyclin O is involved in the translational response to stress pathways and study the participation of Cyclin Oα and Cyclin Oβ in the ER stress pathway.

MATERIALS AND METHODS

1. Anti-Cyclin O antibodies

The N1 and C2 antibodies were generated previously in our laboratory and described in Roig *et al.*[218]. Two new antibodies against Cyclin Oα and Cyclin Oβ were generated in rabbits using peptides as antigens. The sequences of the peptides and their localization are summarized in Figure 1A. The peptides H-ESRSKLLSWLIPVHRQFGLSC-NH2 (alpha1) and H-SLARQPQVEVHPPRC-NH2 (beta1) were coupled with 3-maleimidobenzoic acid N-hydroxysuccinimide ester (MBS, Sigma-Aldrich) to Keyhole Lympet Haemocyanine (KLH). The alpha1 peptide is located in the sequence encoded by exon 2 of the gene, not present in the beta isoform. In contrast, the beta1 peptide is encoded by the junction between exon 1 and exon 3 of the gene, and we expected that the antiserum specifically recognized the sequence of the exon 1-exon 3 junction, the only sequence in the beta isoform not present in the alpha isoform (Figure 1A). Peptides were synthesised by Dr. David Andreu (Grup de Recerca en Proteòmica i Química de Proteïnes, UPF). New Zealand Rabbits were used for immunisation and were kept at the animal facility of the Facultat de Farmàcia, Universitat de Barcelona.

The α1 and β1 sera were affinity purified using the corresponding peptide bound to an EAH-sepharose 4B column according to the manufacturer (GE Healthcare). In all the cases, the production of the specific antibody in the different batches of sera was confirmed and titrated by ELISA, affinity purified using antigen columns and, finally, the titres adjusted with PBS containing Bovine Serum Albumin (BSA) (Sigma-Aldrich) to a final concentration of 1mg/ml. Affinity purified antibodies were aliquoted and kept at -20 ºC until use. In order to rule out crossreactivity with Cyclin Oα protein, the β1 serum was run through a column containing GST-Cyclin Oα-bound to sepharose beads. The flowthrough fraction was then passed

through a β1 peptide column and eluted as described. The specificity of the affinity-purified antibodies was determined by several independent tests, such as Western Blotting (Figure 1B) or immunofluorescence (Figure 1C).

2. ELISA

Antigens used to coat the ELISA plates were crosslinked to the carrier ovoalbumin (OVA) using glutaraldehyde. 96-well Maxisorp microtiter plates (Nunclon) were coated with peptide-OVA conjugates at a concentration of 20 μg/ml. Reactive sites were blocked with 1% gelatine for 30 minutes. For competitive ELISA, affinity purified antibodies were pre-incubated with peptides α1 and β1, at a final concentration of 300 μg/ml for 1h at room temperature (RT). Blocked antibodies (or purified antibodies, in the case of antibody titration) were then serially diluted in PBS containing 1% BSA and incubated for 1 hour at 37 ºC in the antigen-coated wells. After washing three times with PBS-Tween 0.1%, alkaline phosphatase-conjugated swine anti-rabbit immunoglobulins (DAKO) were added and then plates were incubated for 1 hour at 37 ºC. Reactions were developed using 4-methylumbelliferyl-phosphate disodium salt (Sigma-Aldrich) at 1mg/ml diluted in 1M triethanolamine pH 9.5 for 30 minutes at RT, and fluorescence was determined using an Infinite M200 fluorimeter (TECAN).

3. Specificity of the antibodies Cyclin Oα and Cyclin β

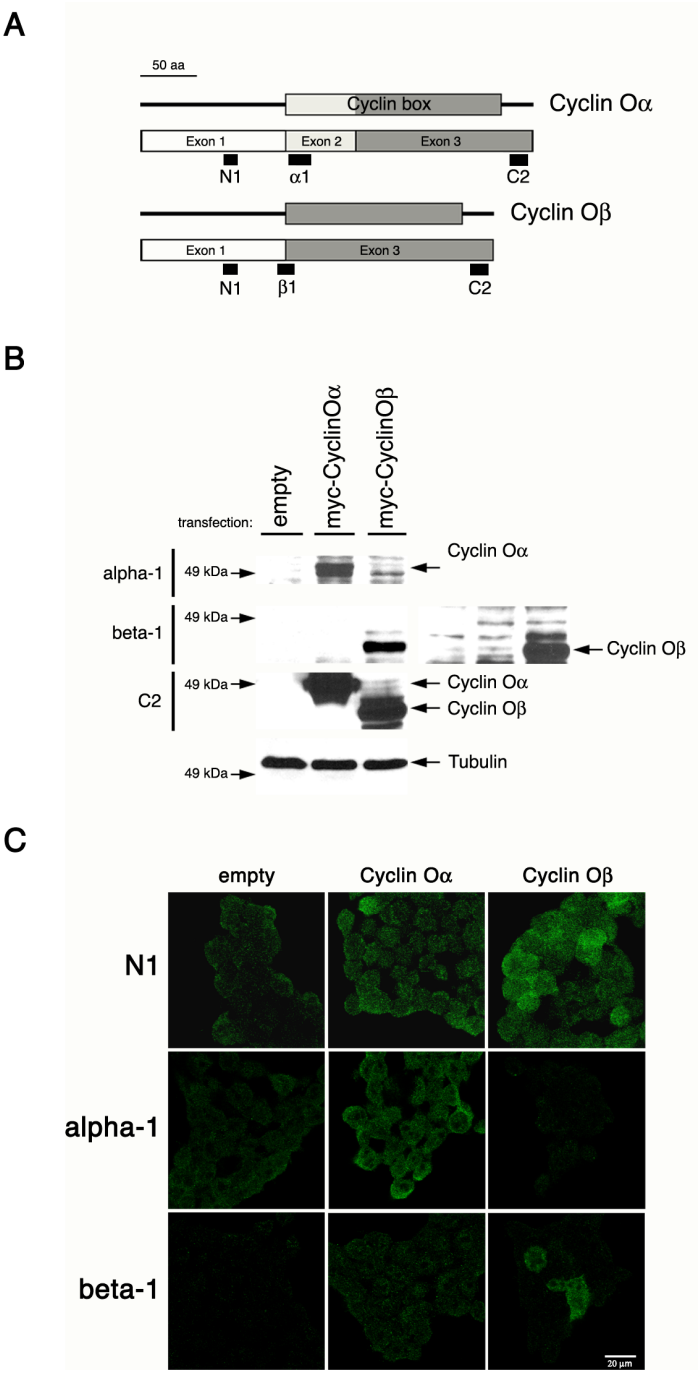

Figure 1. Characterization of anti-Cyclin Oα and β specific antibodies.(A) Location of the peptides used to rise anti-Cyclin Oα plus β serum (N1 and C2, Roig *et al.* 2009[218]), anti-Cyclin Oα (α1) and anti-Cyclin Oβ (β1) sera. The black boxes indicate the position of the peptides in the protein. The structure of the Cyclin Oα and β proteins is represented in the upper diagrams, while the exons encoding them are depicted in the lower diagrams. The light and dark grey boxes (encoded by exon 2 and part of exon 3) indicate the Cyclin Box, which is incomplete in the case of Cyclin Oβ. **(B)** Cellular extracts from HEK-293T cells transfected with empty vector or expression vectors for myc-tagged Cyclins Oα or β were analysed by Western Blotting using the anti-Cyclin O C2 antibody and the isoform specific alpha-1 and beta-1 antibodies. The membrane was reprobed with anti-Tubulin antibodies as a loading control. In the case of the beta1 antibody, the film was overexposed to rule out crossreactivity with Cyclin Oα protein (right panel).**(C)** HEK-293T cells transfected with empty vector or expression vectors for myc-tagged Cyclins Oα or β were analysed by immunofluorescence and confocal microscopy using the anti-Cyclin O N1 antibody and the isoform specific alpha-1 and beta-1 antibodies.

4. Other antibodies

Protein	Antibody	Source	Supplier	Technique used
Anti-Phosphoserine/ threonine	612548	Mouse monoclonal	BD Transduction Laboratories	WB
ATF6-α	H-280	Rabbit polyclonal	Santa Cruz	WB
α-Tubulin	clone DM1A	Mouse monoclonal	Sigma-Aldrich	WB
Calreticulin	F5	Mouse monoclonal	Santa Cruz	WB, IF
Cdc2 p34 (Cdk1)	Clone 17	Mouse monoclonal	Santa Cruz	WB
Cdk2	M2	Rabbit polyclonal	Santa Cruz	WB
DNAJC3 ($p58^{IPK}$)	Ab728885	Rabbit polyclonal	Abcam	WB, IF
eIF2α	FL-135	Rabbit polyclonal	Santa Cruz	WB
GADD153 (CHOP)	F-168	Rabbit polyclonal	Santa Cruz	WB
GFP		Mouse monoclonal	Clontech	WB
GM130		Mouse monoclonal	Kind gift of V.Malhotra (CRG)	IF
GRP78/BiP	N-20	Goat polyclonal	Santa Cruz	WB, IF
GST		Mouse monoclonal	Kind gift of J.Ayte (UPF)	WB
HA-Tag	3F10	Mouse monoclonal	Roche	WB
Histone H3	Ab1791	Rabbit polyclonal	Abcam	WB
HRI	07-728	Rabbit polyclonal	Millipore	IF
Myc-Tag	9E10	Mouse monoclonal	Hybridoma from ATCC	WB, IF
PhosphoSer51-eIF2α	9721	Rabbit polyclonal	Cell Signal	WB
PhosphoThr981-PERK	32577	Rabbit polyclonal	Santa Cruz	WB
PERK	H-300	Rabbit polyclonal	Santa Cruz	WB, IF
PKR	Ab47509	Rabbit polyclonal	Abcam	IF
Piruvate kinase		Goat polyclonal	Chemicon	WB
Ribosomal Protein S6	E-13	Goat polyclonal	Santa Cruz	IF
TIA-1	C-20	Goat polyclonal	Santa Cruz	IF
Tom 20	FL-145	Rabbit polyclonal	Santa Cruz	IF
Vimentin	V4630	Goat polyclonal	Sigma-Aldrich	WB

Table 1. Primary Antibodies used.

Antibody	Supplier	Technique used
Cy™ 3-conjugated AffiniPure Bovine Anti-Goat IgG (H+L)	Jackson ImmunoReserach	IF
Cy™ 3-conjugated AffiniPure Donkey Anti-Rabbit IgG (H+L)	Jackson ImmunoReserach	IF
Cy™ 2-conjugated AffiniPure Donkey Anti-Rabbit IgG (H+L)	Jackson ImmunoReserach	IF
Fluorescein Streptavidin (FITC)	Vector Laboratories IHC	IF
Alexa Fluor® 555 goat Anti-mouse IgG (H+L)	Invitrogen	IF
Alexa Fluor® 488 donkey Anti-goat IgG (H+L)	Invitrogen	IF
Alexa Fluor® 647 donkey Anti-rabbit IgG (H+L)	Invitrogen	IF
EnVision™ Anti-rabbit	DAKO	IHC
Alkaline phosphatase-conjugated swine Anti-rabbit immunoglobulins	DAKO	ELISA
Polyclonal Rabbit Anti-mouse Immunoglobulins/HRP	DAKO	WB
Polyclonal Goat Anti-rabbit Immunoglobulins/HRP	DAKO	WB
Polyclonal Rabbit Anti-goat Immunoglobulins/HRP	DAKO	WB
Peroxidase-conjugated IgG Fraction Monoclonal Mouse Anti-Rabbit IgG, Ligh Chain Specific	Jackson ImmunoReserach	WB

Table 2. Secondary antibodies used.

5. Semiquantitave and quantitative RT-PCR

RNA was obtained using Trizol reagent (Invitrogen) following the manufacturer instructions.

RT-PCR reactions were done using SuperScript III One-Step RT-PCR with Platinum Taq (Invitrogen) using 1 μg of RNA per reaction and the PCR conditions described in Table 3.

Quantitative RT-PCR (qRT-PCR) was performed using QuantiTect Sybr Green reagent (Qiagen) using 1 μg, 500 ng or 100 ng of RNA/reaction (in mouse tissues, WEHI7.2 cells or Mouse Embryonic Fibroblasts (MEFs) cells, respectively) in a final volume of 10 μl. Samples were analysed in triplicate and the data was analysed using SDS2.1 software (Applied Biosystems). PCR cycles are described in Table 3. All qRT-PCR experiments were performed using RNA from at least three independent experiments and until reaching statistical significance.

Semiquantitative RT-PCR			**Quantitative RT-PCR**		
50ºC	30 min		50ºC	30 min	
94ºC	2 min		95ºC	15 min	
94ºC	15 sec		95ºC	15 sec	
55ºC	30 sec	40 cycles*	55ºC	30 sec	40 cycles
68ºC	1min		72ºC	30 sec	
68ºC	5 min		72ºC	10 min	

Table 3. RT-PCR conditions. *40 cycles for mCyclin Oα, mCyclin Oβ and XBP1 detection. For HPRT and exogenous Cyclin (eCyclin O) only 30 cycles were used.

Technique	mRNA	Oligo 1	Oligo 2
RT-PCR	mCyclin Oα	5'-CGCTTGCAAGCAGGTAGAGG -3'	5'-CTACCTCGTGAGGACTTCG-3'
RT-PCR	mCyclin Oβ	5'- CGCGCCAGCCACAAGTAGAGG-3'	5'- CTACCTCGTGATGGACTTCG-3'
RT-PCR	HPRT	5'-GGCCAGACTTTGTTGGATTTG-3'	5'-TGCGCTCATCTTAGGCTTTGT-3'
RT-PCR	XBP1	5'-AAACAGAGTAGCAGCGCAGACTGC-3'	5'-TCCTTCTGGGTAGACCTCTGGGAG-3'
RT-PCR	eCyclin O	5'-GTAGAGGTGCACCCACCTCGCTTG-3'	5'-CTCGTCAAGAAGACAGGGC-3'
qRT-PCR	hCyclin Oα	5'-CGCTTGCAAACAGGTGGAGG-3'	5'-TGCGTGAAATGCTCCAGGAAG-3'
qRT-PCR	hCyclin Oβ	5'-CACGGCAGCCACAAGTGGAGG-3'	5'-TGCGTGAAATGCTCCAGGAAG-3'
qRT-PCR	CHOP	5'-TATCTCATCCCAGGAAACG-3'	5'-GGGCACTGACCACTCTGTTTC-3'
qRT-PCR	CA6	5'-AAATGGTTACCGCAGCACAC-3'	5'-AAAGTGCCGGTTCTTCTTTG-3'
qRT-PCR	HPRT	5'-GGCCAGACTTTGTTGGATTTG-3'	5'-TGCGCTCATCTTAGGCTTTGT-3'

Table 4. Primers used in RT-PCR reactions.

6. Cell culture and transfections

Cells were grown in Dulbecco's modified Eagle's medium (DMEM) (Invitrogen) supplemented with antibiotics and 10% foetal calf serum (Biological Industries). Cells were maintained at 37 ºC with a humid atmosphere of 5% of CO_2. Cell lines used were obtained from American Type Culture Collection (ATCC) and were the following: U2OS, a human osteosarcoma cell line; AR42J, a rat pancreatic adenocarcinoma cell line; HT29-M6 (M6), a human colon adenocarcinoma cell line derived from the HT29 cell line and HEK-293T cells, a variant from the Human Embryonic Kidney cells (HEK-293 cells). This variant contains the SV40 large T antigen, which allows for episomal replication of transfected plasmids containing the SV40 origin of replication. PERK wild-type and knockout immortalized MEFs were kindly provided by Barbara C. McGrath (The Pennsylvania State University, United States). MEFs cells were grown as described above and supplemented with 1x non-essential amino acids and 45 μM β-mercaptoethanol. The mouse T-cell lymphoma cell line WEHI7.2 (obtained from Dr. Roger Miesfeld, University of Arizona, Tucson, Arizona,

USA) was grown in low glucose (1 g/L) DMEM supplemented with antibiotics and 10% foetal calf serum. WEHI7.2 cells that stably express shRNA against GFP (shGFP) or shRNA against Cyclin O (shCyclinO) were previously generated in our laboratory[218]. WEHI7.2 cells were transfected by electroporation with the pSuper-based shRNA constructs. Single cell clones were isolated by serial dilution and selected with 1 μg/ml of puromycin (Sigma-Aldrich).

HEK-293T and U2OS cells were transfected using polyethylimine (PEI, lineal MW 25.000, 1mg/ml) (Polysciences) (see section 6.1).

Cells were treated with a variety of stress-inducing agents, including thapsigargin (0.1 μM) (Sigma-Aldrich), DTT (Ditriothreitol) (4 mM) (Roche), tunicamycin (5 μg/ml) (Sigma-Aldrich), sodium arsenite ($NaAsO_2$) (400 μM), UV irradiation (50 mJ/cm²) or heat shock (44 ºC). After different times of treatment, immunofluorescence were performed or cells were washed with PBS and frozen at -80 ºC until used or fixed with ethanol for flow cytometry analysis (see section 19).

6.1. PEI transfection

Cells were seeded according to the cell type and plate and 24 hours later transfection was performed using the PEI method. A mixture was done with 150 mM NaCl, DNA and PEI 1mg/ml (Table 5). The mixture was incubated 15 minutes at RT and added drop by drop to the target cells. 48 hours later, cells were analysed.

Plate	DNA amount (μg)	PEI (μl)	NaCl (final volume, μl)
24 well plate	0.5 μg	2 μl	42 μl
6 well plate	2 μg	10 μl	200 μl
10 cm²	11.25 μg	58.5 μl	1170 μl

Table 5. Conditions for PEI transfection.

7. Lentiviral production, titration and infection

7.1. Lentiviral production

The vector used for the lentiviral production was the pWPI vector (kind gift of Didier Trono, Tronolab), in which it was inserted an oligonucleotide containing a polylinker to facilitate the cloning. The new vector was called pWPI-linker. The pWPI vector is a bicistronic vector that allows the simultaneous expression of a transgene and EGFP marker to facilitate tracking of transduced cells. The EGFP marker cDNA has been inserted downstream of EMCV IRES (Encephalomyocarditis virus, Internal Ribosomal Entry Site) (Figure 2). Myc-tagged mCyclin Oα, myc-tagged mCyclin Oβ or myc-tagged mCyclin OL3A were cloned into the pWPI-linker vector.

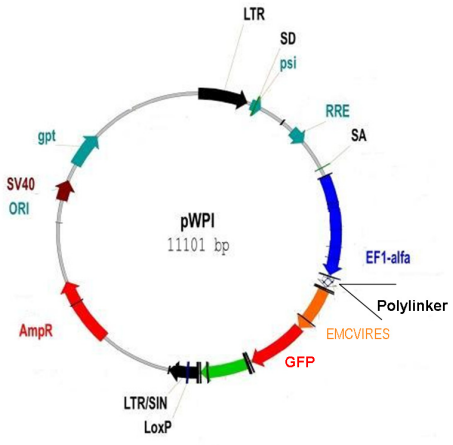

Figure 2. Scheme of the pWPI-linker vector.

mCyclin Oα, mCyclin Oβ, mCyclinOL3A or empty lentivirus were prepared by cotransfecting HEK-293T with helper vectors containing 10% of envelope vector (pMD2G) and 40% of packaging vector (pPAX2) using the PEI method. After 12 hours of transfection the virus-containing cell supernatant was removed and the cells were fed with fresh media. 48 and 72

hours post-transfection the supernatant was collected again, filtrated through a 0.45 μm filter, alicuoted in 1 ml fractions and frozen at -80 ºC until used.

7.2. Titration of the lentiviruses

Before the infection of the cells the titer of the virus was determined measuring by FACS analysis the number of GFP-positive cells, due to the fact that the lentiviral vector encodes an IRES-GFP cassette. The cells were seeded in a 24-well plate and the next day serial dilutions of the virus-containing cell supernatant were added to the cells in the presence of 10 μg/ml of polybrene (hexadimethrine bromide) (Sigma-Aldrich). After 12 hours of infection the medium was changed. 36 hours post-infection, cells were trypsinized, washed, resuspended in 250 μl of PBS and analysed by flow cytometry using a FACScan cytometer (Beckton Dickinson).

To calculate the titer the following formula was used:

Titer of the virus= $N \times D / V$ where N= number of GFP positive cells, D= fold dilution of vector sample for transduction and V= volume (ml) of diluted vector sample added into each well for transduction. In figure 3 it is shown an example of the titration of different viruses (mCyclin Oα, mCyclin Oβ, mCyclinOL3A or the empty virus).

Once the titer of the different viruses is determined, the MOI (Multiplicity Of Infection = ratio of infectious virus particles to cells) was calculated.

To calculate the MOI the following formula was used[223]:

$MOI = - ln P[0]$ [proportion of non infected cells]

In our experiments we used a MOI =1, to avoid that superinfection may trigger ER stress[114]. To obtain a MOI =1 a 63.5 % of cells has to be infected ($MOI = - ln P[0]$ → 1 = -ln ((10000-6350)/10000).

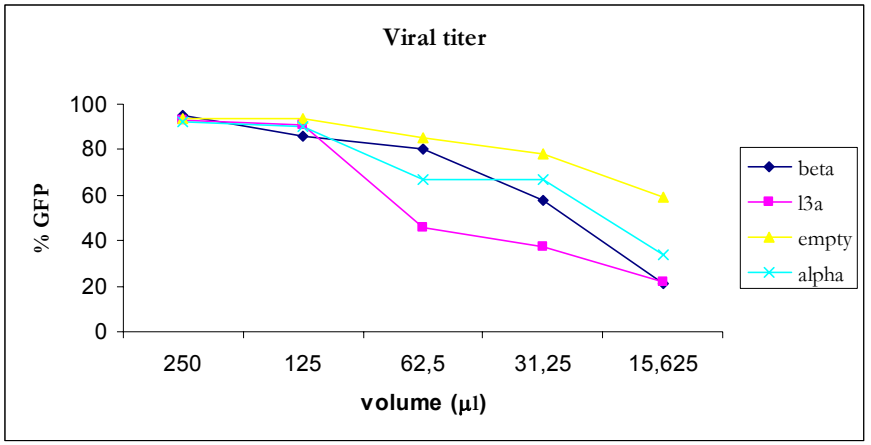

Figure 3. Titration of lentiviruses. This plot shows a representative titration of a batch of the lentiviruses encoding mCyclin Oα, mCyclin Oβ, mCyclin OL3A and the empty virus. In the X axis it is represented the volume of the different dilutions of the virus-containing supernatant added to the indicated cells and in the Y axis it is represented the percentage of GFP-positive cells measured by FACS analysis.

7.3. Lentiviral infection

Cells were infected with mCyclin Oα, mCyclin Oβ, mCyclin OL3A or empty lentivirus at a MOI =1 in the presence of 10 µg/ml of polybrene. After 12 hours of infection the supernatant was removed and the cells were fed with fresh medium. Cells were harvested at different time points afterwards (24, 36 and 48 hours post-infection) and the pellet was frozen at – 80 ºC until used.

8. Site-directed mutagenesis

Site-directed mutagenesis was performed using QuickChange II Site-Directed Mutagenesis kit (Stratagene), according to the manufacturer's protocol. L92, L95 and L97 of pMVHA-mcOα were replaced by alanines using the following primers:

L3AF1: 5'-TACTCAACCCTGCCCAGCCC**GCG**ACAGCG**GCG**GAT**GCC**CAGACCTTCCGAGAATACGG-3'

L3AR1: 5'- CGTATTCTCGGAAGGTCTG**GGC**ATC**CGC**CGCTGT**CGC**GGGCTGGGCAGGGTTGAGTA-3'

The nucleotides encoding the mutated residues are shown in red font.

The new plasmid construction was called pMVHA-mcOL3A.

9. DNA constructs

The constructs pMRFP-C1, pMRFP-mcOα, pMRFP-mcOβ, pEGFP-C1, pEGFP-mcOβ, pCDNA3-MycTag, pcDNAMycTag-mcOα and pcDNAHA-mcOβ were generated previously in our laboratory. pEGFP-TIA-1 was kindly provided by Dr. Juan Valcárcel (CRG).

In table 6 are described the different constructs that have been generated and used in this thesis. General cloning protocols have been used to obtain the different constructs[224]. All constructs were verified by restriction digest and sequencing.

The vectors used to generate the different constructs were the following:

pMRFP-C1/C2: a mammalian expression vector that encodes Monomeric Red Fluorescent Protein (MRFP), kindly provided by Dr. Roger Y. Tsien[225], followed by a polylinker. The Multiple Cloning Site (MCS) of pMRFP-C1/C2 is located after the RFP coding sequences, so genes cloned into the MCS will be expressed as fusions to the C-terminus of MRFP.

pEGFP-C1/C2: a mammalian expression vector that encodes Enhanced Green Fluorescent Protein (EGFP) followed by a polylinker. The MCS of pEGPP-C1/C2 is located after the EGFP coding sequences, so genes cloned into the MCS will be expressed as fusions to the C-terminus of EGFP (Clontech).

pEGFP-N2: The MCS of pEGPP-N2 is located before the EGFP coding sequences, so genes cloned into the MCS will be expressed as fusions to the N-terminus of EGFP (Clontech).

pCDNA3-MycTag: a mammalian expression vector that contains a strong promoter from a cytomegalovirus for high-level expression in mammalian cells and an epitope tag for easy detection of the expressed protein with a monoclonal antibody (kind gift of Susana de la Luna, CRG).

pGEX-6P3: a prokaryotic expression vector for high-level expression of GST-tagged recombinant proteins under the control of the IPTG-inducible *tac* promoter (GE Healthcare).

pWPI-linker: a lentiviral vector for mammalian expression (described in the section 7.1, kind gift of Didier Trono, Tronolab).

Construct	Vector used	Insert used
pEGPC2-mcOL3A	pEGFP-C2	Murine Cyclin Oα ORF, encoding mutated LxL motif
pMRFPC2-mcOL3A	pMRFP-C2	Murine Cyclin Oα ORF, encoding mutated LxL motif
pCDNA3-MycTag-mcOL3A	pCDNA3-MycTag	Murine Cyclin Oα ORF, encoding mutated LxL motif myc tagged
pCDNA3-MycTag-mcOβ	pCDNA3-MycTag	Murine Cyclin Oβ ORF myc tagged
GFP139wt	pEGFP-C2	Murine Cyclin Oα ORF, fragment from nucleotide 1 to 419
GFP139L3A	pEGFP-C2	Murine Cyclin Oα ORF, fragment from nucleotide 1 to 419 encoding mutated LxL motif
GFP-LxL Cyclin Box	pEGFP-C2	Murine Cyclin Oα ORF, fragment from nucleotide 211 to 1059 encoding LxL motif
GFP-L3A Cyclin Box	pEGFP-C2	Murine Cyclin Oα ORF, fragment from nucleotide 211 to 1059 encoding mutated LxL motif
N139GFPwt	pEGFP-N2	Murine Cyclin Oα ORF, fragment from nucleotide 1 to 419
N139GFPL3A	pEGFP-N2	Murine Cyclin Oα ORF, fragment from nucleotide 1 to 419 encoding mutated LxL motif
pGEX-6P3-mcOα	pGEX-6P3	Murine Cyclin Oα ORF
pWPI-linker- mcOβ	pWPI-linker	Murine Cyclin Oβ ORF
pWPI-linker-mcOL3A	pWPI-linker	Murine Cyclin Oα ORF, encoding mutated LxL motif

Table 6. Constructs used in this thesis.

10. Transfection of fusion proteins in U2OS for fluorescence microscopy

Cells were grown overnight on coverslips, previously treated with 10 μg/ml of poly-L-lysine for 1 hour at 37 ºC. 0.5 μg of the plasmid encoding each fusion protein was transfected per well using the PEI method. 48 hours post-transfection the cells were washed twice with PBS and then fixed with 4 % paraformaldehyde for 20 minutes at RT. When required, permeabilization of the cells was performed by treatment with 0.05% Tween-20 dissolved in

PBS and nuclei were stained with TOPRO-3 (Molecular Probes, Invitrogen) (1 μM). Cells were washed twice with PBS and afterwards with miliQ water and mounted with fluoromount. The cells were then examined by confocal microscopy (Leica TCS SP2).

11. Immunohistochemistry

11.1. From tissues

Immunohistochemical analyses were performed using 3 μm sections of paraformaldehyde-fixed, paraffin-embedded mouse or human tissue blocks. Antigen retrieval was done by boiling the slides in 10 mM sodium citrate pH 6 for 10 minutes. Slides were blocked with filtered 5 % non fat milk and 0.04 % Tween-20 dissolved in PBS. Affinity purified antibody against Cyclin O (N1) was incubated for 90 minutes at 27 ºC. As secondary antibody, the EnVision™ anti-rabbit system was applied (DAKO). Sections were counterstained with haematoxylin, dehydrated and mounted.

11.2. From adherent cells

Cells were grown overnight on coverslips and fixed with 4% paraformaldehyde for 20 minutes at RT. After washing with PBS, cells were incubated with 50 mM ammonium chloride for 30 minutes. Permeabilization of the cells was performed with 0.1 % Triton X-100 dissolved in PBS for 10 minutes at RT. Endogenous peroxidase was blocked by treatment with 4% hydrogen peroxide in PBS for 10 minutes. Nonspecific binding sites were blocked with filtered 5% non fat milk and 0.04 % Tween-20 dissolved in PBS for 20 minutes. Primary and secondary antibodies were the same as described above.

12. Immunofluorescence

The initial protocol is the same as the one used for immunohistochemistry of adherent cells until the blocking step. Blocking was carried out for 30 minutes with 5% horse serum dissolved in TBS-BSA 1%. Then, the coverslips were incubated with the primary antibody diluted in TBS-BSA 1% for 1 hour at RT or overnight at 4 ºC. After washing six times with TBS, coverslips were incubated for 40 minutes at RT with the secondary antibody diluted in TBS-BSA 1%. Then, cells were washed four times with TBS and afterwards with miliQ water and mounted with fluoromount. In some cases, nuclei were stained with TOPRO-3 (1 μM) or DAPI (0.5 μg/ml). The cells were examined by confocal microscopy (Leica TCS SP2 and Leica TCS SPE).

For the mitotracker dye, the cells were incubated for 30 minutes with 0.1 μM Mitotracker-red (Invitrogen) at 37 ºC. Then, the medium was removed and replaced it with pre-warmed medium. After washing with PBS, cells were fixed with 4% paraformaldehyde for 20 minutes at RT. The immunofluorescence was done as described above.

13. Assessment of colocalization

Confocal imaging was performed with a Leica TCS SP2 adapted to an inverted Leica DM IRBE microscope using a 63x (NA 1.32, oil) Leica Plan Apochromatic objective. Images of multilabeled specimens were acquired sequentially using the following settings: GFP, Alexa 488 and Cy2 were excited with the 488 nm line of an argon laser and their emission were recorded between 495 and 540nm; RFP, Alexa 555 and Cy3 were excited with a 543 nm helium-neon laser, and were recorded between 555 and 620

nm; TOPRO-3 was excited with a 633 nm helium-neon laser, and was recorded between 640 and 750 nm.

Four colour staining images were acquired with a Leica TCS SPE adapted to an inverted Leica DMI 4000B microscope using a 63x (NA 1.30, oil) Leica ACS APO objective. DAPI, Streptavidin-FITC, Mitotracker-red and Alexa 647 were excited with 405 nm, 488 nm, 532 nm and 635 nm diode lasers respectively; and their emission were sequentially recorded approximately at 425-490 nm, 500-575 nm, 585-650 nm and 645-750 nm, respectively. Z stacks of the whole cellular volume were acquired with a z-step between 0.5 and 1.2 μm.

Imaged cells were zoomed in to fulfill the optical resolution of the objective according to Nyquist sampling criterion. All images were 1024 x 1024 pixels and were acquired at 400 Hz.

Quantification of colocalization was carried out using the colocalization module of ImageJ version 1.43q software package using different parameters informative of the amount of colocalization between the different proteins[226].

Rr (Pearson's correlation coefficient including all the pixels): R is a measure of the strength of the association between two variables (fluorescence of two channels). The values range from 1 to -1. A value of 1 represents perfect correlation; low (close to zero) and negative values for fluorescent images are difficult to interpret.

Rcoloc (Pearson's coefficient including only in the calculation pixels showing colocalization): Returns Pearson's correlation coefficient for pixels where both channel 1 and channel 2 are above their respective threshold. The values range from 1 to -1. A vale of 1 represents perfect correlation; a value equal to 0 represents no correlation and a value of -1 represents perfect inverse correlation.

R (Mander's Overlap coefficient): R is another method of quantifying correlation. The values range from 1 to 0. A value of 1 represents high colocalization and a value of 0 represents low colocalization. The disadvantage of this coefficient is that is insensitive to differences in signal intensities between the two channels.

ICQ (Intensity Correlation Quotient): This quotient is based on the non-parametric sign-test analysis of the PDM (Product of the Differences from the Mean) values and is equal to the ratio of the number of positive PDM values to the total number of pixel values. The PDM value is the (red intensity-mean red intensity) * (green intensity –mean green intensity)[227]. The values range from -0.5 to +0.5. A value between 0 to +0.5 represents dependent staining, a value equal to 0 represents random staining and a value between -0.5 to 0 represents segregated staining.

% Volume colocalized: percentage of volume colocalized compared to the total volume of the cell. The parameter is calculated using Cortes' quoficient[226].

14. Western Blot

Cells to be used for immunoblotting were washed with cold PBS and frozen at -80 ºC until used. Cell pellets where extracted with RIPA buffer (10 mM Tris-HCl pH 7.4, 1% NP-40, 0.1% SDS, 1% sodium deoxycolate and 0.15 M NaCl) to which protease and phosphatase inhibitors were added (2 µg/ml aprotinin, 2 µg/ml leupeptin, 2 µg/ml antipain, 20 µg/ml soybean trypsin inhibitor, 1 mM DTT, 1 M NaF, 0.5 M β-glycerol phosphate, 0.1 M sodium pyrophosphate, 1 mM Pefablock™ and 20 mM sodium ortovanadate) and protein quantified using the Bradford reagent (BioRad). Equal amounts of protein from total cellular extracts were loaded on each lane, resolved by SDS-Polyacrylamide Gel Electrophoresis (SDS-PAGE) and transferred into a nitrocellulose membrane (Protran). Membranes were blocked with 5%

non-fat milk prepared in TBS-T (20 mM Tris HCl pH 7.6, 137 mM NaCl, 0.1% Tween 20) either for 1 hour at RT or overnight at 4 ºC with constant agitation. Primary antibodies were diluted in TBS-T containing 2% BSA and were incubated for 1h at RT or overnight at 4 ºC. After extensive washing with TBS-T, membranes were incubated for 1 hour with the corresponding secondary HRP (Horse Radish Peroxidase)-conjugated antibody (all purchased from DAKO). Membranes where then blotted using either the standard ECL chemiluminiscent substrate (Pierce) or SuperSignal West Pico (Pierce). For stripping the antibody, membranes were incubated for 30 minutes at 50 ºC with 62.5 mM Tris-HCl pH 6.8, 2% SDS, 100 mM β-mercaptoethanol.

15. Immunoprecipitation and kinase assays

HEK-293T cells were transfected with empty vector or expression vectors for myc-tagged Cyclin Oα, β or L3A using the PEI method. 48 hours after transfection cells were collected by scrapping, washed with PBS and lysed with Lysis Buffer (50 mM Tris HCl pH 7.4, 0.5% NP-40, 20 mM EDTA, 0.15 M NaCl) to which protease and phosphatase inhibitors were added (2 µg/ml aprotinin, 2 µg/ml leupeptin, 2 µg/ml antipain, 20 µg/ml soybean trypsin inhibitor, 1 mM DTT, 1 mM NaF, 1 mM β-glycerol phosphate, 1 mM sodium orthophosphate, 1 mM Pefablock™ and 200 mM sodium ortovanadate). For the immunoprecipitation first, 50 µl of the supernatant of the 9E10 anti-myc hybridoma were bound to 25 µl of Protein-G Sepharose beads (GE Healthcare). As a negative control, 50 µl of an irrelevant hybridoma of the same immunoglobulin isotype was used. 750 µg of cell extract was then mixed with the antibody beads and incubated for 3 h at 4 ºC with constant agitation. After this time the immunoprecipitates were split in 2 aliquots, one for Western Blot analysis (95%) and the other for the kinase assay (5%). For Western Blotting, beads were extensively washed, boiled

with Laemmli Buffer 2X and separated by SDS-PAGE. Western Blotting was performed against Cdk2. Membranes were then stripped and probed against Cyclin O using the polyclonal anti-Cyclin O antibody C2 to detect the immunoprecipitated Cyclin Oα, β and L3A. To achieve minimal cross-reaction to Mouse IgG it was used the peroxidase-conjugated IgG Fraction Monoclonal Mouse Anti-Rabbit IgG, Ligh Chain Specific as a secondary antibody (Jackson ImmunoResearch). For the kinase assay, beads were washed extensively with Kinase Buffer (50 mM Tris-HCl pH 7.5, 10 mM $MgCl_2$, 1 mM DTT) and finally resuspended in 20 µl of Hot Mix (50 mM Tris-HCl pH 7.5, 10 mM $MgCl_2$, 20 µM ATP, 10 µCi [$\gamma-^{32}$P] dATP, 1 mM DTT, 2 µg Histone H1). Kinase reactions were incubated 30 minutes at 30 ºC and then stopped by adding 20 µl of Laemmli Buffer 2X. 20 µl of the reaction were loaded on a SDS-PAGE, Coomassie Blue stained, drained and signal detected by autoradiography.

16. Kinase assay after subcellular fractionation

Different subcellular extracts of MEFs were obtained using the ProteoExtract Subcellular Proteome extraction kit (S-PEK) (Calbiochem). This kit yields the total proteome fractionated into four subproteomes of decreased complexity. With extraction buffer I cytosolic proteins are released (fraction 1), membranes and membrane organelles are solubilised with Extraction Buffer II, without impairing the integrity of nucleus and cytoskeleton (fraction 2). Next, nucleic proteins are enriched with Extraction Buffer III (fraction 3). Components of the cytoskeleton are finally solubilised with Extraction Buffer IV (fraction 4).

The different subcellular extracts were immunoprecipitated using 10 µl of C2 antiserum against Cyclin O or the corresponding preimmune serum as a negative control covalently bound to 25 µl of protein A-Sepharose Beads.

Beads were washed extensively with Kinase Buffer and finally resuspended in 20 µl of Hot Mix. The kinase assay was carried out as describe above.

We controlled the subcellular fractionation by Western Blotting using different protein markers: Piruvate Kinase for fraction 1, BiP for fraction 2, Histone H3 for fraction 3 and Vimentin for fraction 4. The different subcellular extracts were quantified using the MicroBCA™ Protein Assay kit (Pierce). Equal amounts of protein from each fraction were analysed by Western Blotting.

17. Production of recombinant proteins in *Escherichia coli*

17.1. Vectors and strains

For the production of recombinant proteins we used the *Escherichia coli* (E. coli) strain BL21 (DE3) transformed with the corresponding expression vectors. For production of GST fusion proteins we used the pGEX vectors (GE Healthcare).

17.2. Production of bacterial lysate

An inoculum of 10 mL of LB medium plus antibiotic with the bacteria carrying the plasmid of interest were incubated at 37 ºC overnight. The following morning, the saturated culture was diluted 1:1000 and incubated at 37 ºC with constant agitation at 200 rpm for 3h in LB medium plus antibiotic. For the production of GST-Cyclin O the saturated culture was incubated at 30 ºC during four hours to avoid degradation of the protein. After the indicated time, recombinant protein expression was induced by adding IPTG (Isopropyl-beta-D-thiogalactopyranoside) 1 mM to the media. The culture was incubated at 30 ºC with constant agitation at 200 rpm for 5 hours. After the indicated time, culture was harvested by centrifuging at 3500 rpm for 30 minutes. The cell pellet was frozen at -80 ºC for at least 1h.

Bacteria were then resuspended with 1/10 volume of NTEN (20 mM Tris-HCl pH 8, 150 mM NaCl, 1 mM EDTA, 0.5% NP40, 1 mM DTT, 2 µg/ml aprotinin, 2 µg/ml leupeptin, 2 µg/ml antipain, 20 µg/ml soybean trypsin inhibitor, 1 mM Pefablock™) and lysed by sonication. To obtain a clear lysate, the extract was centrifuged at 10.000 rpm for 10 minutes at 4 ºC and the pellet was discarded. The supernatant was aliquoted and stored at -80 ºC until used.

17.3. Check the expression of recombinant proteins

We checked the quality and quantity of the recombinant proteins generated before. Different amounts of the cleared lysate (between 2 and 500 µl) were incubated with 25 µl of Glutathione-Sepharose beads (GE Healthcare) during 3 h with constant agitation at 4 ºC. Beads were extensively washed with NTEN buffer and boiled with 30 µl of Laemmli Buffer 2X. 15 µl of the eluted were loaded on a SDS-PAGE and stained with Coomassie Blue. The same amount of the different recombinant proteins (about 5 µg) will be used for the pull-down experiment.

18. Pull-down

Cell extracts from exponentially growing M6 cells were prepared using Lysis Buffer (1% Triton, 150 mM NaCl, 20 mM HEPES, 10% glycerol, 1 mM EDTA, 100 mM NaF) to which protease and phosphatase inhibitors were added (2 µg/ml aprotinin, 2 µg/ml leupeptin, 2 µg/ml antipain, 20 µg/ml soybean trypsin inhibitor, 1 mM Pefablock™, 10 mM sodium pyrophosphate, and 17.5 mM β-glycerol phosphate) and protein quantified using the Bradford reagent. We then precleared the extracts by incubation with glutathione sepharose-bound GST-RFP fusion protein. 0.5-1 mg of M6 cell extracts were incubated with 25 µl of GST-RFP fusion protein previously bound to 25 µl of Glutathione-Sepharose beads for 2 hours at

4ºC. After this time, beads were centrifugated 5 minutes at 14000 rpm and the supernatant was separated from the beads. On the other hand, GST-fusion proteins (GST, GST-GFP, GST-Cyclin Oα) previously bound to 25 µl of Glutathione-Sepharose beads were incubated with 20 mg /ml of BSA for at least 3 hours at 4 ºC to avoid inespecific binding. Then, beads were incubated with the precleared M6 extracts overnight at 4 ºC. The following morning, beads were washed with lysis buffer three times and boiled with 30 µl of Laemmli Buffer 2X. 5-25 µl of the eluted were loaded on a SDS-PAGE and transferred to a nitrocellulose membrane. The presence of different proteins in the beads was analysed by Western Blotting.

19. Flow cytometry: measurement of cell cycle and apoptosis by DNA content

In order to analyse the cell cycle profile and apoptosis, shGFP or shCyclin O WEHI7.2 cells (0.5 * 10^6) were centrifuged at 2000 rpm for 5 minutes and resuspended in 200 µl of PBS. Cells were fixed by adding drop by drop 2 ml of 70% ethanol and kept at 4 ºC for at least 24h. For the DNA staining, cells were washed twice and resuspended in Staining Solution (10 µg/ml RNAase A, 10 µg/ml Propidium Iodide (PI) in PBS) at a final concentration of 10^6 cells/ml and incubated at 4 ºC for 24 hours. Samples were analysed by flow cytometry using a FACScan flow cytometer (Beckton Dickinson). Data analysis was performed using BD CellQuestTM software.

20. Colony assay

U2OS osteosarcoma cells (1 * 10^6) were plated in a 10 cm^2 plate. Next day, the cells were transfected with pCDNA3-MycTag empty vector (Invitrogen) or pCDNA3-MycTag-mCyclin Oα, β or L3A using the PEI method. All the plasmids used were previously linearized with *AhdI*. 48 hours after

transfection, cells were trypsinised, each plate was diluted 1/100 and plated in triplicate in six-well plates in the presence of 1 mg/ml G418 (Gibco). Selection media were replaced every three days. Two weeks after transfection, cells were fixed with 4% paraformaldehyde, stained with Coomassie Blue and counted. Transfection efficiency between the different transfected cell lines was normalized by cotransfection of each plasmid with an EGFP expression plasmid. The GFP positive cells were analysed 48 hours post-transfection by flow cytometry.

21. Stadistical analysis

Data were expressed as the mean ± S.E.M. (Standard Error of the Mean) of the values from the number of the experiments as indicated. Data were evaluated statistically by Student's t-test. Significance levels: P=0.05, *; 0.05 >P>0.01,**; 0.01>P>0.005, ***; 0.005>P>0.001, **** and 0.001>P>0.0005, *****.

22. Commercial suppliers

Commercial suppliers	Localisation
Abcam	Cambridge, UK
American Type Culture Collection (ATCC)	Rockville, MD, USA
Amersham Biosciences	Uppsala, Sweden
Applied Biosystems	Warrington, UK
BD Transduction Laboratories	California, USA
Beckton Dickinson	California, USA
Biological Industries	Kibbutz Beit Haemez, Israel
Biorad	Madrid, Spain
Calbiochem	Ireland
Cell Signalling Technology (Cell Signal)	Boston, MA, USA
Chemicon (Milipore)	Billeberica, MA, USA
Clontech	Mountain View, CA, USA
Dako Cytomation (DAKO)	Glostrup, Denmark
GE Healthcare	Buckinghamshire, UK
Gibco (Invitrogen)	Carlsbad, CA, USA
Invitrogen	Carlsbad, CA, USA
Jackson ImmunoResearch Laboratories, Inc.	West Grove, PA, USA
Millipore	Billeberica, MA, USA
Nunclon	SanDiego, USA
Pierce	Rockford, IL, USA
Polysciences	Pennsylvania USA
Promega	Madison, WI, USA,
Protran	Schleicher & Schuell GmbH, Germany
Qiagen	Hilden, Germany
Roche	Madrid, Spain
Santa Cruz Biotechnology	CA, USA
Sigma-Aldrich	St. Lois, MO, USA
Stratagene	La Jolla, CA , USA
Tecan	Switzerland
Tronolab	Switzerland
Vector Laboratories IHC	Burlingame, CA, USA

Table 7. Commercial suppliers.

RESULTS

1. Cyclin O expression

1.1. Expression of endogenous Cyclin O

Our group has identified different mRNA isoforms encoded by the gene *cyclin O*[218] (Figure 1A): Cyclin Oα mRNA encoded by exons 1 to 3; the alternative splicing product Cyclin Oβ encoded by exons 1 and 3; Cyclin Oε, product of an alternative 3' splicing donor site of exon 1 plus exons 2 and 3 and the product of an alternative promoter: murine Cyclin Oδ and human Cyclin Oγ. The function of Cyclin Oε, Cyclin Oδ and Cyclin Oγ is still unknown and neither the gamma nor the delta forms are protein coding. This work will focus on the study of Cyclin Oα and Cyclin Oβ.

We analysed the expression pattern of Cyclin Oα and Cyclin Oβ in mouse tissues by semi-quantitative RT-PCR (Figure 1B). The mRNA of Cyclin Oα is expressed at low levels in a wide range of tissues, with the highest expression found in testis. A different expression pattern between both isoforms is observed, without an obvious relationship. We have to take into account that some tissues that did not express any of the two mRNAs constitutively, for instance the thymus or the spleen, did express them in response to stimuli such as γ-radiation or glucocorticoid treatments[218].

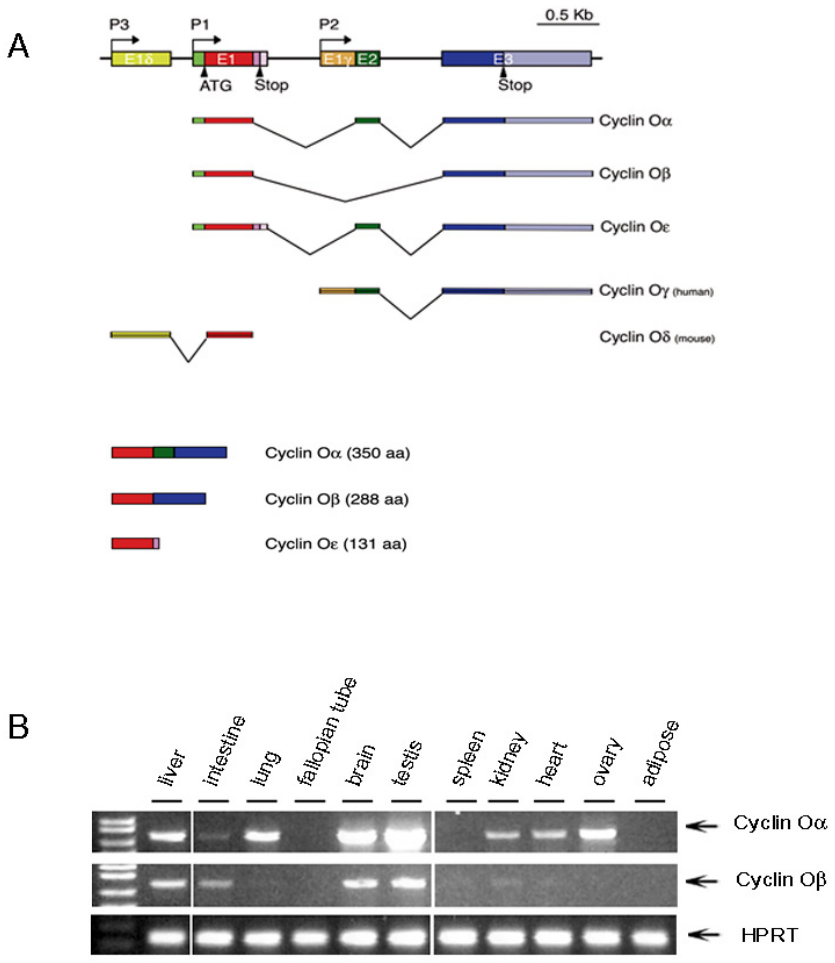

Figure 1. *Cyclin O* locus and expression. (A) Generic structure of the *cyclin O* locus. The *cyclin O* locus encodes four transcripts that arise from the use of two alternative promoters and alternative splicing: P1 (human/mouse Cyclin Oα, Cyclin Oβ and Cyclin Oε), and P2/P3 (human Cyclin Oγ, mouse Cyclin Oδ). Red, green and dark blue boxes denote exons 1, 2 and 3, respectively. The other coloured boxes denote non-coding regions. **(B)** Expression of Cyclin Oα and β mRNAs was measured by semi-quantitative RT-PCR in mouse tissues. As a loading control, HPRT levels were measured.

In order to determine the subcellular localisation of Cyclin O proteins, we performed immunohistochemistry experiments in normal mouse and human tissues and cell lines. We have observed that Cyclin O is expressed in most tissues, in agreement with the semi-quantitative RT-PCR data. In most of the cases, Cyclin O shows a clear cytoplasmic punctate pattern, like in murine brain cortical neurons (Figure 2a) or in normal human colon epithelium (Figure 2b). However, in some tissues with high expression levels Cyclin O is expressed both in the nucleus and cytoplasm, like in some cells of the mouse small intestine (Figure 2c). The same cytoplasmic distribution seen in the tissues is observed in different cell lines, such as in MEFs (Figure 2d), HT29-M6 (human colon adenocarcinoma cell line) (Figure 2e) and U2OS (human osteosarcoma cell line) (Figure 2f).

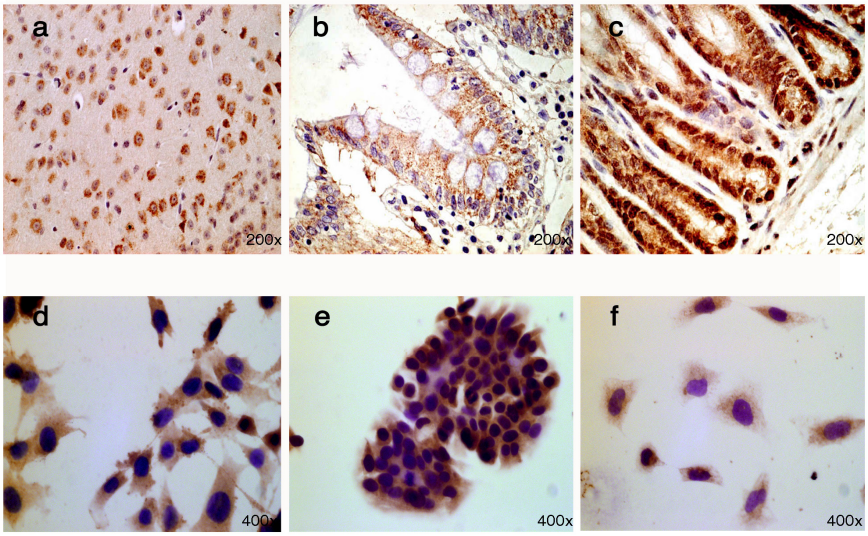

Figure 2. Expression of Cyclin O in mouse, human tissues and cell lines by immunohistochemistry. Cyclin O was detected by immunohistochemistry in murine brain cortical neurons **(a),** in normal human colon epithelium **(b)**, in murine small intestine **(c)**, in mouse embryonic fibroblasts **(d)**, in a human colon adenocarcinoma cell line (HT29-M6) **(e)** and in a human osteosarcoma cell line (U2OS) **(f)**. Cyclin O was detected using the N1 antibody and the EnVision™ system with the colorimetric substrate DAB.

All these immunohistochemistry experiments were performed with the N1 antibody, which recognizes both the α and β isoforms. In order to determine the specific subcellular distribution of each isoform we generated antibodies recognizing only Cyclin Oα or Cyclin Oβ (see Materials & Methods section). By immunofluorescence, we observed a different cytoplasmic pattern between Cyclin Oα and β in two different cell lines (Figure 3). Anti-Cyclin Oα staining shows a fine, uniform dotted pattern, whereas Cyclin Oβ immunostaining reveals a coarse punctate pattern (dots up to 300 nm in diameter). The punctate pattern of Cyclin Oβ is comparable to its distribution in transient transfection experiments (see section 1.2). Furthermore, from this experiment we can also conclude that endogenous Cyclin Oα is expressed at higher levels than Cyclin Oβ.

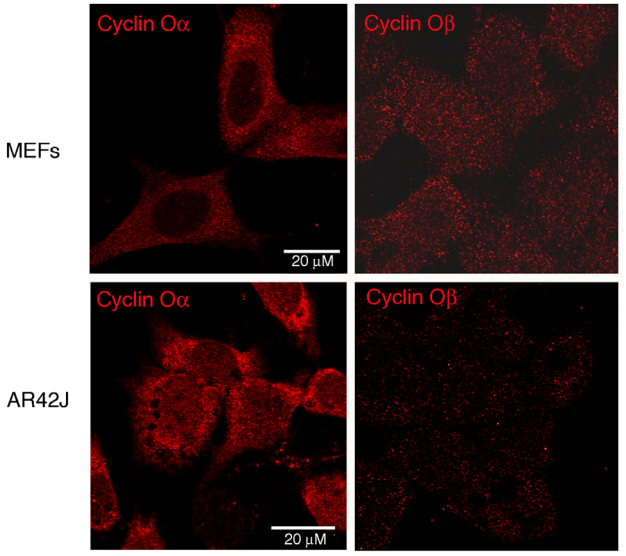

Figure 3. Subcellular distribution of endogenous Cyclin Oα and β isoforms. The subcellular localization of endogenous Cyclin Oα and Cyclin Oβ was determined in mouse embryonic fibroblasts (MEFs) (upper panels), and in a rat exocrine pancreas adenocarcinoma cell line (AR42J) (lower panels) by confocal microscopy using the specific α1/β1 antibodies detected with a Cy3-labeled donkey anti-rabbit secondary antibody.

1.2. Expression of exogenous Cyclin O

We also checked the subcellular localization of the α and β isoforms when Cyclin O is transiently transfected into different cell types. Surprisingly, we observed that when expression vectors encoding the fusion protein RFP-Cyclin Oα were transiently transfected in the U2OS osteosarcoma cell line, the protein was mostly nuclear; however the transiently transfected beta isoform shows a cytoplasmic punctate pattern (Figure 4). We hypothesized that the nuclear localization of the transfected Cyclin Oα is most likely due to an overexpression of the protein, which may exceed a putative cytoplasmic retention mechanism, since the subcellular localization of endogenous Cyclin Oα is mainly cytoplasmic. The cytoplasmic punctate pattern of Cyclin Oβ resembles the distribution observed in the case of the endogenous protein in figure 3, although the amount of the transfected protein and the size of the dots are much higher.

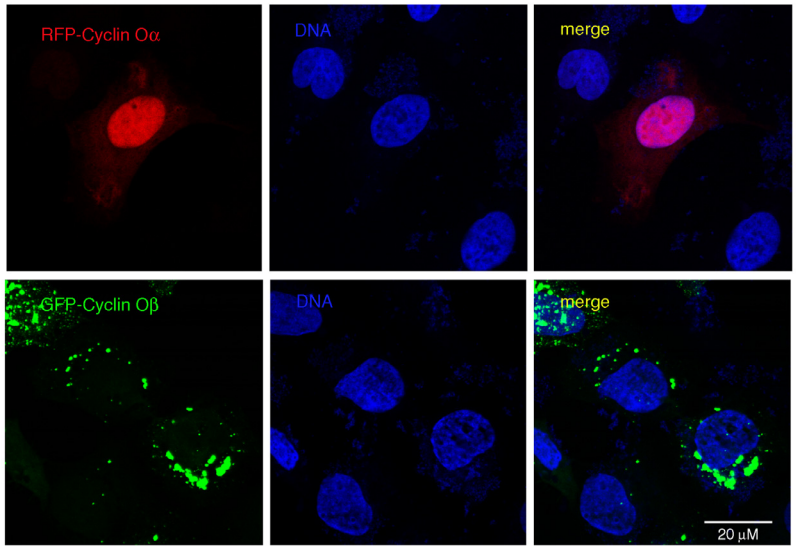

Figure 4. Expression of transfected mCyclin Oα and mCyclin Oβ. Subcellular localization of RFP-mCyclin Oα (upper panels) and GFP-mCyclin Oβ fusion proteins (lower panels) in the U2OS osteosarcoma cell line. Vectors encoding the fusion proteins were transfected and their subcellular distribution was analysed by confocal microscopy. Nuclei were stained with TOPRO-3 (DNA) and are shown in blue colour.

To try to understand the reasons for the different subcellular distribution of Cyclin O between the endogenous and the transfected protein, we took profit of lentiviruses that we generated in our laboratory encoding Cyclin Oα and β. We observed that the expression levels of Cyclin Oα and β in cells infected with these viruses is much lower compared with the cells where Cyclin Oα or β are transiently transfected (data not shown). We observed that in recombinant lentivirus infected cells Cyclin Oα shows a mixed nuclear and cytoplasmic pattern, whereas Cyclin Oβ is exclusively located in the cytoplasm (data not shown).

Altogether, these data indicate that the subcellular localization of Cyclin Oα depends on the amount of protein expressed.

2. Structure of Cyclin O

Cyclin O is a highly conserved gene present in all the vertebrate genomes sequenced so far. About two thirds of the protein sequence encompasses a highly conserved C-terminal Cyclin box, being the N-terminal part (composed by about 100 amino acids) much less conserved. However, this N-terminal part contains several highly conserved putative regulatory motifs, suggesting a regulatory role. In figure 5 it is shown the alignment of the N-terminal region of Cyclin O in different species. The conserved motifs include a putative NLS, a β-Trcp/GSK3 degron and the LxxLxL motif, which resembles a NES.

Figure 5. Structure of Cyclin O. Alignment of the N-terminal region of Cyclin O of different species showing the high degree of homology in the putative regulatory motifs. Several conserved motifs are indicated: KKSRRxxRRK corresponds to a putative NLS (Nuclear Localization Signal) (purple), DSGxxxDxxxSPSS corresponds to a β-Trcp/GSK3 (Beta-transducin repeats-containing protein, Glycogen synthase Kinase-3) degron (green), and the LxxLxL motif corresponds to a putative NES (Nuclear Export Signal) (red).

2.1. The L3A mutant

The subcellular localization of Cyclin O might be important for its function. We thought that the study of the conserved putative regulatory motifs of the N-terminal part of the Cyclin could help us to understand the localization and regulation of this protein. The NLS and NES could be crucial for its subcellular localization, and the phosphorylation sites could modulate them. In an attempt to mutagenize the putative NES (LxxLxL motif), by means of site-directed mutagenesis, we replaced L92, L95 and L97 residues by alanines (L3A mutant) (see Materials & Methods section). A NES is a short amino acid sequence of 5-6 hydrophobic residues in a protein that targets it for export from the cell nucleus to the cytoplasm through the nuclear pore complex. Our first idea was that if we mutated the NES of the Cyclin O, the transfected protein would be located in the nucleus constitutively. We then transiently transfected the L3A mutant fused to RFP or EGFP in the U2OS osteosarcoma cell line (Figure 6). Surprisingly, we could observe that the L3A mutant showed a cytoplasmic punctate pattern, reminiscent of the distribution of the beta isoform. These results suggest that this sequence does not correspond to a NES.

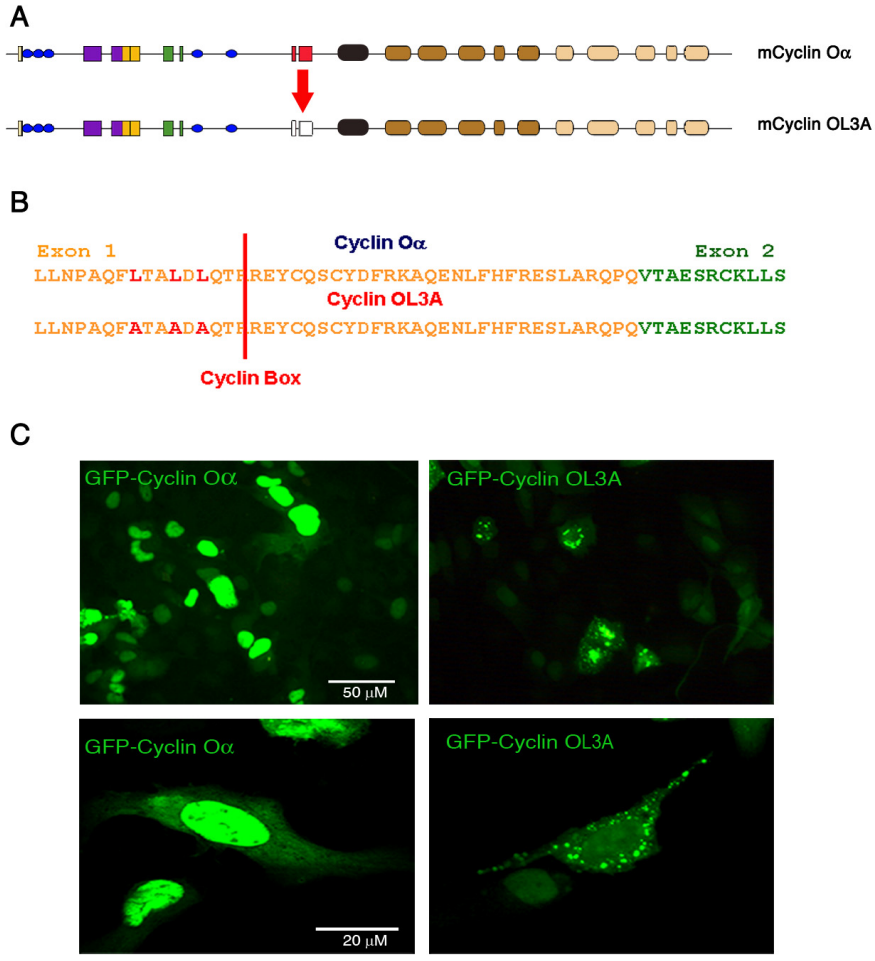

Figure 6. Comparison between mCyclin Oα and mCyclin OL3A. (A) Scheme of mCyclin Oα and mCyclin OL3A where are represented the different motifs of the protein. The L3A mutation is indicated by a white box. The correspondence of each symbol can be found in the section 9.1 of the Introduction part. **(B)** Amino acid sequence of mCyclin Oα and mCyclin OL3A. The mutagenized amino acids are indicated in red colour. **(C)** GFP-mCyclin Oα (left panel) and GFP-mCyclin OL3A (right panel) expression plasmids were transiently transfected into the U2OS osteosarcoma cell line. Subcellular distribution of the fusion proteins was analysed by fluorescence microscopy.

3. Study of the cytoplasmic punctate pattern of Cyclin O

The dotted distribution of Cyclin O in the cytoplasm indicated that it was not evenly distributed but concentrated in unknown cytoplasmic structures. To further characterise this pattern, we transiently cotransfected vectors encoding the fusion protein RFP-mCyclin Oα together with an expression plasmid for GFP-mCyclin Oβ. When both isoforms are coexpressed, the localisation of the β isoform changes the nuclear localization of the transfected α isoform, resulting in a cytoplasmic punctate pattern with complete colocalization of both proteins (Figure 7A). We then transiently cotransfected expression vectors encoding the fusion proteins RFP-mCyclin Oα and GFP-mCyclin OL3A. The L3A mutant relocates Cyclin Oα to the cytoplasm, similarly to what happens when we cotransfected the α and β isoforms, resulting again in a cytoplasmic punctate pattern with complete colocalization of both proteins (Figure 7B). Finally, we transiently cotransfected expression plasmids for the fusion proteins GFP-mCyclin Oβ and RFP-mCyclin OL3A. Again, we obtained a punctate pattern containing both proteins (Figure 8).

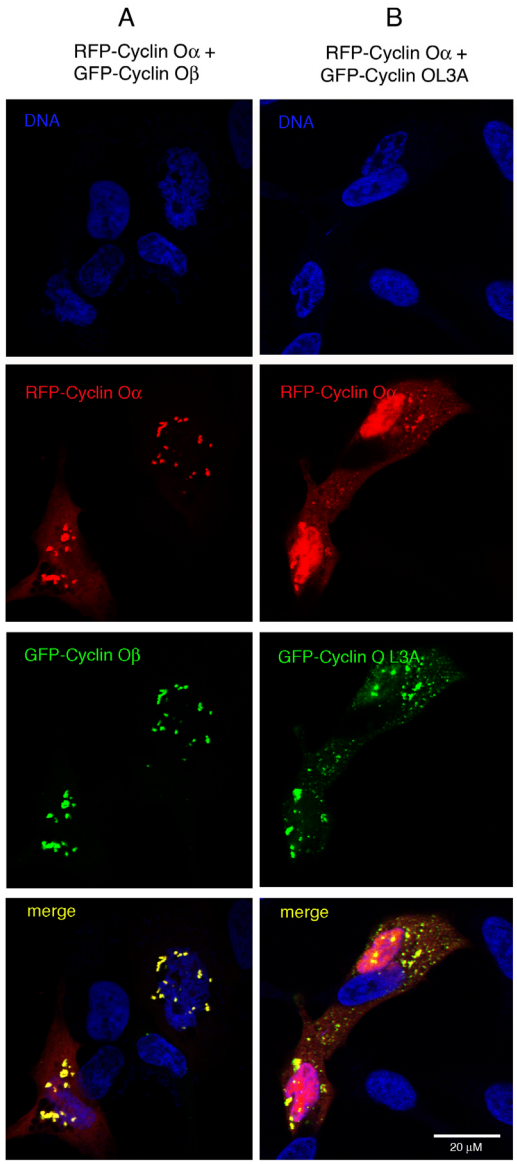

Figure 7. Subcellular distribution of cotransfected mCyclin Oα and mCyclin Oβ or mCyclin Oα and mCyclin OL3A. RFP-mCyclin Oα and GFP-mCyclin Oβ **(A)** or RFP-mCyclin Oα and GFP-mCyclin OL3A expression plasmids **(B)** were transiently cotransfected in the U2OS osteosarcoma cell line. Subcellular distribution of the fusion proteins was analysed by confocal microscopy. Nuclei were stained with TOPRO-3 (DNA) and are shown in blue colour.

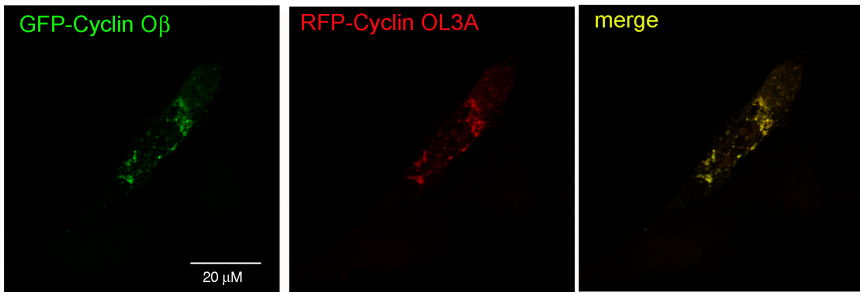

Figure 8. Subcellular distribution of cotransfected mCyclin Oβ and mCyclin OL3A. GFP-mCyclin Oβ and RFP-mCyclin OL3A expression plasmids were transiently cotransfected in the U2OS osteosarcoma cell line. Subcellular distribution of the fusion proteins was analysed by confocal microscopy.

Taking into account all these experiments, we wondered what type of cytoplasmic bodies these aggregates could correspond to. We can find three main different cytoplasmic bodies in eukaryotic cells[228]: Aggresomes, Processing Bodies and Stress Granules. For its shape and size, the Cyclin O cytoplasmic structures are not likely to correspond to aggresomes and for its irregular shape we discarded that they could correspond to PBs. So we speculated that the cytoplasmic punctate pattern of Cyclin O would correspond to SGs.

3.1. The cytoplasmic punctate pattern of Cyclin O corresponds to SGs

In order to investigate if the cytoplasmic punctate pattern of Cyclin O corresponds to SGs, we used the protein TIA-1 as a marker. TIA-1 protein exhibits a remarkably altered subcellular distribution in stressed cells, moving from the nucleus into the cytoplasm where it accumulates in the SGs. Thus, TIA-1 acts downstream of eIF2α phosphorylation to promote SG assembly during stress[66]. We transiently cotransfected RFP-mCyclin Oα and GFP-TIA-1 expression plasmids in the U2OS cell line and stressed the cells with different stimuli, such as sodium arsenite or heat shock (Figure 9), which

activate different eIF2α kinases. As a result, we observed that in response to these environmental stresses Cyclin Oα colocalitzed with TIA-1 in the cytoplasmic granules. These results demonstrated that in stressed cells, Cyclin Oα localization is compatible with SGs.

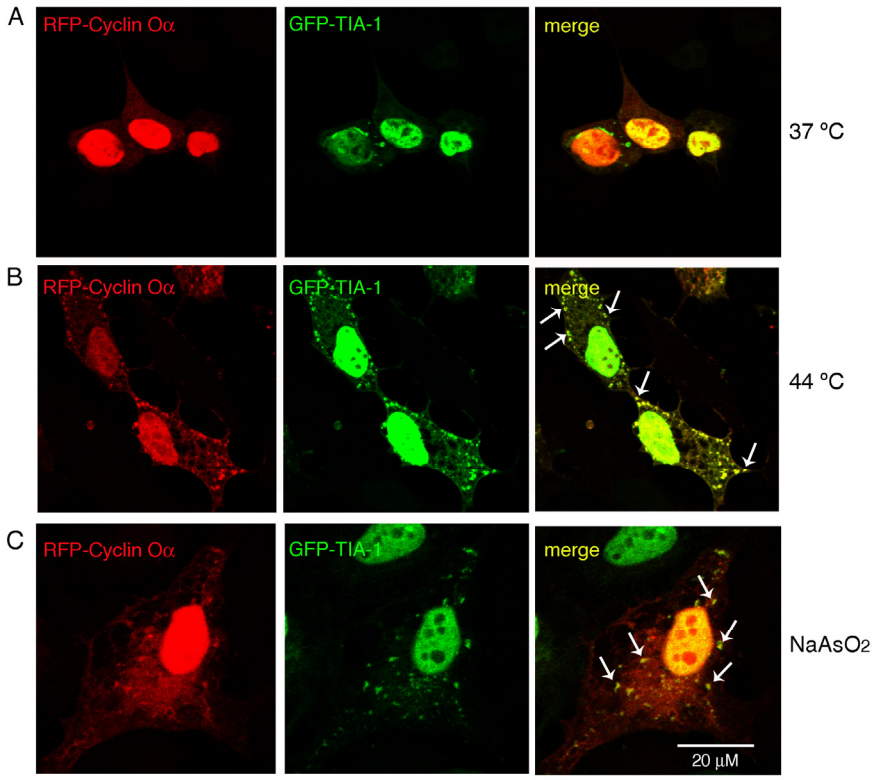

Figure 9. mCyclin Oα colocalizes with TIA-1 in the SGs in response to environmental stresses. Subcellular localization of GFP-TIA-1 and RFP-mCyclin Oα espression plasmids transiently cotransfected in the U2OS osteosarcoma cell line. Cells were incubated in standard conditions **(A)**, at 44º C for 3 hours **(B)** or in medium containing sodium arsenite ($NaAsO_2$; 400 µM) for 30 minutes **(C)**. The subcellular localization of both proteins was analysed by confocal microscopy. White arrows indicate examples of colocalization of both proteins in the SGs.

Since the previous data showed that mCyclin Oβ and mCyclin OL3A show a constitutive cytoplasmic punctate pattern, we hypothesized that without any environmental stress these two proteins would directly localize to the SGs.

To check this, we transiently cotransfected expressing vectors encoding RFP-mCyclin OL3A or RFP-mCyclin Oβ with vectors for GFP-TIA-1 in the U2OS osteosarcoma cell line. The results showed that mCyclin OL3A colocalizes with TIA-1 in the cytoplasmic granules (Figure 10). For unknown reasons we could not get coexpression of Cyclin Oβ and TIA-1 in any of three independent experiments. However, we have demonstrated that Cyclin Oβ colocalizes with L3A and L3A colocalizes with TIA-1. Thus, these results let us to speculate that Cyclin Oβ and TIA-1 most likely would colocalize. Therefore, we can conclude that the L3A mutant and the β isoform of Cyclin O are constitutively localized to cytoplasmic granules compatible with being SGs.

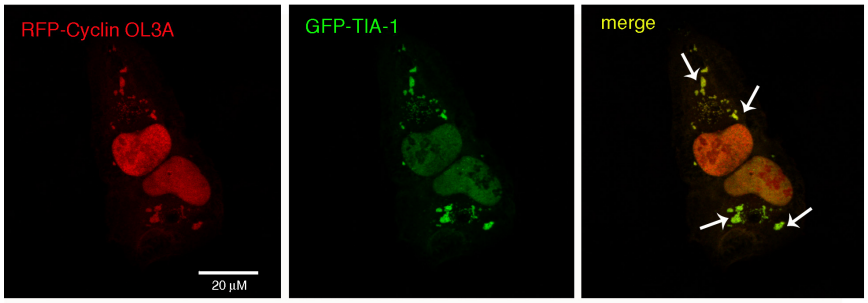

Figure 10. mCyclin OL3A colocalizes constitutively with TIA-1. Subcellular localization of RFP-mCyclin OL3A and GFP-TIA-1 expression plasmids transiently cotransfected in the U2OS cell line was analysed by confocal microscopy. White arrows indicate examples of colocalization of both proteins in the SGs.

Taking all these experiments together, we can conclude that in normal conditions transfected Cyclin Oα has a nuclear distribution, most likely due to an overexpression of the protein, but when the cell is stressed either with an environmental stress or because of the expression of Cyclin Oβ or Cyclin OL3A, Cyclin Oα translocates to the cytoplasm and localizes to cytoplasmic granules compatible with being SGs. Moreover, the L3A mutant is constitutively localized to these granules, suggesting that the mutated residues are critical for this response. To further characterise the features of the L3A mutant responsible of its constitutive localization to the SGs, we

generated chimaeric proteins containing different parts of the L3A mutant fused to GFP (Figure 11A). When we transiently transfected these constructs in the U2OS osteosarcoma cell line and independently of the treatment of the cells with thapsigargin (an ER stress inducer), we observed that they did not show a cytoplasmic punctate distribution. With this experiment we can reach two conclusions. First, that there is not an SG targeting sequence in the region we studied. Second, that the information necessary to target the protein to the SGs is more complex than the primary sequence of the protein and may involve changes in the tridimensional structure. In figure 11B are summarized the different subcellular localizations of the constructs transfected in the U2OS cell line.

A

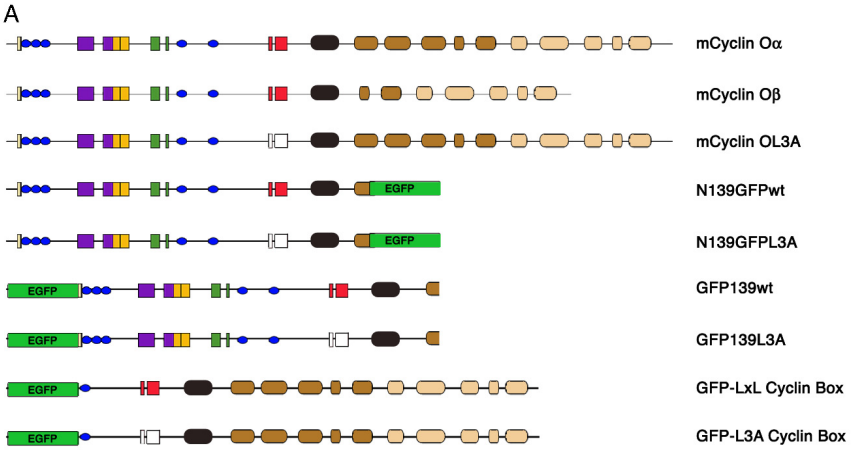

B

Construct		Nuclear	Cytoplasmic	
			Homogeneous	Punctated
Cyclin Oα	C	+++	+	-
	T	++	-	++
Cyclin Oβ	C	+	-	+++
	T	ND	ND	ND
Cyclin OL3A	C	+	-	+++
	T	ND	ND	ND
N139GFPwt	C	++	++	-
	T	++	++	-
N139GFPL3A	C	++	++	-
	T	++	++	-
GFPN139wt	C	+++	+	-
	T	+++	+	-
GFPN139L3A	C	+++	+	-
	T	+++	+	-
GFP-LxL CyclinBox	C	++	++	-
	T	++	++	-
GFP-L3A CyclinBox	C	++	++	-
	T	++	++	-

C: control
T: thapsigargin
ND: not determined

Figure 11. Representation of different constructs of Cyclin O. (A) Scheme of mCyclin Oα, mCyclin Oβ, mCyclin OL3A and the GFP fusion constructs containing different parts of the protein (N139GFPwt, N139GFPL3A, GFPN139wt, GFPN139L3A, GFP-LxL Cyclin Box, GFP-L3A Cyclin Box). The correspondence of each symbol can be found in the section 9.1 of the Introduction part. **(B)** Subcellular localization of the constructs after transient transfection into the U2OS osteosarcoma cell line. The subcellular localization of the transfected constructs was analysed in normal conditions (C) or after treatment with thapsigargin (T) (0.1 μM, 30 minutes). ND (not determined) indicates that the experiment was not done in these specific conditions. (–) indicates that the construct was negative for this specific localization, whereas (+) indicates that the construct was localized there. The number of crosses indicates the amount of protein present in this specific localization.

3.2. Endogenous Cyclin O partially colocalizes with TIA-1

Given the fact that when we stress the cells transfected Cyclin Oα colocalizes with TIA-1 in the SGs, we decided to further substantiate these findings by studying the effect of stress on the endogenous Cyclin O. We analysed by double immunofluorescence the expression of endogenous Cyclin Oα and TIA-1 after triggering ER stress by thapsigargin treatment. As it is shown in figure 12, endogenous Cyclin Oα partially colocalizes with TIA-1 in stressed cells. In addition to this, we have found that upon thapsigargin treatment there is an increase in the intensity of both TIA-1, Cyclin O and in the degree of colocalization. These results are consistent with the results showed with the transfected Cyclin Oα.

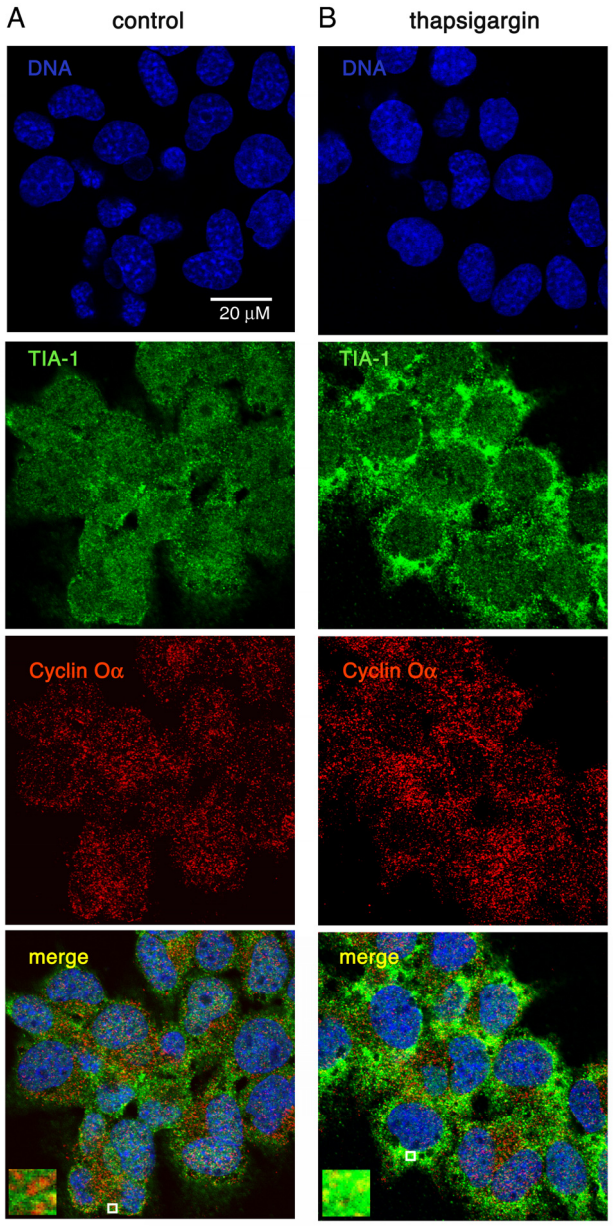

Figure 12. mCyclin O partially colocalizes with TIA-1. Subcellular localization of endogenous Cyclin Oα and TIA-1 in the pancreatic adenocarcinoma AR42J cell line was determined by confocal microscopy using anti-TIA-1 and anti-Cyclin O antibodies detected with Alexa 488-labeled anti-goat and Cy3-labeled donkey anti-rabbit secondary antibodies. Cells were incubated in standard conditions (control) **(A)** or in medium containing thapsigargin (0.1 μM) for 30 minutes **(B)**. Nuclei were stained with TOPRO-3 (DNA) and are shown in blue colour. Colocalized pixels are shown in yellow colour. Insets show the selected area at higher zoom.

4. Cyclin Oα is located in the cytoplasm, in the ER and in the mitochondria

Since Cyclin Oα is the most abundant isoform found in the cells, we focused on the study of the localization of this specific isoform. By immunohistochemistry and immunofluorescence, we have observed that endogenous Cyclin Oα is present mostly in the cell's cytoplasm showing a punctate pattern both in normal mouse, human tissues and cell lines. We have also seen that in a few cases Cyclin Oα is localized in the nucleus correlating with elevated levels of expression of the protein. Since previous evidences from our laboratory demonstrated that Cyclin Oα can bind and activate Cdk2[218], to confirm the immunolocalization experiments, we checked which subcellular fraction contained Cyclin O protein and Cyclin O--associated kinase activity. Thus, we detected Cyclin O by Western Blotting and measured Cyclin O-associated Histone H1 kinase activity using subcellular extracts from MEFs. Anti-Cyclin O immunoprecipitates show kinase activity mostly from the cytosolic fraction and minor amounts from the membrane and nuclear fractions (Figure 13A). These results correlate with the results of the immunolocalization of Cyclin Oα and Western Blotting detection in the same cellular fractions. We controlled the subcellular fractionation by Western Blotting using different protein markers (Piruvate Kinase for cytosol, BiP for ER, Histone H3 for nucleus and Vimentin for cytoskeleton) (Figure 13B), showing the correct fractionation of the cell's proteome according to its subcellular localization.

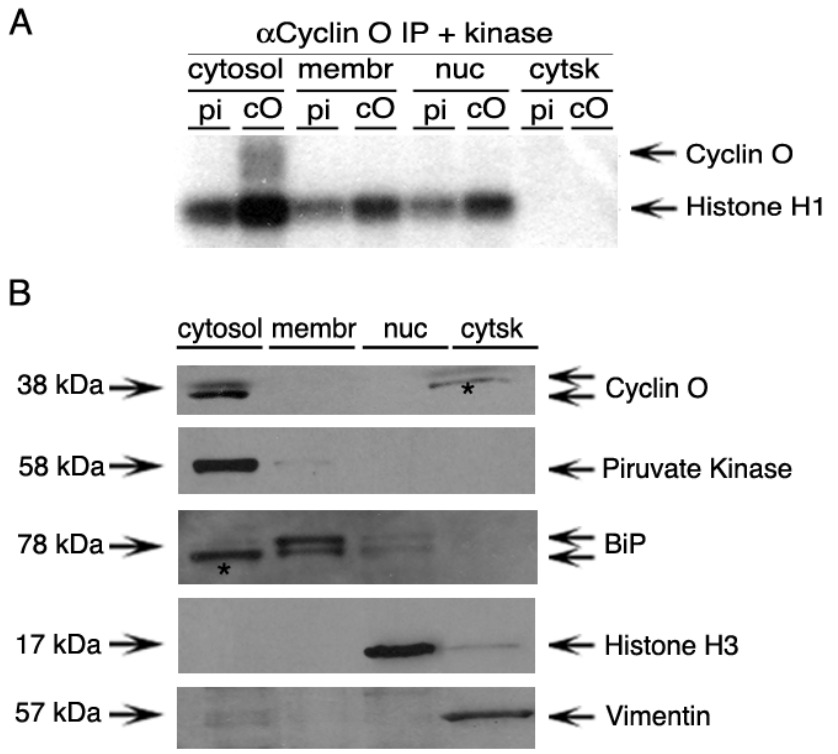

Figure 13. Endogenous Cyclin O protein and Cyclin O-associated kinase activity in subcellular fractions of MEFs. Four different fractions (cytosol, membranes (membr), nucleus (nuc) and cytoskeleton (cytsk) were obtained from MEFs after subcellular fractionation. **(A)** The different extracts were immunoprecipitated either with a preimmune serum (pi) or with anti-Cyclin O C2 antibody (cO) bound to protein-A-Sepharose beads. Immunoprecipitates were incubated with [γ-^{32}P] ATP and the exogenous substrate Histone H1 and analysed by SDS-PAGE and autoradiography. Cyclin O phosphorylation band is also indicated. **(B)** As a control of the subcellular extraction, the different extracts were analysed by Western Blotting with Piruvate Kinase, BiP, Histone H3 and Vimentin antibodies. A Western Blotting against Cyclin O done with the anti-Cyclin O C2 antibody is also shown. Asterisks indicate inespecific bands.

The previous experiments suggest that part of Cyclin Oα is associated to cellular membranes. To investigate in which organelle Cyclin Oα is present, we used confocal microscopy. Using Calreticulin and BiP as ER markers, we found that part of Cyclin Oα is located in the ER (Figure 14A and 14B). We then investigated whether Cyclin Oα colocalizes with ribosomes using RpS6 as a ribosomal protein marker (Figure 14C). We have also determined if Cyclin Oα colocalizes with other cytoplasmic structures such as the Golgi apparatus or the mitochondria. As it is shown in figure 14D, Cyclin Oα does not colocalize with the Golgi marker GM130. We have used two different methods to study the colocalization of Cyclin O with the mitochondria. First, we have used an antibody against Tom20, a protein present in the outer membrane of the mitochondria, detected by a Cy3-labeled donkey anti-rabbit secondary antibody and a biotinilated anti-Cyclin O antibody detected by Streptavidin-FITC (Figure 14E). Second, we used Mitotracker-red (Invitrogen), a mitochondria specific dye, and the N1 antibody (anti-Cyclin O) detected by a Cy2-labeled donkey anti-rabbit secondary antibody (Figure 14F). In table 1 are shown different parameters informative of the amount of colocalization found (see section 13 of the Materials & Methods part). The best colocalization parameters found are for the Cyclin O and the mitochondrial markers (Tom20 and Mitotracker). A significant colocalization between Cyclin O and Calreticulin is also observed. Although the values of colocalization between Cyclin O and BiP and Cyclin O and RpS6 are not very high, there are some areas of the confocal images where we could observe good colocalizations. The values of colocalization between Cyclin O and GM130 are very low.

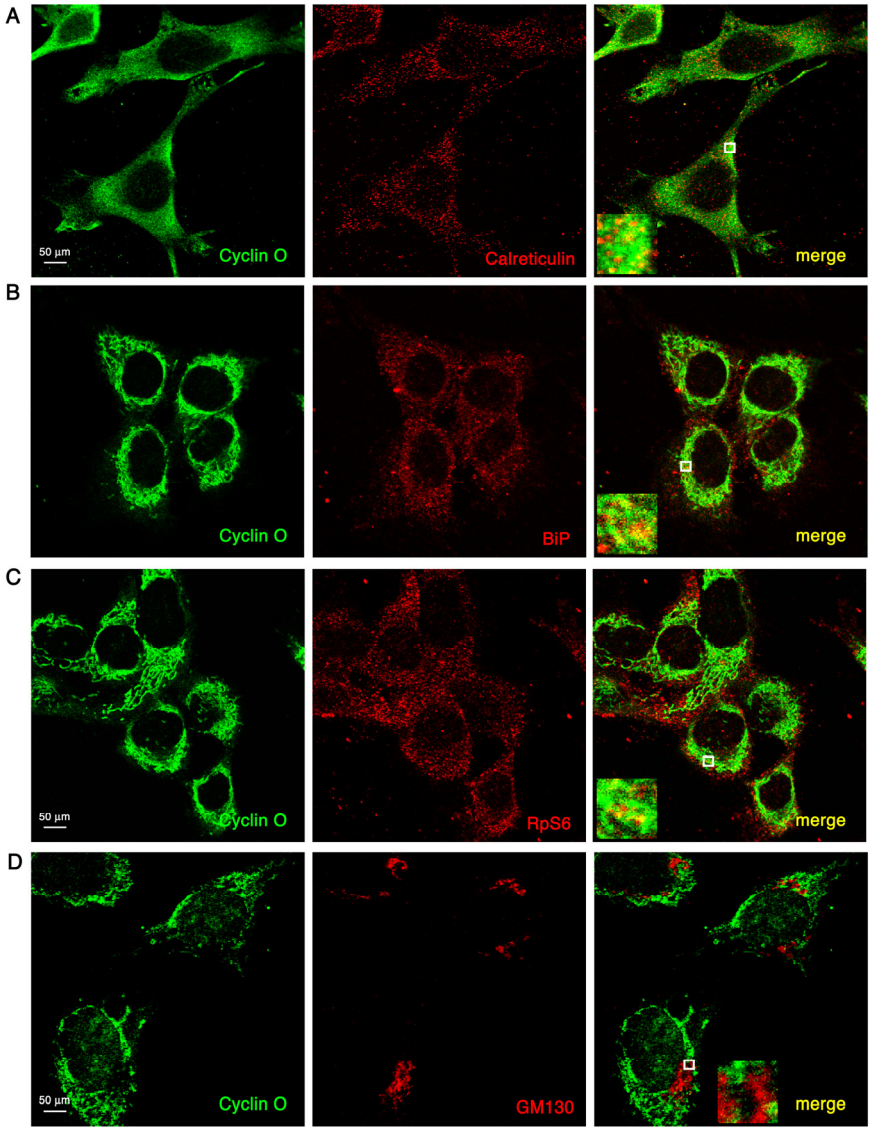
A
50 µm
Cyclin O
Calreticulin
merge
B
Cyclin O
BiP
merge
C
50 µm
Cyclin O
RpS6
merge
D
50 µm
Cyclin O
GM130
merge

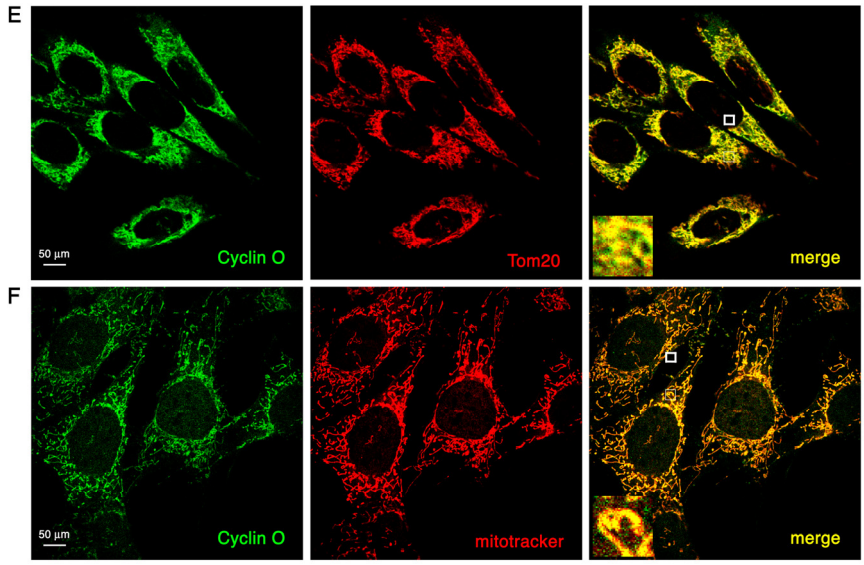

Figure 14. Cyclin Oα colocalization markers. (A) Colocalization of endogenous Cyclin O and Calreticulin in MEFs was determined by confocal microscopy using anti-Calreticulin and anti-Cyclin O antibodies detected with Alexa 555-labeled anti-mouse and Cy2-labeled donkey anti-rabbit secondary antibodies. **(B)** Colocalization of endogenous Cyclin O and BiP in MEFs was determined by confocal microscopy using anti-BiP and anti-Cyclin O antibodies detected with Cy3-labeled bovine anti-goat and Cy2-labeled donkey anti-rabbit secondary antibodies. **(C)** Colocalization of endogenous Cyclin O and RpS6 in MEFs was determined by confocal microscopy using anti-RpS6 and anti-Cyclin O antibodies detected with Cy3-labeled bovine anti-goat and Cy2-labeled donkey anti-rabbit secondary antibodies. **(D)** Colocalization of endogenous Cyclin O and GM-130 in U2OS osteosarcoma cell line was determined by confocal microscopy using anti-GM130 and anti-Cyclin O antibodies detected with Alexa 555-labeled anti-mouse and Cy2-labeled donkey anti-rabbit secondary antibodies. **(E)** Colocalization of endogenous Cyclin O and Tom20 in MEFs was determined by confocal microscopy using anti-Tom20 and biotinilated anti-Cyclin O antibodies detected with a Cy3-labeled donkey anti-rabbit secondary antibody and Streptavidin-FITC respectively. **(F)** Colocalization of endogenous Cyclin O and the mitochondria-specific Mitotracker-red dye was determined by confocal microscopy using the anti-Cyclin O antibody detected with a Cy2-labeled donkey anti-rabbit secondary antibody. Insets show the selected area at higher zoom.

	Rr	R	ICQ	Rcoloc	Percentage of Volume colocalized (%)
Cyclin O / Calreticulin	0.31 ±0.04	0.53 ±0.03	0.21 ±0.02	0.77 ±0.01	3.5 ±0.4
Cyclin O / BiP	0.2 ±0.04	0.38 ±0.03	0.23 ±0.01	0.85 ±0.02	1.1 ±0.2
Cyclin O / RpS6	0.12 ±0.03	0.37 ±0.03	0.19 ±0.01	0.89 ±0.01	1.1 ±0.4
Cyclin O / GM130	0.12	0.23	0.11	0.66	1.7
Cyclin O / Tom20	0.83 ±0.02	0.88 ±0.01	0.38 ±0.01	0.9 ±0.01	12.1 ±1.7
Cyclin O / Mitotracker	0.73 ±0.02	0.85 ±0.01	0.29 ±0.01	0.87 ±0.01	15.0 ±1.0

Table 1. Analysis of the amount of colocalization between Cyclin O and different markers. The Pearson's correlation coefficient including all the pixels (Rr); the Manders's Overlap coefficient (R); the Intensity Correlation Quotient (ICQ); the Pearson's coefficient including only in the calculation pixels showing colocalization (Rcoloc) and the percentage of Volume colocalized are shown. The values calculated with the ImageJ software are represented as the mean ± SEM.

5. Cyclin O is upregulated by ER stress and is necessary for ER stress-induced apoptosis

5.1. Cyclin O is upregulated during drug-induced ER stress

SGs are heterogeneous cytoplasmic granules not surrounded by membranes and associated with the ER. Given the fact that upon stress Cyclin Oα localized to SGs and a significant part of Cyclin Oα colocalizes with the ER, we decided to characterise if Cyclin O is related to the ER stress pathway. We then check whether ER stress modulates Cyclin O mRNA abundance. We treated WEHI7.2 cells, a cell line derived from a mouse T-cell lymphoma, with thapsigargin and DTT (ER stress inducers) and we isolated RNAs after different times. Thapsigargin blocks the ER calcium ATPase pump, leading to the depletion of ER calcium stores, whereas DTT induces protein misfolding by reducing their disulfide bonds. By means of quantitative RT-PCR we measured the abundance of Cyclin Oα and Cyclin Oβ mRNAs in the treated WEHI7.2 cells (Figure 15). We observed that Cyclin Oα and β are upregulated in a time-dependent fashion upon ER stress induction by both drugs. These results correlate with the results shown in figure 12, where upon thapsigargin treatment there is an increase in the fluorescence intensity of Cyclin O. With thapsigargin treatment the upregulation of Cyclin Oα and β mRNA is higher than with DTT. We also noticed that with both ER stress inducers the upregulation of Cyclin Oα is much higher than that of Cyclin Oβ, in agreement with the amounts of the endogenous protein levels of each isoform.

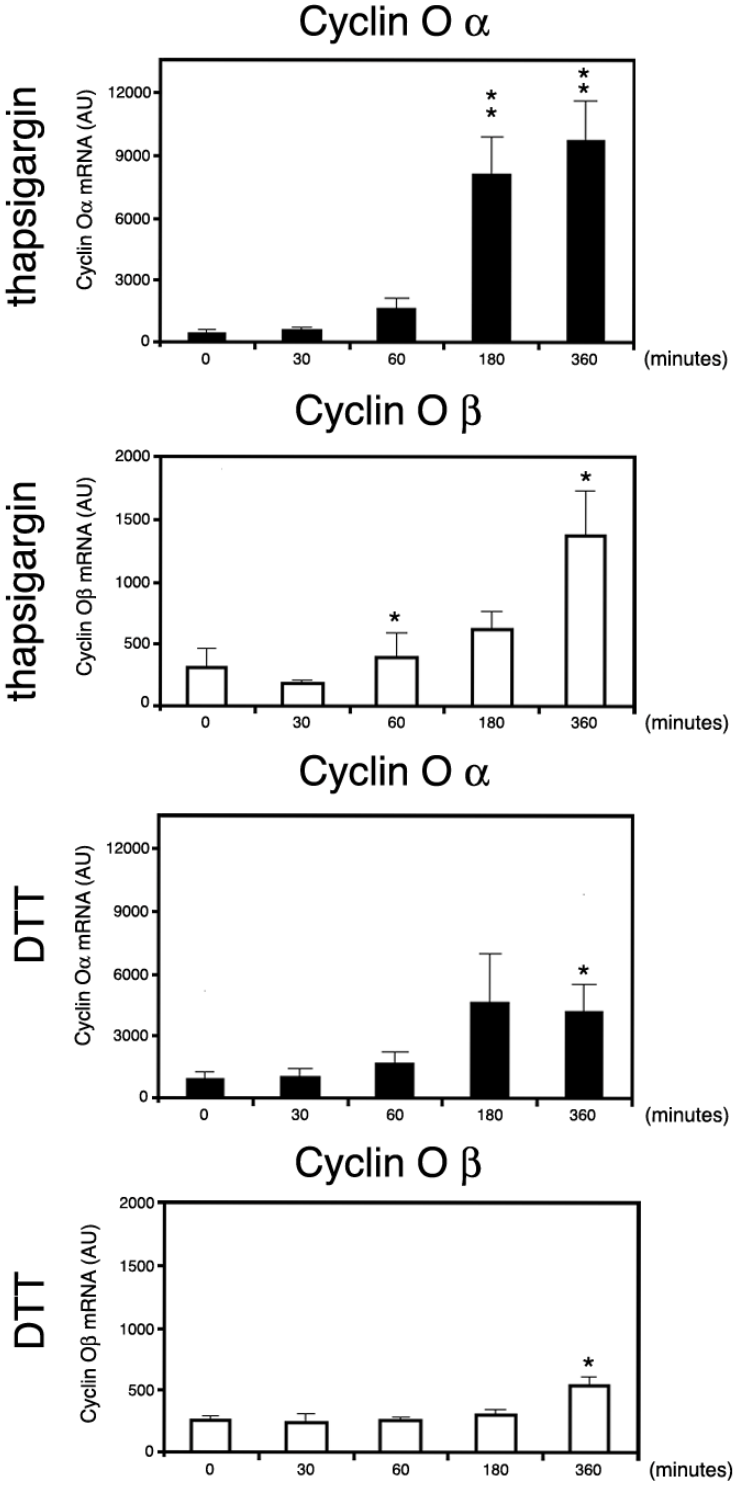
Cyclin O α
thapsigargin
Cyclin Oα mRNA (AU)
12000
9000
6000
3000
0
0
30
60
180
360
(minutes)
Cyclin O β
thapsigargin
Cyclin Oβ mRNA (AU)
2000
1500
1000
500
0
0
30
60
180
360
(minutes)
Cyclin O α
DTT
Cyclin Oα mRNA (AU)
12000
9000
6000
3000
0
0
30
60
180
360
(minutes)
Cyclin O β
DTT
Cyclin Oβ mRNA (AU)
2000
1500
1000
500
0
0
30
60
180
360
(minutes)

Figure 15. Cyclin Oα and β are upregulated by ER stress. WEHI7.2 cells were treated with 0.1 μM thapsigargin or 4 mM DTT and RNA purified from samples taken at the indicated times. The abundance of Cyclin Oα (black bars) and β (white bars) mRNAs were measured by quantitative RT-PCR. Samples were analysed in triplicate and the results shown are the mean ± the SEM of at least three independent experiments. Asterisks indicate statistically significant measures as determined by the Student's t-test.

5.2. Cyclin O is necessary for ER stress-induced apoptosis

In mammalian cells, one of the first responses to ER stress is transient global translation attenuation. This is mediated by the PERK signalling pathway. Once PERK is activated, it phosphorylates Serine-51 of eIF2α that leads to the inhibition of global protein synthesis. However, phosphorylated eIF2α allows the activation of some specific target genes such as CHOP, which can induce apoptosis[186]. To investigate if downregulation of Cyclin O expression had any effect on the signalling by ER stress, we studied the activation of the PERK pathway in a cell line transfected with an shRNA against Cyclin O. In our laboratory we have previously generated and characterised cell clones of the WEHI7.2 cell line that stably express shRNAs directed against Cyclin O or, as a control, shRNAs directed against GFP[218]. The shRNA Cyclin O expression vector used downregulates both the α and β isoforms of Cyclin O. We measured by Western Blotting the levels of phospho-Ser51-eIF2α and the induction of CHOP in WEHI7.2 cells stably transfected with a control or a Cyclin O-specific shRNA expression vector after thapsigargin or tunicamycin treatment (Figure 16). Tunicamycin is another ER stress inducer that inhibits N-linked glycosylation leading to the accumulation of non-glycosylated proteins in the ER. We observed that both the phosphorylation of eIF2α and the induction of CHOP are attenuated when Cyclin O is downregulated, which means that Cyclin O is needed to signal ER stress in WEHI7.2 cells. In agreement with this, the ER stress target gene CHOP needs longer times to be induced after downregulation of Cyclin O.

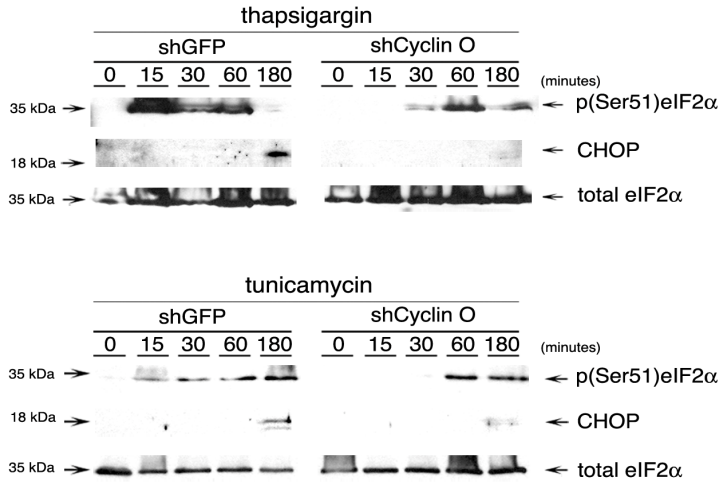

Figure 16. Downregulation of Cyclin O mRNA impairs ER stress in WEHI7.2 cells. WEHI7.2 cells stably transfected with a control (shGFP) or a Cyclin O-specific (shCyclin O) shRNA expression vectors were treated with 0.1 μM thapsigargin (upper panel) or 5 μg/mL of tunicamycin (lower panel) and samples taken at the indicated times. The levels of phospho-Ser51 eIF2α, CHOP and total eIF2α (as a control) were measured by Western Blotting. The experiment was performed at least three times with each ER stress inducer and a representative result is shown.

To further define the role of Cyclin O in the ER stress pathway, we measured the percentage of apoptosis in the control and shRNA Cyclin O WEHI7.2 cells upon ER stress treatment. Therefore, we treated these cell lines with thapsigargin, DTT or tunicamycin at different times and measured the percentage of apoptotic cells (Figure 17). In contrast to the control, the cells with Cyclin O downregulated were refractory to apoptosis induced either by thapsigargin, DTT or tunicamycin. So we can conclude that Cyclin O is necessary for ER stress-induced apoptosis. As it happened in the quantitative RT-PCR experiments shown in figure 15, the results are more evident with thapsigargin or tunicamycin than with DTT treatment.

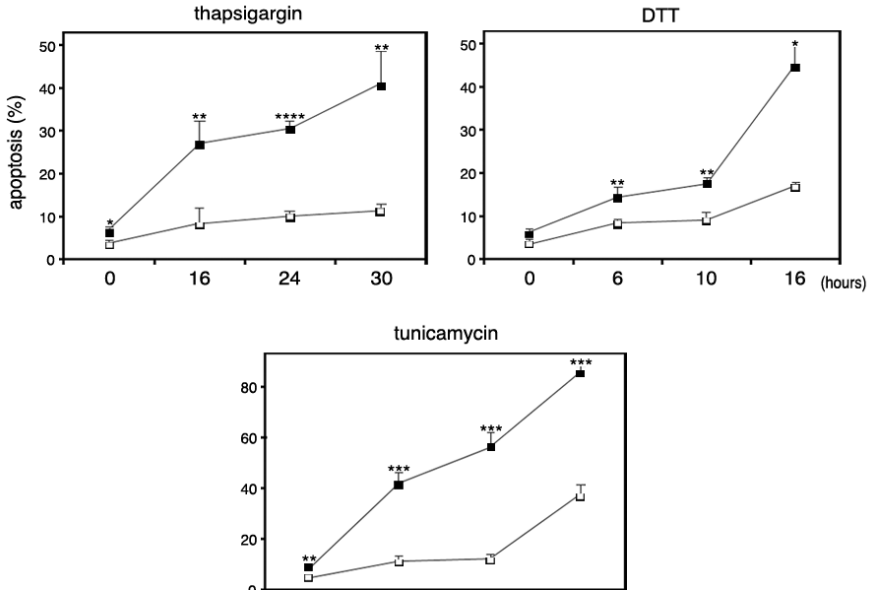

Figure 17. Cyclin Oα and β are necessary for ER stress-induced apoptosis. WEHI7.2 cells stably transfected with a control (white squares) or a Cyclin O-specific (black squares) shRNA expression vectors were treated with 0.1 μM thapsigargin, 4mM DTT or 5 μg/mL of tunicamycin, samples taken at the indicated times and processed for measuring the cellular DNA content by flow cytometry. The percentage of apoptosis (indicating the percentage of cells with subdiploid DNA content) is indicated. Samples were analysed in triplicate and the results shown are the mean ± the SEM of at least three independent experiments. Asterisks indicate statistically significant measures as determined by the Student's t-test.

6. Different apoptosis signalling mechanisms between Cyclin Oα and Cyclin Oβ

We have shown that Cyclin Oα and Cyclin Oβ are upregulated by ER stress and are necessary for ER stress-induced apoptosis. We have proven the involvement of Cyclin Oα in apoptosis[218], but we did not have any evidence for the function of the beta isoform. On the other hand, we have also shown that in transiently transfected cells, Cyclin Oα moves to TIA-1-containing cytoplasmic granules when it is cotransfected with Cyclin Oβ or Cyclin OL3A. We found interesting to find out whether Cyclin Oβ and the L3A mutant share biochemical properties with Cyclin Oα.

We first performed co-immunoprecipitation experiments using HEK-293T cells transiently transfected with either HA or myc-tagged mCyclin Oα, mCyclin Oβ or mCyclin OL3A, to detect the interaction of these proteins with Cdk2 *in vivo*. Then, we studied whether the α and β isoforms and the L3A mutant activated Cdk1/2 kinase activity using substrates such as Histone H1. As it is shown in figure 18A, Cyclin Oα and Cyclin OL3A bind to Cdk2, whereas Cyclin Oβ does not bind either Cdk2 or Cdk1 (data not shown). In agreement with these results, only Cyclin Oα and Cyclin OL3A efficiently phosphorylate Histone H1 (Figure 18B).

Finally, we have also studied if these proteins are able to induce apoptosis using colony forming experiments. Due to the poor transfectability of our reference lymphoid cell line, we have used the highly transfectable U2OS cell line to do the experiment. U2OS cells were transfected with expression vectors for mCyclin Oα, β or L3A (including the neomycin resistance gene) or with empty vector as a control, and then selected with G418 for two weeks. Colonies were fixed, stained with Coomassie Blue and counted. As it

is shown in figure 18C, about fourfold more colonies were consistently obtained in the empty vector-transfected cells versus the Cyclin Oα, β, or L3A-transfected cells. So we can conclude that Cyclin Oα, Cyclin Oβ and Cyclin OL3A are proapoptotic, but only Cyclin Oα and Cyclin OL3A coimmunoprecipitate with Cdk2 and show kinase activity. This implies that the apoptosis signalling mechanism of the β isoform does not involve Cdk1/2 activation and, then, differs from the mechanism of Cyclin Oα.

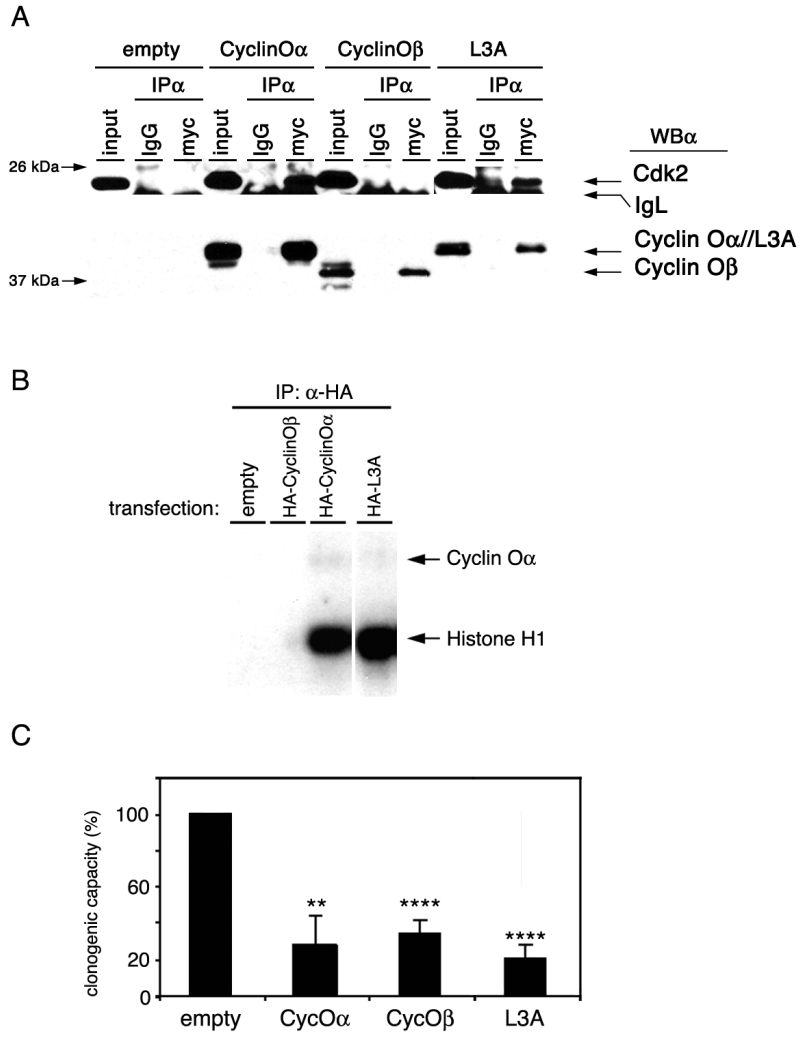

Figure 18. Interaction of Cyclin Oα and β isoforms with Cdk2. (A) Cellular extracts from HEK-293T cells transfected with empty vector or expression vectors for myc-tagged Cyclin Oα, β or L3A were immunoprecipitated with purified normal mouse IgGs or with the anti-myc tag antibody 9E10 bound to Protein-G Sepharose beads. Immunoprecipitated proteins were analysed for the presence of Cdk2 by Western Blotting. The membrane was stripped and reprobed with the anti-Cyclin O antibody C2 to detect the immunoprecipitated Cyclins Oα, β and the L3A mutant. IP: immunoprecipitation; WB: Western Blotting; IgL: Immunoglobulin light chain. **(B)** Cellular extracts from HEK-293T cells transfected with empty vector or expression vectors for HA-tagged Cyclin Oα, β or L3A were immunoprecipitated with the anti-HA tag antibody 12CA5 bound to Protein-A Sepharose beads. Immunoprecipitates were incubated with [γ-^{32}P] ATP and the exogenous substrate Histone H1 and analysed by SDS-PAGE and autoradiography. Cyclin O phosphorylation band is also indicated. **(C)** The U2OS osteosarcoma cell line was transfected with either empty pCDNA3-MycTag plasmid, or with the same plasmid driving the expression of myc-tagged Cyclin Oα, Cyclin Oβ and Cyclin OL3A. After G418 selection, colonies were stained and counted. Transfection efficiency between the different plasmids was normalized by cotransfection with an EGFP expression plasmid and quantitation by FACS of GFP positive cells 48 hours after transfection. The ratio between the number of colonies obtained for each plasmid and the number of colonies obtained by transfection of the empty vector (clonogenic capacity) is represented. The results shown are the mean ± the SEM of at least four independent experiments. Asterisks indicate statistically significant measures as determined by the Student's t-test.

7. Cyclin O overexpression leads to PERK pathway activation

We have shown that Cyclin O may be involved in the ER stress pathway since its downregulation impairs the phosphorylation of eIF2α and the induction of CHOP upon ER stress induction. These evidences indicate that Cyclin O might activate the PERK pathway. To check this, we overexpressed Cyclin O by means of infection of the pancreatic adenocarcinoma AR42J cell line with lentiviruses encoding Cyclin Oα, β or L3A. We used this pancreatic cell line because it is a well established cellular model for the study of the ER stress pathway. Lentiviral infection leads to a highly efficient expression of moderate levels of the exogenous proteins. We then checked the activation of the PERK pathway by measuring the levels of phospho-Thr980 PERK, phospho-Ser51 eIF2α and the induction of CHOP. We used thapsigargin treated cells infected with a control lentivirus as a positive control. As it is shown in figure 19, AR42J infection of the cells with lentivirus encoding Cyclin Oα, β or L3A leads to the phosphorylation of PERK-Thr980, eIF2α-Ser51 and the induction of CHOP. No effect was detected in control lentivirus-infected cells. To rule out that these results are not cell-type dependent, we performed the same experiment using MEFs obtaining similar results (data not shown). From these observations we can conclude that overexpression of Cyclin O leads to PERK pathway activation.

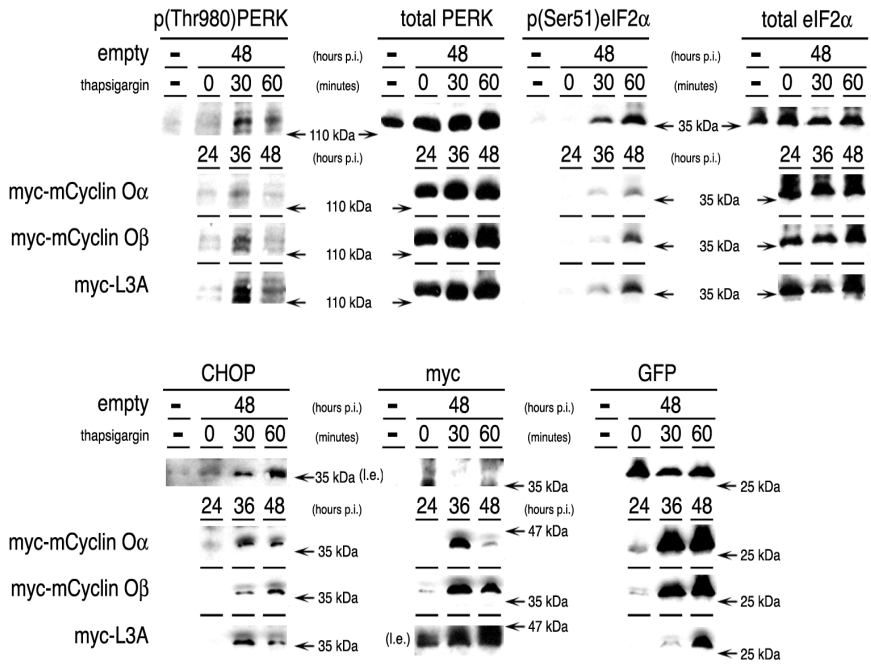

Figure 19. Cyclin O overexpression leads to PERK pathway activation. AR42J cells were infected with control (empty) or myc-tagged Cyclin Oα, β or L3A lentiviruses at a MOI of 1, harvested at the indicated times after infection and the levels of total and phospho-Thr980 PERK, total and phospho-Ser51 eIF2α and CHOP measured by Western Blotting. As a control of ER stress, cells infected with the empty lentivirus were treated with 0.1 μM thapsigargin 48 hours post-infection (hours p.i.), harvested at the indicated times and processed as the rest of the samples. The levels of expression of the proteins encoded by the lentivirus (myc-tagged Cyclin Oα, β and L3A) were detected using the anti-myc tag antibody 9E10. As a control of the efficiency of the lentiviral infection, the levels of GFP expressed from the IRES-GFP cassette encoded by the lentiviral vector were measured by Western Blotting. The experiments were performed at least three times and a representative result is shown. l.e.: long exposure.

8. Cyclin O signals ER stress through the PERK/CHOP pathway

The UPR can be initiated by three different ER membrane receptors: PERK, IRE1 and ATF6. We wished to investigate which receptor activates the expression of Cyclin O to trigger the ER stress response and rule out that this is not due to an inespecific activation of the UPR due to for example, to an overload of the protein folding capacity of the cell.

We isolated RNA from MEFs after 24, 36 or 48 hours post-infection of lentiviruses encoding Cyclin Oα, β or L3A or after thapsigargin treatment as positive control, and we studied the IRE1 pathway by measuring the IRE1-dependent splicing of XBP1 by RT-PCR. As it is shown in figure 20A, we only detected the splicing of XBP1 in cells treated with thapsigargin. So we can conclude that Cyclin O overexpression does not activate the XBP1 pathway. We then determined whether Cyclin O induces the activation of the ATF6 pathway. AR42J cells were treated with thapsigargin, as a positive control, or infected with Cyclin Oα, β or L3A encoding lentiviruses. As it is shown in figure 20B, only in the cells treated with thapsigargin the full length ATF6α band (90kDa) diminishes in intensity, which means that the cleavage of ATF6α is not produced when Cyclin O is overexpressed. These data suggest that Cyclin O overexpression does not activate the ATF6 pathway.

Finally, to demonstrate the functionality of the PERK/CHOP pathway, we measured the mRNA expression of CHOP (Figure 20C) and its target gene CA6 (Figure 20D) by quantitative RT-PCR after Cyclin O expression in MEFs. We observed that, at variance with infection with a control lentivirus, 24 hours post-infection of lentiviruses encoding Cyclin Oα, β and L3A there is a transient upregulation of the CHOP and CA6 mRNAs. So we can

conclude that Cyclin O induces the ER stress pathway by a specific activation of the PERK pathway.

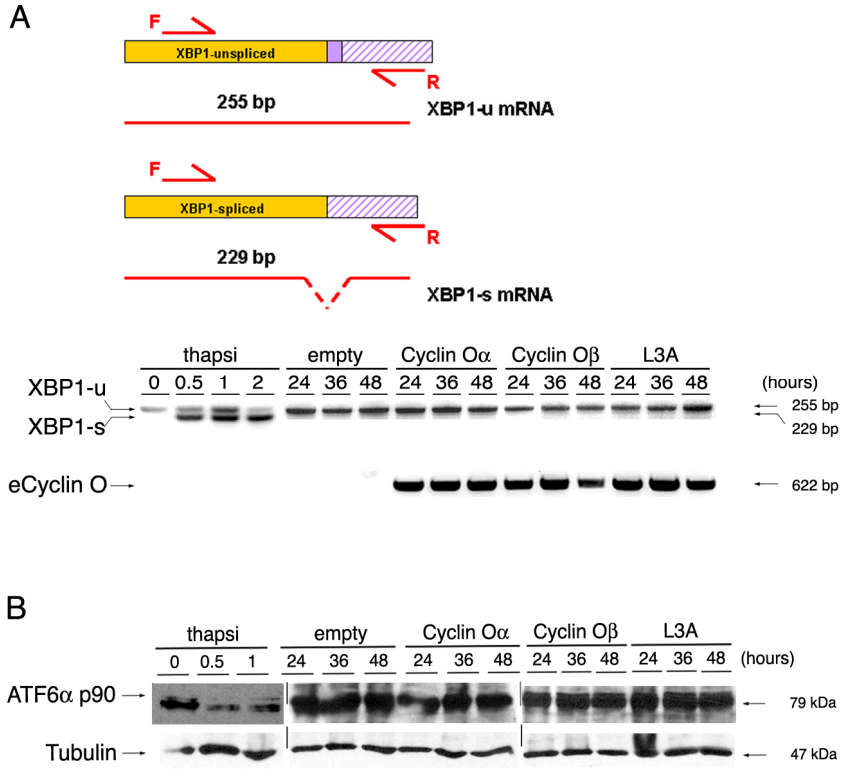

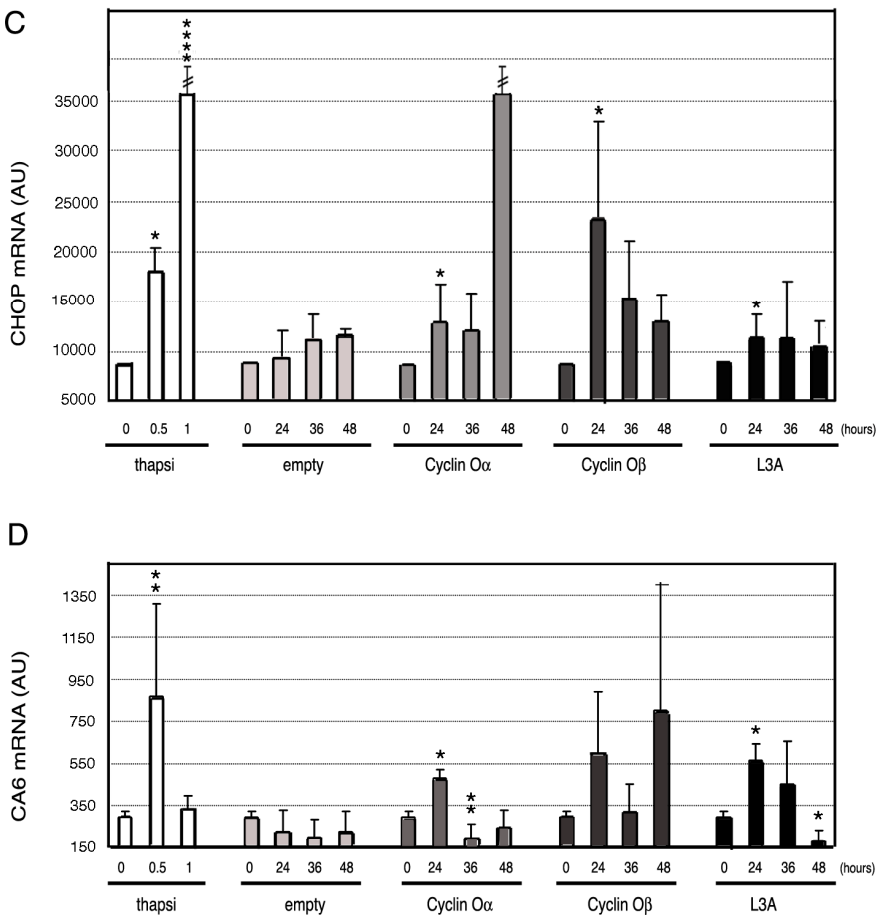

Figure 20. Cyclin O signals ER stress by selective activation of the PERK/CHOP pathway. (A) Schematic representation of unspliced (XBP1-u) and spliced (XBP1-s) forms of XBP1 mRNA**.** The red arrows represent the forward (F) and reverse (R) primers for XBP1 RT-PCR. Mouse fibroblasts were treated with 0.1 μM thapsigargin (thapsi) or infected with control (empty) or Cyclin Oα, β or L3A lentiviruses at a MOI of 1, harvested at the indicated times after infection and RNA isolated. The IRE1-dependent splicing of XBP1 was assessed by RT-PCR and detection of the unspliced product (XBP1-u) of 255 bp and the spliced product (XBP1-s) of 229 bp (upper panel). Expression of the two isoforms or the L3A mutant of Cyclin O encoded by the lentivirus (eCyclin O) was assessed in the same RNA samples by RT-PCR (lower panel). **(B)** AR42J cells were treated with 0.1 μM thapsigargin (thapsi) or infected with control (empty) or Cyclin Oα, β or L3A lentiviruses at a MOI of 1, harvested at the indicated times after infection and the levels of full length ATF6α (p90) measured by Western Blotting. The membrane was reprobed with anti-Tubulin antibody as a loading control. In (A) and (B) the

experiments were performed at least three times and a representative result is shown. Expression levels of CHOP **(C)** and its target gene CA6 **(D)** mRNAs were measured in the same RNA samples described in (A) by quantitative RT-PCR. Measures were done in triplicate. Represented are the mean values from at least three independent experiments. Bars correspond to the mean ± the SEM. Asterisks indicate statistically significant measures as determined by the Student's t-test.

9. Mechanism of PERK activation by Cyclin Oα

9.1. Cyclin Oα interacts with PERK, BiP and p58^{IPK} *in vitro*

Given the fact that part of Cyclin O is located in the ER and that Cyclin O activates the PERK pathway at a very proximal step (PERK activation) (Figure 19), we aimed to further characterise the mechanism by which the PERK pathway is activated by Cyclin O. The first approach to elucidate this question was to determine whether Cyclin O interacts directly with PERK. We performed a pull-down experiment were recombinant GST-GFP (negative control) and GST-Cyclin Oα previously bound to Glutathione-Sepharose Beads were incubated with M6 cell extracts. M6 human colon adenocarcinoma cells where used because of the high levels of expression of endogenous Cyclin O and PERK. The M6 cell extracts were previously precleared with the fusion protein GST-RFP bound to glutathione beads, to avoid non-specific interactions. After exhaustive washing, the proteins bound to the beads were analysed by Western Blotting. As it is shown in figure 21, Cyclin Oα interacts with PERK, whereas the negative control does not. We speculated that the bands observed in the anti-PERK Western Blotting could be due to different phosphorylation status of this Ser/Thr protein kinase that have different gel mobility shifs. Since the analysis of this Western Blot with the phospho-Thr980 PERK antibody did not yield conclusive results, we probed the membrane with an anti-phosphoserine/threonine antibody. This Western Blotting yielded a single group of bands with the same mobility than the bands obtained in the anti-PERK Western Blot, supporting the idea that they correspond to phosphorylated forms of PERK. We also checked whether Cyclin Oα interacts with Cdk2 and Cdk1 in these conditions. Surprinsgly, we found that neither Cdk2 nor Cdk1 is detectable in the complexes recovered.

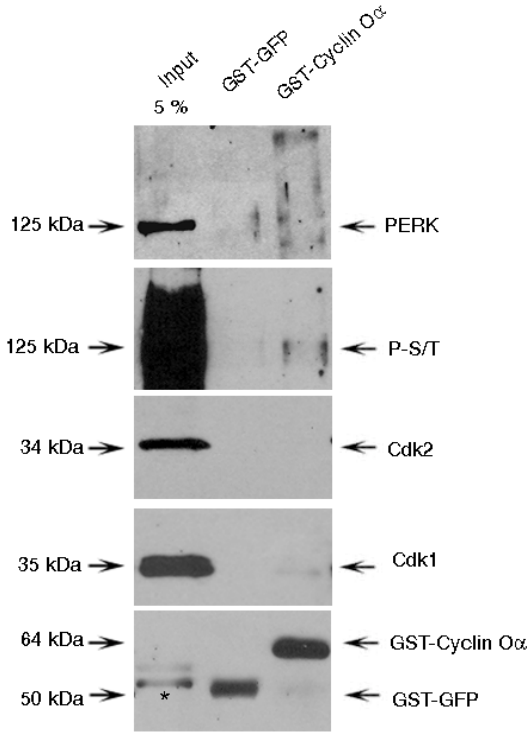

Figure 21. Cyclin Oα interacts with PERK *in vitro*. 5 μg of recombinant protein (GST-GFP, GST-Cyclin Oα) were incubated with 25 μl of Glutathione-Sepharose beads (3 hours, 4 ºC). After extensive washing, samples were incubated with 20 mg/ml BSA to avoid inespecific binding (3 hours, 4 ºC). Then, beads were incubated o/n at 4 ºC with the M6 cell extracts, previously precleared with GST-RFP recombinant protein. The proteins bound to the beads were analysed by Western Blotting using the indicated antibodies: PERK, phosphoserine/threonine (P-S/T), Cdk2 and Cdk1. The membrane was reprobed with anti-GST antibody to detect the recombinant proteins. 5 % represents the amount of protein loaded in the input with respect to the total amount of extract used in the pull-down samples. Asterik indicates inespecific bands.

These results suggest that Cyclin Oα and PERK are part of the same protein complex, but it cannot be concluded whether this interaction is direct or mediated via other proteins. PERK is a transmembrane protein that binds to other proteins such as BiP or p58^{IPK}. To check whether Cyclin O can interact with these proteins, we performed pull-down experiments in which the proteins bound to GST-Cyclin Oα beads were analysed by Western

Blotting against BiP or p58$^{IPK.}$ As a negative control, instead of using the recombinant protein GST-GFP we used GST alone, since the GST-GFP fusion protein comigrates with p58^{IPK} and impairs its detection. In figure 22 we show that BiP is present in the Cyclin Oα complexes. These findings correlate with the results shown in figure 14 where we observed that Cyclin Oα colocalizes with BiP by confocal microscopy.

Similar experiments showed that Cyclin Oα interacts with p58^{IPK} (Figure 23). We also observed that the interaction of Cyclin Oα with p58^{IPK} is independent of the thapsigargin treatment.

All these results suggest that Cyclin Oα interacts with PERK, BiP and p58^{IPK}.

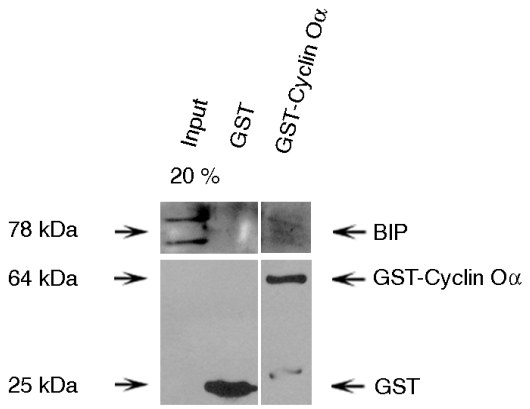

Figure 22. Cyclin Oα interacts with BiP *in vitro*. 5 μg of recombinant protein (GST, GST-Cyclin Oα) were incubated with 25 μl of Glutathione-Sepharose beads (3 hours, 4 ºC). After extensive washing, samples were incubated with 20 mg/ml BSA to avoid inespecific binding (3 hours, 4 ºC).Then, beads were incubated o/n at 4 ºC with the M6 cell extracts, previously precleared with GST-RFP recombinant protein. The proteins bound to the beads were analysed by Western Blotting using the BiP antibody. The membrane was reprobed with anti-GST antibody to detect the recombinant proteins. 20 % represents the amount of protein loaded in the input with respect to the total amount of extract used in the pull-down samples.

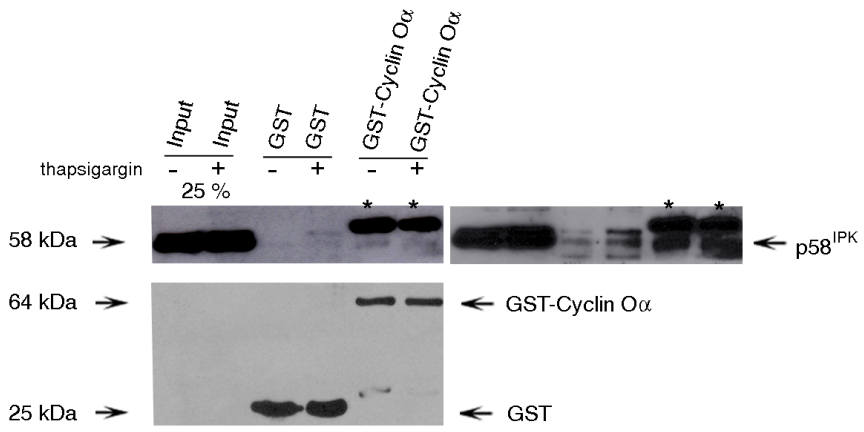

Figure 23. Cyclin Oα interacts with p58^{IPK} *in vitro*. 5 μg of recombinant protein (GST, GST-Cyclin Oα) were incubated with 25 μl of Glutathione-Sepharose beads (3 hours, 4 ºC). After extensive washing, samples were incubated with 20 mg/ml BSA to avoid inespecific binding (3 hours, 4 ºC). Then, beads were incubated o/n at 4 ºC with the M6 cell extracts, previously precleared with GST-RFP recombinant protein. M6 cell extracts were cultured in standard conditions (-) or treated with thapsigargin (0.1 μM, 30 minutes) (+). The proteins bound to the beads were analysed by Western Blotting using the p58^{IPK} antibody. The film was overexposed to enhance the detection of the bands (right panel). The membrane was reprobed with anti-GST antibody to detect the recombinant proteins. Asterisks indicate the recombinant proteins detected inespecifically by the p58^{IPK} antibody. 25 % represents the amount of protein loaded in the input with respect to the total amount of extract used in the pull-down samples.

9.2. Cyclin Oα colocalizes with p58^{IPK}

To corroborate that Cyclin Oα interacts with p58^{IPK} we used colocalization experiments using confocal microscopy. We performed a triple staining with Cyclin O, mitotracker and p58^{IPK} (Figure 24). As we showed before in other cell types, Cyclin Oα colocalizes significantly with the mitochondria in M6 cells. We also observed that a substantial amount of Cyclin Oα is associated with p58^{IPK}. P58^{IPK} also colocalizes partially with mitotracker, but the amount of colocalization is smaller than with Cyclin Oα. The high degree of colocalization of Cyclin Oα with p58^{IPK} is in agreement with the strong

interaction of these two proteins observed in the pull-down experiments. M6 cells are epithelial-like cells that grow forming compact colonies. We observed that the distribution of Cyclin Oα, mitotracker and p58^{IPK} is not uniform in the colony, being their levels higher in the periphery of the colony than in the centre. We did not observe these differences in non-epithelial cells such as MEFs. The fact that Cyclin Oα, p58^{IPK} and mitotracker have similar distribution inside the cell and in the context of the colony may indicate that they are involved in the same function. In table 2 are shown different parameters indicative of the amount of colocalization between the different proteins. The values of colocalization of Cyclin O with mitotracker and Cyclin O with p58^{IPK} are comparable. The colocalization parameters between mitotracker and p58^{IPK} indicate a poorer degree of colocalization.

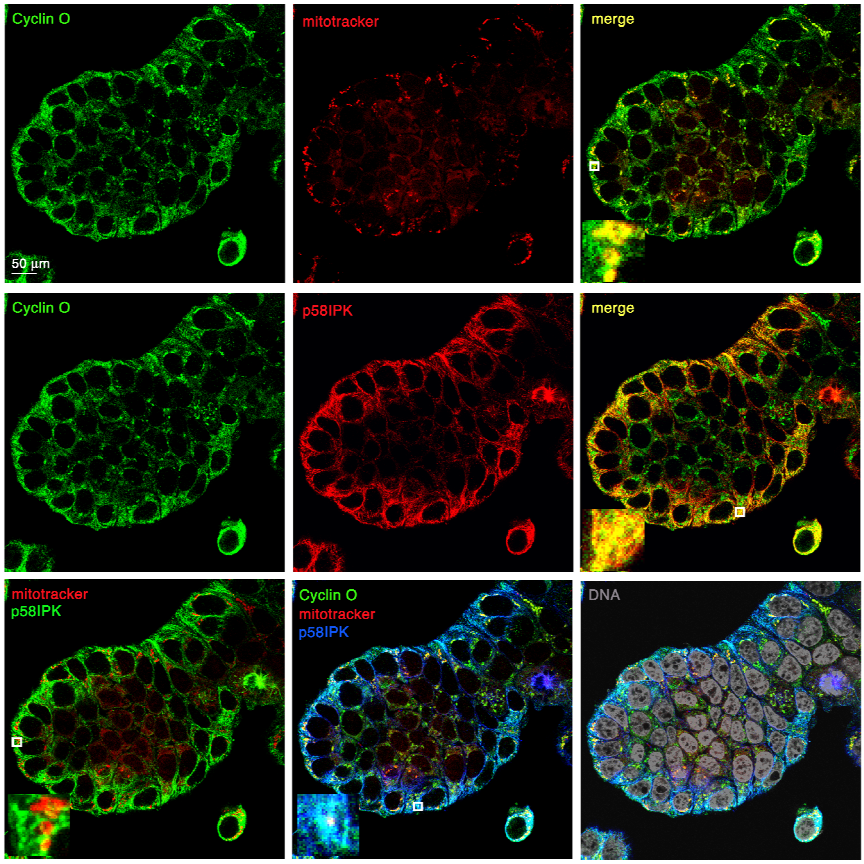

Figure 24. Cyclin Oα is partially located in the mitochondria and colocalizes with p58^{IPK}. Colocalization of Cyclin O, mitotracker and p58^{IPK} in M6 cell line was determined by confocal microscopy using anti-p58^{IPK} and biotinilated anti-Cyclin O antibodies detected with Alexa 647-labeled anti-rabbit secondary antibody and Streptavidin-FITC. Nuclei were stained with DAPI (DNA) and are shown in purple colour. Insets show the selected area at higher zoom.

	Rr	R	ICQ	Rcoloc	Percentage of Volume colocalized (%)
Cyclin O / Mitotracker	**0.54** ±0.05	**0.79** ±0.03	**0.19** ±0.01	**0.82** ±0.02	**25** ±6
Mitotracker / p58^{IPK}	**0.31** ±0.07	**0.62** ±0.04	**0.15** ±0.02	**0.76** ±0.03	**18** ±5
Cyclin O / p58^{IPK}	**0.58** ±0.08	**0.77** ±0.05	**0.26** ±0.03	**0.8** ±0.02	**30** ±4

Table 2. Analysis of the amount of colocalization between Cyclin O, Mitotracker and p58^{IPK}. The Pearson's correlation coefficient including all the pixels (Rr); the Manders's Overlap coefficient (R); the Intensity Correlation Quotient (ICQ); the Pearson's coefficient including only in the calculation pixels showing colocalization (Rcoloc) and the percentage of Volume colocalized are shown. The values calculated with the ImageJ software are represented as the mean ± SEM.

10. Participation of Cyclin O in the activation of other eIF2α kinases

10.1. Downregulation of Cyclin O mRNA impairs stress induced by sodium arsenite or UV irradiation

Cells respond to different types of stress reducing global translation by triggering the phosphorylation of the α-subunit of eIF2 at residue Ser51. The phosphorylation of eIF2α is mediated by four distinct proteins kinases: HRI, GCN2, PKR and PERK. HRI, present mostly in erythroid cells, is activated under conditions of low haem or treatment with arsenite, osmotic or heat shock[84]. GGN2 is activated in response to amino acid starvation[229] and UV irradiation[230]. PKR is activated by double-stranted RNA[231] and finally PERK is activated in response to ER stress. We have previously seen that Cyclin O activates the PERK pathway, and we wandered whether other eIF2α kinases could also be activated by Cyclin O. To investigate this, we treated WEHI7.2 cells stably transfected with a control or a Cyclin O-specific shRNA expression vector with different types of stress such as sodium arsenite or UV irradiation. We measured by Western Blotting the levels of phospho-eIF2α after treating the cells for different times with sodium arsenite (Figure 25A) or UV light (Figure 25B). We found that in both cases the phosphorylation of eIF2α is decreased when Cyclin O is downregulated. So we can conclude that downregulation of Cyclin O mRNA impairs stress produced by sodium arsenite treatment or UV irradiation in WEHI7.2 cells. Thus, Cyclin O may also be involved in the activation of other eIF2α kinases.

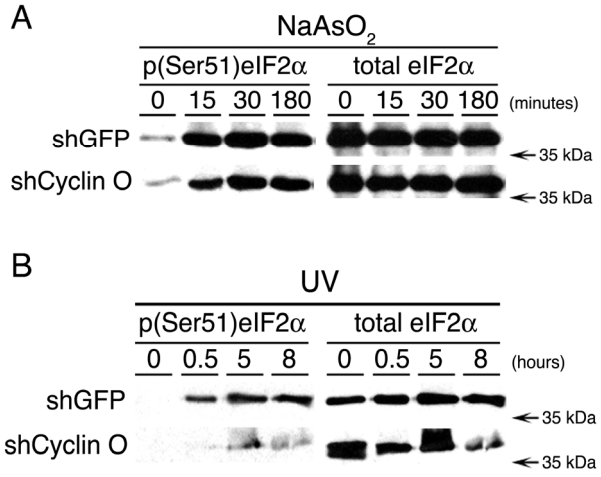

Figure 25. Downregulation of Cyclin O mRNA impairs stress produced by arsenite treatment or UV irradiation in WEHI7.2 cells. WEHI7.2 cells stably transfected with a control (shGFP) or a Cyclin O-specific shRNA expression vector (shCyclin O) were treated with 400 μM sodium arsenite ($NaAsO_2$) **(A)** or 50 mJ/cm^2 of UV irradiation **(B)** and samples taken at the indicated times. The levels of phospho-Ser51 eIF2α and total eIF2α (as a control) were measured by Western Blotting. The experiment was performed at least three times with each stress inducer and a representative result is shown.

10.2. Cyclin O colocalizes with eIF2α kinases

To further investigate the involvement of Cyclin O in the activation of other eIF2α kinases, we studied the colocalization of Cyclin O with PERK, PKR and HRI. We performed three colour labelling of Cyclin O, mitotracker and each eIF2α kinase in MEFs. Cyclin O partially colocalizes with PERK (Figure 26). We found significant colocalization between Cyclin O and PERK in other cells types such as AR42J or M6 cells, characterised by having a well developed ER (data not shown). Cyclin O colocalizes significantly with PKR (Figure 27) and HRI (Figure 28). In tables 3, 4 and 5 are shown different parameters indicating the amount of colocalization of

the proteins studied. For all the stainings, the values of colocalization of Cyclin O with mitotracker are comparable. The best colocalization parameters found are for Cyclin O and mitotracker. The colocalization parameters between the different eIF2α kinases and Cyclin O are better than with mitotracker. Among the eIF2α kinases studied, HRI/Cyclin O shows the best colocalization parameters, but the differences are subtle.

Taking all these results together, we can conclude that Cyclin O may be involved in the activation of all the eIF2α kinases and its function may be related to its localization in the mitochondria.

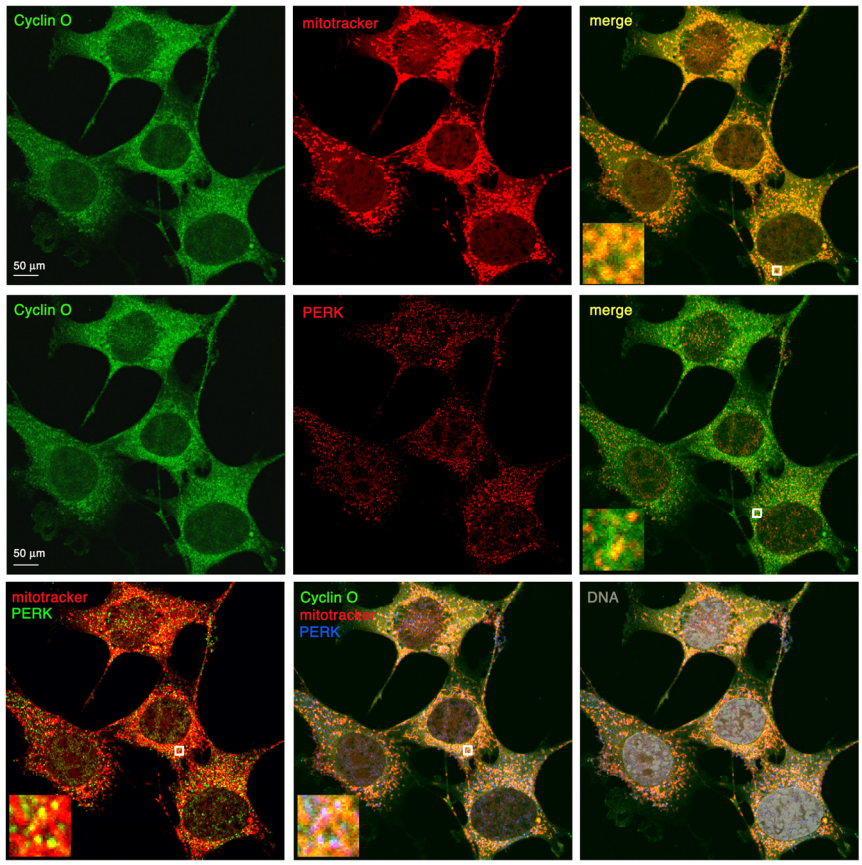

Figure 26. Cyclin Oα is partially located in the mitochondria and colocalizes with PERK. Colocalization of endogenous Cyclin O, mitotracker and PERK in MEFs was determined by confocal microscopy using anti-PERK and biotinilated anti-Cyclin O antibodies detected with Alexa 647-labeled anti-rabbit secondary antibody and Streptavidin-FITC and the mitochondria-specific dye Mitotracker-red. Nuclei were stained with DAPI (DNA) and are shown in purple colour. Insets show the selected area at higher zoom.

	Rr	R	ICQ	Rcoloc	Percentage of Volume colocalized (%)
Cyclin O / Mitotracker	**0.73** ±0.02	**0.85** ±0.01	**0.3** ±0.01	**0.87** ±0.01	**18** ±1
Mitotracker/ PERK	**0.43** ±0.03	**0.64** ±0.02	**0.25** ±0.01	**0.71** ±0.01	**11** ±1
Cyclin O/ PERK	**0.46** ±0.04	**0.66** ±0.02	**0.24** ±0.02	**0.77** ±0.01	**9** ±1

Table 3. Analysis of the amount of colocalization between Cyclin O, Mitotracker and PERK. The Pearson's correlation coefficient including all the pixels (Rr); the Manders's Overlap coefficient (R); the Intensity Correlation Quotient (ICQ); the Pearson's coefficient including only in the calculation pixels showing colocalization (Rcoloc) and the percentage of Volume colocalized are shown. The values calculated with the ImageJ software are represented as the mean ± SEM.

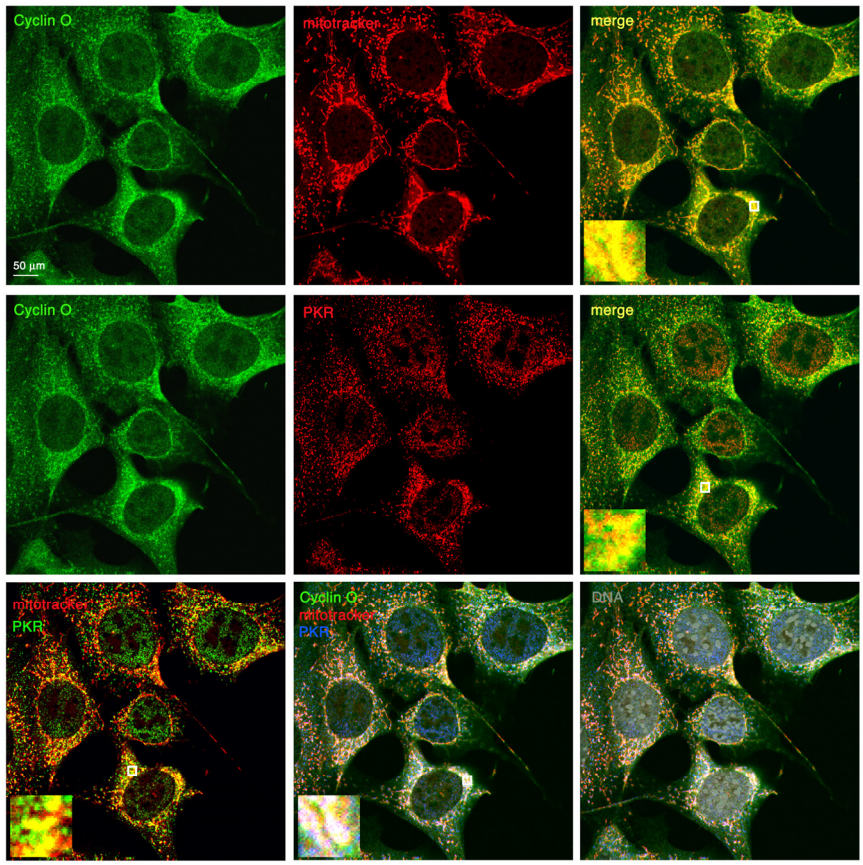

Figure 27. Cyclin Oα is partially located in the mitochondria and colocalizes with PKR. Colocalization of endogenous Cyclin O, mitotracker and PKR in MEFs was determined by confocal microscopy using anti-PKR and biotinilated anti-Cyclin O antibodies detected with Alexa 647-labeled anti-rabbit secondary antibody and Streptavidin-FITC and the mitochondria-specific dye Mitotracker-red. Nuclei were stained with DAPI (DNA) and are shown in purple colour. Insets show the selected area at higher zoom.

	Rr	R	ICQ	Rcoloc	Percentage of Volume colocalized (%)
Cyclin O / Mitotracker	0.75 ±0.01	0.85 ±0.01	0.29 ±0.01	0.89 ±0.01	15 ±2
Mitotracker / PKR	0.52 ±0.02	0.7 ± 0.01	0.25 ±0.01	0.79 ±0.01	10 ±2
Cyclin O / PKR	0.52 ±0.04	0.7 ± 0.02	0.26 ±0.01	0.82 ±0.01	10 ±3

Table 4. Analysis of the amount of colocalization between Cyclin O, Mitotracker and PKR. The Pearson's correlation coefficient including all the pixels (Rr); the Manders's Overlap coefficient (R); the Intensity Correlation Quotient (ICQ); the Pearson's coefficient including only in the calculation pixels showing colocalization (Rcoloc) and the percentage of Volume colocalized are shown. The values calculated with the ImageJ software are represented as the mean ± SEM.

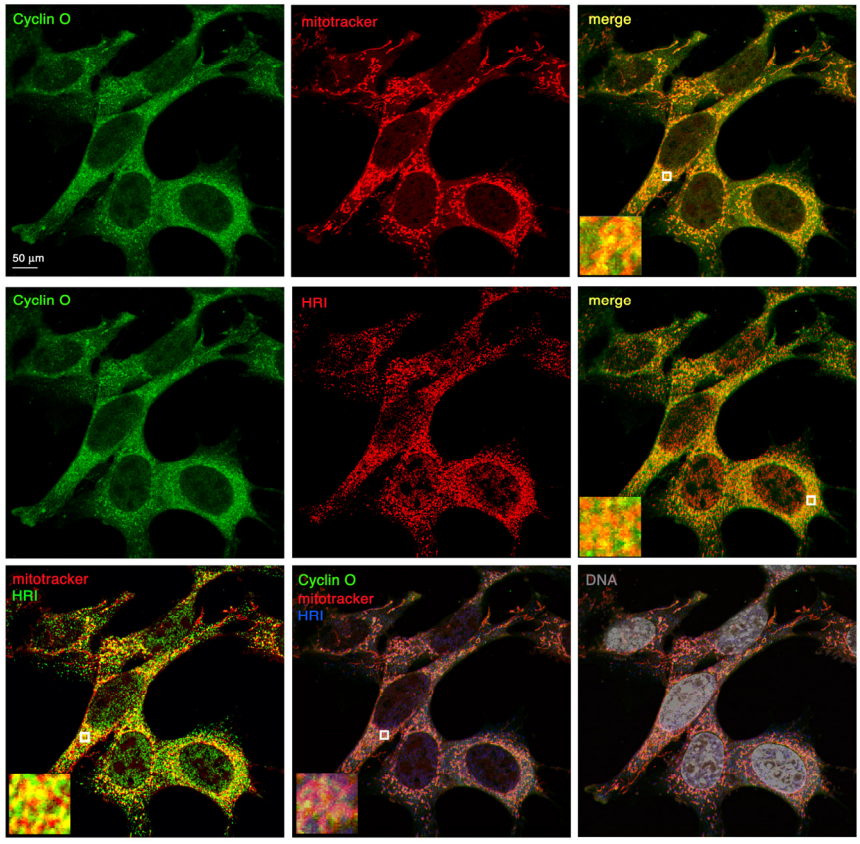

Figure 28. Cyclin Oα is partially located in the mitochondria and colocalizes with HRI. Colocalization of endogenous Cyclin O, mitotracker and HRI in MEFs was determined by confocal microscopy using anti-HRI and biotinilated anti-Cyclin O antibodies detected with Alexa 647-labeled anti-rabbit secondary antibody and Streptavidin-FITC and the mitochondria-specific dye Mitotracker-red. Nuclei were stained with DAPI (DNA) and are shown in purple colour. Insets show the selected area at higher zoom.

	Rr	R	ICQ	Rcoloc	Percentage of Volume colocalized (%)
Cyclin O / Mitotracker	**0.71** ±1.4	**0.85** ±0.4	**0.28** ±0.7	**0.86** ±0.8	**19** ±0.4
Mitotracker / HRI	**0.55** ±4.3	**0.73** ±2.1	**0.26** ±0.9	**0.76** ±1.2	**16** ±2
Cyclin O / HRI	**0.59** ±5.4	**0.76** ±2.9	**0.26** ±1.8	**0.8** ±1.2	**16** ±3

Table 5. Analysis of the amount of colocalization between Cyclin O, Mitotracker and HRI. The Pearson's correlation coefficient including all the pixels (Rr); the Manders's Overlap coefficient (R); the Intensity Correlation Quotient (ICQ); the Pearson's coefficient including only in the calculation pixels showing colocalization (Rcoloc) and the percentage of Volume colocalized are shown. The values calculated with the ImageJ software are represented as the mean ± SEM.

DISCUSSION

1. Expression pattern of Cyclin O

The expression pattern of Cyclin Oα and Cyclin Oβ in mouse tissues was analysed by semi-quantitative RT-PCR. The expression levels of Cyclin O mRNA in normal conditions are low in most tissues. About 40 cycles of PCR are necessary to detect the mRNA of Cyclin O, whereas for HPRT 30 cycles are enough. This means that Cyclin O is approximately 1000 times less abundant than HPRT. Although the mRNA levels are low we can detect its expression in a wide range of tissues (Figure 1B of the Results section). A different expression pattern between both isoforms is observed without an evident relationship. We can detect the expression of both Cyclin Oα and Cyclin Oβ in several tissues including liver, intestine, brain, testis and kidney and the expression of Cyclin Oα alone in lung, heart and ovary. The highest expression of both isoforms is detected in testis and brain. However, we have not further characterised the physiology of their expression in these tissues.

By immunohistochemistry we can detect expression of Cyclin O in a wide range of tissues, in agreement with the semi-quantitative RT-PCR data, and also in cell lines (Figure 2 of the Results section). In the majority of tissues and cell lines Cyclin O expression is cytoplasmic. Most of the members of the Cyclin family perform their function in the nucleus. This suggests that either Cyclin O is localized in the cytoplasm and goes to the nucleus when is needed or, on the contrary, it performs its function in the cytoplasm. Nuclear export and import of proteins and RNAs is a regulated process that permits the control of protein expression during cell development and differentiation. In all eukaryotic organisms transport of proteins to specific cellular compartments requires specific signalling sequences[232]. Most proteins that shuttle between the nucleus and the cytoplasm have NLS and/or NES signals. As the N-terminal part of Cyclin O contains putative regulatory

motifs, including an NLS and an NES, we hypothesize that both motifs regulate its subcellular localization (see section 2).

2. Structure of Cyclin O

Cyclin O is composed by a highly conserved C-terminal Cyclin Box and a less conserved N-terminal part composed by the first 100 amino acids. This N-terminal part is rich in basic amino acids and contains several conserved putative regulatory motifs, including an NLS [$_{30}$***KK***S***RR***PCL***RRK***$_{40}$], a Cy motif, a GSK3β phosphorylation site [$_{63}$***S***PS***S***$_{66}$], a β-Trcp interacting motif [$_{54}$***DS***GVC***D***$_{59}$] and an [$_{92}$***L***TA***L***D***L***$_{97}$]motif, which resembles a NES (Figure 5 of the Results section). Dingwall *et al.*[233] proposed the consensus sequence [K-K/R-x-K/R] (x = any amino acid) for monopartite NLS. Based on Ikuta *et al.*[234] the consensus sequence of a NES is [Lx$_{1-3}$ Lx$_{2-3}$ LxL], where the last leucine can be replaced by conservative substitutions (isoleucine, valine, etc). To check if the $_{92}$***L***TA***L***D***L***$_{97}$ motif corresponds to a NES, we mutated the ***L***TA***L***D***L*** motif to ***A***TA***A***D***A*** which we called L3A mutant (Figure 6B of the Results section). Transient transfection experiments showed that the ***L***TA***L***D***L*** motif does not correspond to a functional NES (Figure 6C of the Results section). Further analysis of a database of NES[235] has detected one more putative NES motif located in the α3' helix between the residues 284 and 292 (Figure 18 of the Introduction section). Further mutagenesis studies of this element and of the bipartite NLS motif predicted by bioinformatics tools, (http://cubic.bioc.columbia.edu/cgi/var/nair/resonline.pl), will be necessary to understand if the subcellular localization of the Cyclin O is regulated or not by the NLS/NES system.

GSK3 is a serine-threonine kinase that was initially identified as a kinase which phosphorylated and inactivated Glycogen Synthase. GSK3 has two isoforms (alpha and beta), being the most common the beta isoform. GSK3β is a key regulatory component of a large number of cellular processes such as glucose metabolism, protein synthesis, neuronal cell development and body pattern formation[236]. The consensus sequence for a

GSK3 substrate is [S/T-xxx-S/T (P)], where the first serine or threonine is the target residue and x can be any amino acid. The SCF (Skp1, Cul1, F-box protein) complex E3 ubiquitin ligases target many proteins for proteolysis in diverse cellular processes[237]. β-Trcp, an F-box protein of the $SCF^{\beta\text{-Trcp}}$, recognizes the doubly phosphorylated DSG motif [DpSGΦxpS], where Φ represents a hydrophobic amino acid and x represents any amino acid, in various $SCF^{\beta\text{-Trcp}}$ target proteins. The phosphoserine residues within the DSG motif are essential for the target proteins to bind β-Trcp[238]. The GSK3 phosphorylation motif of the transcription factor Snail[239] and the β-Trcp destruction box of both mouse Snail and human Cdc25A[240] proteins are similar to the sequence identified in the Cyclin O protein: [$_{95}$***DSG***KG***S***QPP***S***PP***S***$_{107}$] (mSnail), [$_{81}$***DSG***FCL***DS***$_{88}$] (hCdc25A) and [$_{54}$***DSG***VC***D***LFE***S***PS***S***$_{66}$] (mCyclin O). As it happens in the regulation of the transcription factor Snail[239], we speculate that GSK3β binds and phosphorylates Cyclin O, which regulates its β-Trcp-mediated ubiquitination and hence, its proteasome-mediated degradation. Previous results of our laboratory support this hypothesis since we observed that Cyclin O can be phosphorylated by GSK3 *in vitro*, and Li^+ treatment (a GSK3 inhibitor) stabilizes Cyclin O (data not shown). Cyclin O contains a highly conserved consensus sequence [$_{63}$***S***PS***S***$_{66}$], which could be phosphorylated by GSK3β. Most substrates of GSK3β must first be phosphorylated by another protein kinase at a serine or threonine residue located four residues C-terminal to the site of the GSK3 phosphorylation, that it is called *priming phosphorylation site*. In the case of Cyclin O at this position is found an aspartic acid residue (D69), which because of its negative charge could mimic the *priming phosphorylation site*. The GSK3β phosphorylation motif of Cyclin O overlaps with the putative β-Trcp binding motif [$_{54}$***DSG***VC***D***$_{59}$]. We hypothesize that, as happens with the human Cdc25A [$_{81}$***DSG***FCL***DS***$_{88}$], negative charges near the DSG motif function to upregulate β-Trcp binding in the Cyclin O

protein. Both the putative β-Trcp binding motif and the GSK3β phosphorylation site (the D69 residue of murine Cyclin O) are conserved in all the Cyclin O sequences known (Figure 5 of the Results section).

3. The cytoplasmic puntacte pattern of Cyclin O

All the immunohistochemistry experiments presented in this thesis have been performed using the N1 antibody, which recognizes both α and β isoforms (Figure 2 of the Results section). We have generated antibodies recognizing only Cyclin Oα or Cyclin Oβ and demonstrated their specificity. Both isoforms show a cytoplasmic punctate pattern by immunofluorescence (Figure 3 of the Results section). Cyclin Oα shows a fine and uniform dotted pattern compared to Cyclin Oβ. Cyclin Oβ immunostaining reveals coarse cytoplasmic dots up to 300 nm in diameter. According to the size of the Cyclin Oβ granules, they could correspond to Stress Granules (0.1-2.0 μM) or Processing Bodies (0.1-1.0 μM)[70].

To further characterise the subcellular localization of Cyclin O, we transiently transfected Cyclin Oα and Cyclin Oβ in the U2OS cell line. Surprisingly we observed that Cyclin Oα was mostly nuclear whereas Cyclin Oβ shows a cytoplasmic punctate pattern reminiscent of the pattern observed with the β1 antibody (Figure 4 of the Results section). The different subcellular localization found between endogenous and transfected Cyclin Oα in U2OS cells seems paradoxical. We hypothesize that the nuclear localization of the transfected Cyclin Oα is due to the high overexpression of the protein achieved in transient transfection respect to the endogenous levels, which may exceed a putative cytoplasmic retention mechanism. Previous results of our group support this idea, since the subcellular localization of Cyclin Oα in clones of U2OS cells stably transfected with expression vectors is almost completely cytoplasmic, reminiscent of the localization of the endogenous protein. These stable clones were difficult to establish and express very low amounts of the exogenous protein. In most of the cases, we confirmed that the levels of endogenous Cyclin O are low and

comparable to the levels of the transfected protein (data not shown). To further investigate this point, we have analysed the expression pattern of both isoforms in cells infected with recombinant lentiviruses encoding Cyclin Oα or Cyclin Oβ, where the amount of protein produced is lower than in transient transfection experiments. We found that Cyclin Oα shows a mixed nuclear and cytoplasmic pattern, whereas Cyclin Oβ is exclusively cytoplasmic. The amounts of the β isoform are lower compared with the amounts of α protein. These low levels could determine that the localization of Cyclin Oβ was always cytoplasmic, at variance with the subcellular localization of Cyclin Oα that is variable, depending on the amount of protein expressed. Cyclin Oα could be retained bound to a cytoplasmic protein, but when an excess of Cyclin is expressed, the cytoplasmic anchor protein gets saturated and Cyclin Oα gets translocated to the nucleus. A putative candidate for this cytoplasmic anchor could be $p58^{IPK}$ (Figure 23 of the Results section).

We observed that transfected Cyclin Oβ and transfected Cyclin OL3A showed a similar cytoplasmic punctate pattern (Figure 8 of the Results section). When we cotransfected the α and the β isoforms or the α isoform and the L3A mutant, the localization of Cyclin Oα changes from the nucleus to the cytoplasm (Figure 7 of the Results section). So, coexpression of Cyclin Oβ or the L3A mutant relocalizes Cyclin Oα to the cytoplasm forming a punctate pattern. This pattern consists in dense protein aggregates in the cytoplasm that we speculate that could correspond to SGs. TIA-1 is an RNA-binding protein that promotes the assembly of SGs and can be used as a marker for these cytoplasmic structures[66]. Transiently transfected TIA-1 and Cyclin O colocalize in the U2OS cell line, suggesting that these cytoplasmic aggregations are most likely SGs (Figure 9 and 10 of the Results section). In contrast to Cyclin Oβ or Cyclin OL3A, Cyclin Oα needs

additional environmental or oxidative stresses or expression of Cyclin Oβ or Cyclin OL3A to relocalize from the nucleus to TIA-1 positive cytoplasmic granules.

In eukaryotic cells, we can found a wide variety of cytoplasmic bodies that can be classified in three different structures depending on the proteins they contain and the stimuli by which they are induced to form[228]. The different structures are: Aggresomes, Processing Bodies and Stress Granules. Aggresomes form when the proteosome degradative capacity is exceeded. This cytoplasmic structure forms around the microtubule organizing center, adjacent to the cell's centrosomes and appears as a single large cellular garbage bin-like structure[107]. For its size, number and cellular localization we discarded that the cytoplasmic structures that we found in the cells could correspond to aggresomes. SGs are dense aggregations found in the cytoplasm that appear when the cell is under stress and PBs are cytoplasmic compartments where translational repression and mRNA turnover may occur. It is known that SGs and PBs share some proteins and mRNA components as well as some functional properties[70]. A number of useful SGs markers, such as TIA-1, TIAR and HuR, are not entirely SG specific and may associate with PBs in unstressed cells[241]. This raises the possibility that a crosstalk between SGs and PBs is required to ensure cell protection against stress. Due to the use in our experiments of TIA-1 as the SG protein marker, we can not completely discard that the cytoplasmic structures found in the cells correspond to PBs. Both SGs and PBs are induced by stress, but only SGs assembly requires eIF2α phosphorylation[70]. Two experiments support the idea that these cytoplasmic structures correspond to SGs. First, that phosphorylation of eIF2α is attenuated when the Cyclin O is downregulated. Second, that overexpression of Cyclin O leads to phosphorylation of eIF2α.

We have two hypotheses to explain the localization of Cyclin Oα and β isoforms or the L3A mutant in the SGs (Figure 1). The first hypothesis (direct model) proposes that Cyclin Oα due to environmental stress or because of the expression of Cyclin Oβ or Cyclin OL3A is postranslationally modified and then localizes to the SGs. The L3A mutant has three leucines substituted for three alanines in the N-terminal part of the protein and the β isoform lacks the amino acids encoded by exon 2 of the gene. It is possible that Cyclin Oβ and the L3A mutant mimic the stress-induced modification of Cyclin Oα, leading to their constitutive localization to the SGs. To test this model we investigated whether the L3A mutant contains a sequence critical for the localization of Cyclin O to the SGs, but we were unable to find a SG targeting sequence in the region we studied. In addition to this, even after triggering ER stress with thapsigargin, SGs containing any of the chimaeric proteins tested are not formed (Figure 11 of the Results section). These results suggest that what makes that Cyclin OL3A localizes constitutively to the SGs is not the primary sequence of the protein. The second hypothesis (indirect model) proposes that the expression of the beta isoform or the L3A mutant elicit a permanent cellular stress and, consequently, the protein localizes to the SGs as an indirect effect. This hypothesis is supported by several observations. First, transfection of Cyclin OL3A or Cyclin Oβ in U2OS cells leads to death of most of the transfected cells (Figure 18C of the Results section). However, at variance with the case of transfection of Cyclin Oα, the rare colonies surviving the transfection do not express either the β isoform or the L3A mutant (data not shown), suggesting a strong selection against expression of these proteins. Second, overexpression of Cyclin Oβ and the L3A mutant leads to the activation of the PERK pathway as a consequence of ER stress induction (Figure 19 of the Results section).

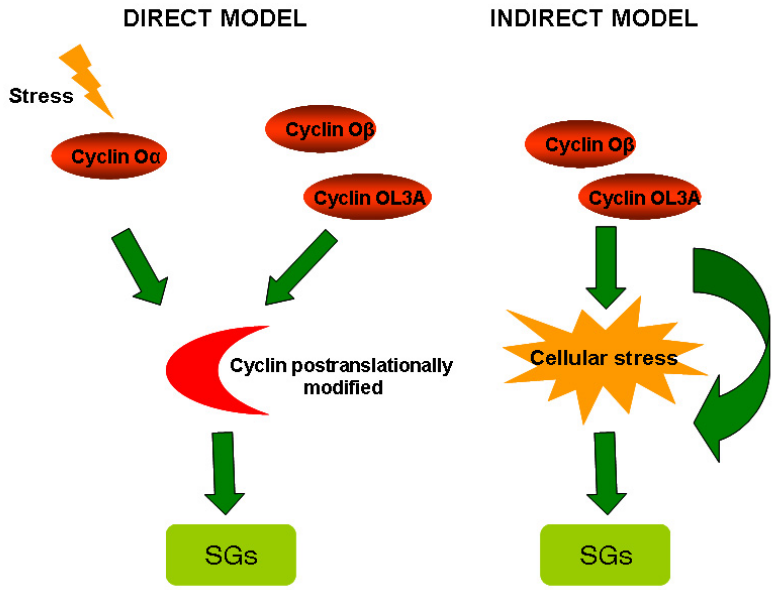

Figure 1. Two models may explain the localization of Cyclin Oα, β or the L3A mutant in the SGs. Direct model: Cyclin Oα upon stress is postranslationally modified and then localizes to the SGs. Cyclin Oβ and the L3A mutant are modified in such a way that mimics Cyclin Oα upon stress and they localize to the SGs constitutively. Indirect model: expression of the beta isoform and the L3A mutant elicit a permanent cellular stress and the protein localizes to the SGs as an indirect effect.

We have observed that endogenous Cyclin Oα partially colocalizes with TIA-1 in stressed cells (Figure 12 of the Results section). Although with transfected GFP-TIA-1 and endogenous TIA-1 the pattern observed is somewhat different, there is a clear increase in the fluorescence intensity of endogenous TIA-1 and a relocalization from the nucleus to the cytoplasm upon thapsigargin treatment. The increase of TIA-1 in response to stress is well documented, since it is known that upon environmental stress this protein accumulates in the SGs in the cytoplasm[61]. In agreement with the mRNA data (Figure 15 of the Results section), upon ER stress the fluorescence intensity of endogenous Cyclin O is also increased, suggesting

that Cyclin O is upregulated upon ER stress induction. It is unclear why the β isoform and the L3A mutant can induce constitutively ER stress. We have observed that next to the amino acid residues mutated in the L3A mutant begins the first α helix of the Cyclin Box (N-terminal α-helix, Figure 18 of the Introduction section). The three point mutations of the L3A mutant located near the N-terminal helix of the Cyclix Box and the lack of the α1, α2 and α3 helixes of the N-terminal repeat of the Cyclix box in the beta isoform could change the conformation of the Cyclin O triggering ER stress more efficiently than the α isoform. Another possibility is that the L3A mutant and the β isoform are partially folded or misfolded proteins which can activate the UPR pathway non-specifically.

4. Cyclin Oα localization in the cytoplasm, in the ER and in the mitochondria

We have demonstrated that Cyclin O binds and activates preferentially Cdk2 and Cdk1[218]. We have also shown in this work that the subcellular localization of Cyclin O is mainly cytoplasmic but we do not know whether it forms active complexes with Cdk2 in these conditions. In the experiments of subcellular fraccionation we observed that anti-Cyclin O immunoprecipitates show kinase activity mostly from the cytosolic fraction and minor amounts from the membrane and nuclear fractions (Figure 13A of the Results section).

Given the fact that Cyclin O may be located in the SGs and we can detect kinase activity in the membrane fraction, we hypothesized that it could be associated with some organelle. Determining the exact subcellular localization of Cyclin O is important for understanding its function. To investigate in which organelle Cyclin O is present, we used confocal microscopy and different parameters informative of the amount of colocalization[226]. We found that Cyclin O partially colocalizes with the mitochondria and the ER (Figure 14 of the Results section). The best colocalization is found with the mitochondrial markers, suggesting a possible function there. The fact that a significant part of Cyclin O is localized in the ER where the SGs are located, suggests that Cyclin O might have a function in this organelle. Although Cyclin O shows some colocalization with ribosomes we do not know whether they are free or membrane-bound ribosomes. Given the fact that Cyclin O colocalizes with the ER it is possible that they are present in the rough ER. It is note that Cyclin O does not have either an ER targeting sequence or a mitochondrial signal peptide. We rather think that the colocalization with ER and mitochondrial markers indicate association of Cyclin O with the cytosolic side of these organelles.

5. Cyclin O is involved in the ER stress pathway

We used three drugs to experimentally induce ER stress: tunicamycin, thapsigargin and DTT. Although these chemicals target different components of the ER, their common effect is to interfere with ER functions and thereby cause ER protein misfolding[242]. Tunicamycin inhibits N-linked glycosylation, while thapsigargin blocks the ER calcium ATPase pump, leading to the depletion of ER calcium stores. DTT induces protein misfolding by reducing their disulfide bonds.

The expression of both Cyclin Oα and Cyclin Oβ mRNA is rapidly elevated after ER stress induction in the lymphoid cell line WEHI7.2 (Figure 15 of the Results section). In agreement with the amount of endogenous protein, the upregulation of Cyclin Oα is much higher than that of Cyclin Oβ. We also found that thapsigargin treatment upregulated both Cyclin Oα and β mRNAs to higher levels than DTT treatment, probably because DTT is more toxic to the cells. This holds true when we measured the percentage of apoptosis upon ER stress induction in these cells. With thapsigargin or tunicamycin treatment, we can detect living cells until 30-40 hours after adding the drug, whereas after 16 hours of DTT treatment most of the cells are dead (Figure 17 of the Results section). Further support to the idea that Cyclin O has a role in the ER stress pathway came from the use of the shRNA technique in the WEHI7.2 cells. Clones expressing an shRNA against Cyclin O have lower levels of phosphorylation of eIF2α and lower induction of CHOP upon ER stress induction, and they were protected against apoptosis induced by ER stress (Figure 16 and 17 of the Results section). We have also demonstrated that overexpression of Cyclin O leads to activation of the PERK pathway (Figure 19 of the Results section).

Probably the most significant ER stress-induced apoptotic pathway is mediated through CHOP. CHOP (-/-) cells are protected from ER stress-induced apoptosis[243], indicating the significance of this pathway. Two different approaches proved that Cyclin O induces the expression of CHOP. First, we demonstrated that Cyclin O expression upregulates CHOP mRNA and protein and its target gene CA6 mRNA by quantitative RT-PCR (Figure 19, 20C and 20D of the Results section). Second, we observed that Cyclin O downregulation attenuates the induction of CHOP (Figure 16 of the Results section). Although the precise mechanism by which CHOP mediates apoptosis is unknown, it activates the transcription of several genes that may potentiate apoptosis. These genes include GADD134, ERO1α, DR5 and CA6. ERO1α encodes an ER oxidase that increases the oxidizing potential of the ER[186]. DR5 encodes a cell-surface death receptor that may activate Caspase cascades[244] and CA6 may decrease the intracellular pH during ER stress[170].

Previous results of our laboratory showed that Cyclin O expression induces apoptosis through the intrinsic pathway by activating apical Caspases in a transcription and translation dependent manner[218]. We showed that Cyclin O/Cdk2 complexes induce Caspase-8 activation[217,218]. However, the mechanisms leading to Caspase-8 activation can not be direct because we demonstrated that *de novo* gene expression is needed downstream of Cyclin O/Cdk2 complexes to activate Caspase-8. One possibility is that Cyclin O/Cdk2 complexes activate the transcription factor CHOP, which induces the target gene DR5. DR5 activates the extrinsic apoptotic pathway by recruiting Procaspase-8 into the DISC, which promotes cleavage of Bid by Caspase-8 and then the activation of the mitochondrial pathway[245]. It is known that other factors might collaborate with CHOP in ER stress-mediated DR5 induction[244]. Recently Caspase-2 has been identified as the premitochondrial protease that cleaves Bid in response to ER stress[246].

However, it is still not clear how Caspase-2 is activated by ER stress or whether it is downstream of one or more of the three stress pathways of the UPR. So another possibility is that CHOP induces the activation of Caspase-2 that ultimately leads to apoptosis (Figure 2).

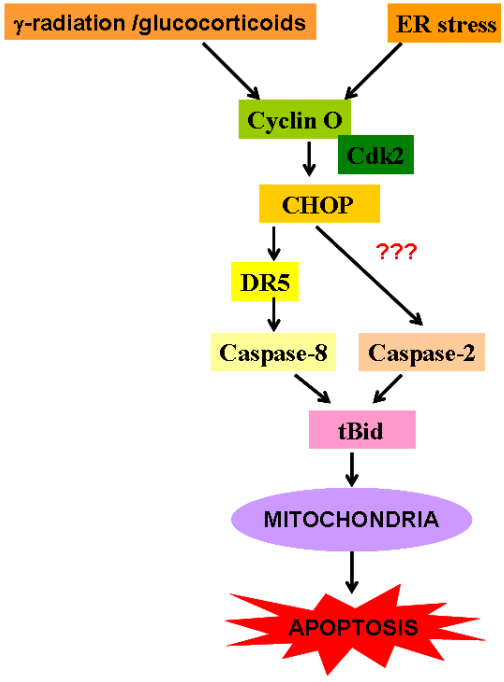

Figure 2. Model of Cyclin O-mediated Caspase-8 and Caspase-2 activation. Cyclin O/Cdk2 complexes activate the transcription factor CHOP, which induces the target gene DR5. DR5 promotes cleavage of Bid by Caspase-8 and then the activation of the mitochondrial pathway, leading to apoptosis. The target gene CHOP might also activate Caspase-2, which cleaves Bid and leads to apoptosis.

We have seen that Cyclin O is involved in two different apoptotic pathways: in the DNA damage[218] and in the ER stress pathways. The CHOP gene was initially identified in a search for genes induced by genotoxic stress, such as UV light, γ-radiation and alkylating agents such as methyl methanesulfonate (MMS)[247]. We measured by Western Blotting the induction of CHOP in the control shRNA and Cyclin O shRNA transfected WEHI7.2 cells after γ-

radiation treatment. We observed that the induction of CHOP is attenuated when Cyclin O is downregulated (data not shown). So it seems that CHOP is a common target gene of Cyclin O in both DNA damage and ER stress pathways (Figure 3).

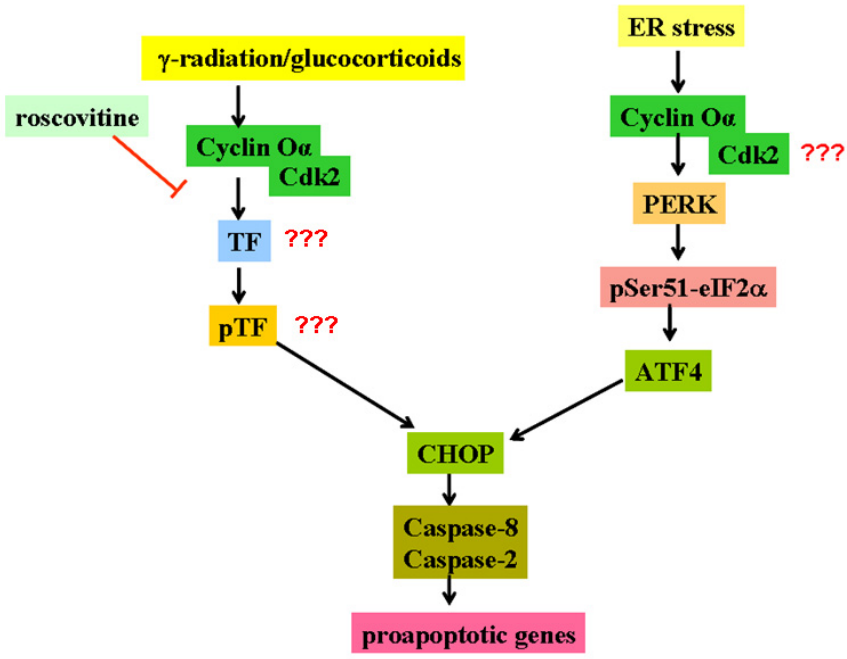

Figure 3. Crosstalk between ER stress and DNA damage pathways. Cyclin O is involved in both DNA damage and ER stress pathways. The common target gene of both pathways is the transcription factor CHOP, which ultimately induces apoptosis. TF: Transcription Factor.

ER stress induces a coordinated adaptive program namely UPR from which PERK, IRE1 and ATF6 are the transducer proteins[173]. We have demonstrated that Cyclin O induces ER stress by a specific activation of the PERK pathway by two different approaches. First, we analysed the activation of the IRE1 pathway by measuring the IRE1-dependent splicing of XBP1 by RT-PCR. Second, we analysed the activation of the ATF6 pathway by measuring the cleavage of ATF6 by WB. We observed that

Cyclin O expression does not activate the IRE1 or the ATF6 pathway. These experiments demonstrate that the activation of the ER stress pathway is not a non-especific event due, for example, to an overload of the protein folding capacity of the cell. Unfolded or misfolded Cyclin O could accumulate and it activates the UPR non-specifically. The fact that Cyclin O shows kinase activity both in the cytosol and in the membrane fractions suggests that it is not misfolded when it is located in the ER.

We have demonstrated that Cyclin O activates specifically the PERK pathway and it is necessary for ER stress-induced apoptosis. These results are consistent with the fact that it is known that under prolonged stress conditions, the IRE1 and ATF6 responses are attenuated and only the PERK response is maintained activated, which ultimately induces apoptosis[181]. Lin *et al.*[182] reported that sustained PERK signalling was harmful to cell viability whereas the equivalent duration of IRE1 signalling was not. So chronic PERK signalling promotes cell death in contrast with IRE1 activity, which enhances cell survival. The PERK pathway is the best candidate to be activated in Cyclin O induced apoptosis upon ER stress.

We have also shown that the L3A mutant behaves similarly to Cyclin Oα. The L3A mutant binds, activates Cdk2 and the PERK pathway but does not activate the IRE1 or the ATF6 pathways and induces apoptosis (Figure 18, 19 and 20 of the Results section).

6. Different signalling between Cyclin Oα and Cyclin Oβ

We currently do not know whether the β isoform is associated with any organelle. Only Cyclin Oα can interact and activate Cdk1/2 (Figure 18A and 18B of the Results section). The shRNA Cyclin O expression vector used in WEHI7.2 cells can trigger downregulation of both α and β isoforms of Cyclin O[218]. So the results obtained with these clones are most likely the consequence of the downregulation of both isoforms. On the other hand, both α and β isoforms are upregulated upon ER stress at the mRNA level and their overexpression induce activation of the PERK pathway (Figure 15 and 19 of the Results section). Expression of the β isoform does not activate the IRE1 or the ATF6 pathway (Figure 20A and 20B of the Results section). So it seems that Cyclin Oβ is also involved in the PERK pathway and can induce apoptosis as demonstrated in colony forming experiments (Figure 18C of the Results section). Given all these findings, we propose that Cyclin Oα and Cyclin Oβ may have a different apoptosis signalling mechanism, since Cyclin Oβ neither binds nor activates Cdk2 but it can induce ER stress and apoptosis. However, we cannot rule out that the kinase activation might be necessary for ER stress induction by the α isoform and the L3A mutant, whereas the β isoform does so by activation of the misfolded protein pathway.

7. Mechanism of PERK activation by Cyclin Oα

The results shown in this thesis provide strong evidence that Cyclin Oα activates the PERK pathway at a proximal level promoting PERK activation. PERK is a type I ER-resident transmembrane protein that senses ER stress through its lumenal domain. Under normal conditions PERK is bound to the ER chaperone BiP which maintains it in an inactive monomeric state. Upon ER stress, BiP dissociates, allowing PERK to be activated[248]. We have two hypotheses to explain how Cyclin O can activate PERK. The first hypothesis is that Cyclin O activates PERK through binding to its kinase domain, directly or through the interaction with other protein(s). The second hypothesis is that Cyclin O activates PERK in an indirect way, binding to BiP and promoting its dissociation from PERK leading to the activation of the PERK pathway. Subcellular fractionation and protease protection experiments are required to elucidate whether Cyclin O is localized in the luminal or in the cytosolic side of the ER. Although no ER targeting sequence has been detected in Cyclin O, we cannot exclude that it is translocated to the ER lumen by a non-conventional mechanism[249]. By pull-down experiments we have demonstrated that Cyclin Oα can interact at least with some phosphorylated forms of PERK (Figure 21 of the Results section).

However, from these experiments we cannot find out whether the Cyclin O-PERK interaction is direct or mediated through other protein(s). It is known that PERK binds to BiP through its lumenal domain, but PERK can also bind with other proteins through its cytoplasmic kinase domain, such as $p58^{IPK}$. $P58^{IPK}$ is a member of the tetratricopeptide repeat (TPR) family of proteins that negatively regulates PERK activity by direct binding to its kinase domain[152]. We studied whether Cyclin Oα can also interact with BiP and/or with $p58^{IPK}$. We observed that in unstressed conditions Cyclin Oα

binds to BiP, although the interaction is weak (Figure 22 of the Results section). So BiP is present in the Cyclin Oα complexes probably interacting indirectly via PERK. The partial colocalization of Cyclin Oα with BiP observed by confocal microscopy corroborates these results (Figure 14B of the Results section). We have also demonstrated that Cyclin Oα interacts strongly with p58^{IPK} both in normal and stress conditions (Figure 23 of the Results section). So the interaction of Cyclin Oα with p58^{IPK} is independent of ER stress treatment. The high colocalization of Cyclin Oα with p58^{IPK} observed by confocal microscopy corroborates these results (Figure 24 of the Results section). We have discussed previously the possibility that the cytoplasmic localization of Cyclin Oα could be due to its binding to a cytoplasmic protein, which retains it in the cytoplasm. One plausible candidate is the p58^{IPK} protein.

Although we know that Cyclin Oα binds to p58^{IPK} and that p58^{IPK} binds to PERK through its kinase domain, we do not know whether the binding of Cyclin Oα to p58^{IPK} is necessary for the interaction of p58^{IPK} to PERK. It is possible that Cyclin Oα binds to p58^{IPK} in the cytoplasm of the cells independently of PERK. This idea is supported by the fact that we have found that Cyclin Oα interacts with p58^{IPK} in PERK knockout cells (data not shown). So perhaps Cyclin Oα /p58^{IPK} complexes perform other functions independently of the PERK pathway. Since p58^{IPK} negatively regulates the kinase activity of PERK[152], the formation of Cyclin Oα /p58^{IPK} complexes upon Cyclin O upregulation may result in the sequestering of p58^{IPK} from its interaction with PERK leading to its activation. Gale *et al.*[250] described p52^{rIPK} as a protein that binds to p58^{IPK} blocking the PKR regulatory function of p58^{IPK} and restoring the eIF2α phosphorylation function of PKR as a consequence. So perhaps Cyclin Oα performs a function similar to p52^{rIPK} protein.

Previous experiments demonstrated that Cyclin Oα binds and activates Cdk2 and we could recover active Cyclin O/Cdk1/2 complexes from cytosolic extracts (Figure 13A of the Results section). Surprisingly, we observed that very little amounts of Cdk1/2 are present in the GST-Cyclin Oα pull-down complexes (Figure 21 of the Results section). However, the previous pull-down and immunoprecipitation experiments were performed using either whole cell lysates or cell lysates obtained using a buffer similar to the lysis buffer used in the GST pull-down experiments but using frozen cell pellets. Moreover, when we performed a Western Blotting against Cdk2 in the different subcellular extracts, we only detected Cdk2 in the nuclear fraction (data not shown), suggesting that the interaction of Cyclin O with Cdk2 might occur during the immunoprecipitation procedure. In addition to this, we can detect Cdk2 in the input of the pull-down complexes. We believe that little amounts of Cdk2, which they can not be detected by Western Blotting but they can be detected by the Kinase assay, could be present in the pull-down complexes being active when bound to Cyclin O. It will be necessary to measure the kinase activity of the pull-down complexes and check different selective chemical Cdk inhibitors to find out whether Cdk2 or a related Cdk is present.

Based on the hypothesis that Cyclin Oα binds to PERK through its kinase domain, we have two models to explain how this interaction can take place (Figure 4). Model A proposes that Cyclin Oα binds to PERK indirectly, through its interaction with $p58^{IPK}$. $P58^{IPK}$ negatively regulates the kinase activity of PERK[152], so Cyclin Oα would inactive the PERK's inhibitory function of $p58^{IPK}$. Model B proposes a direct binding of Cyclin Oα to PERK. In both model A and B, we can find Cyclin Oα bound to $p58^{IPK}$ and Cyclin Oα bound to Cdk2 in the cytoplasm of the cells.

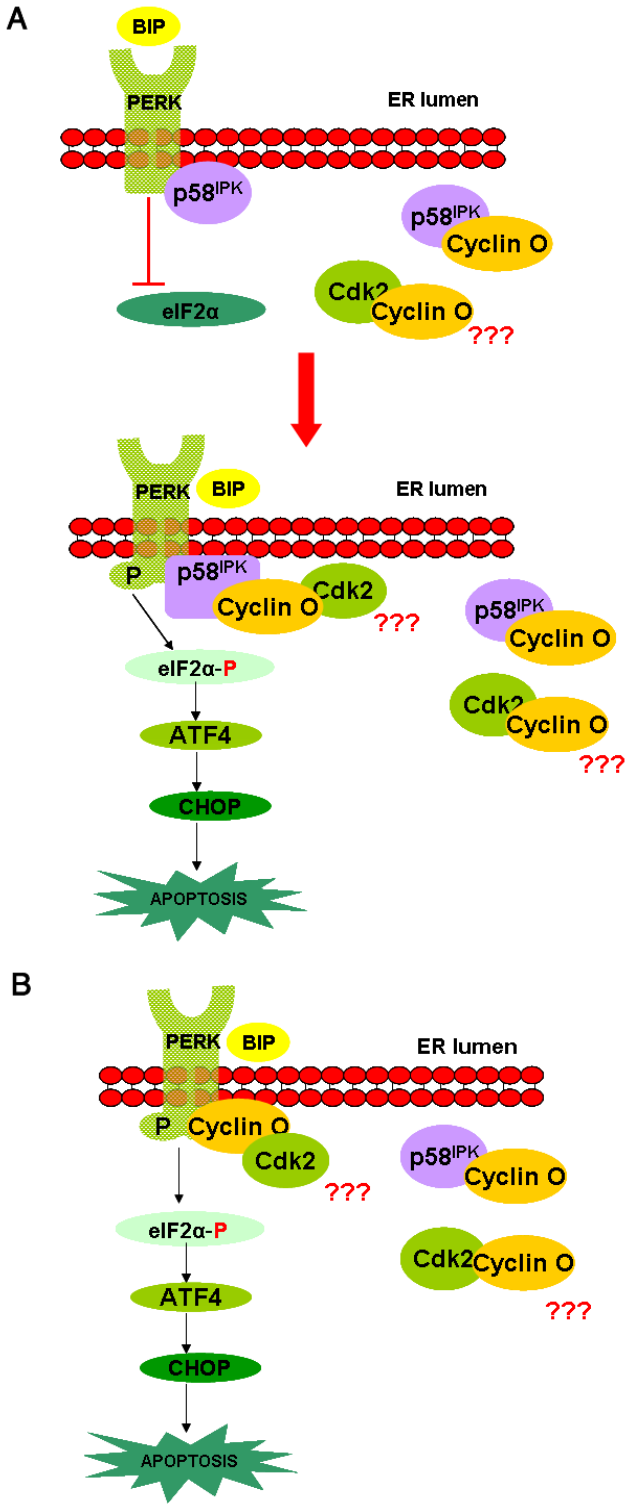
A
BIP
PERK
ER lumen
p58IPK
eIF2α
p58IPK
Cyclin O
Cdk2
Cyclin O
???
PERK
BIP
ER lumen
P
p58IPK
Cyclin O
Cdk2
???
eIF2α-P
ATF4
CHOP
APOPTOSIS
p58IPK
Cyclin O
Cdk2
Cyclin O
???
B
PERK
BIP
ER lumen
P
Cyclin O
Cdk2
???
eIF2α-P
ATF4
CHOP
APOPTOSIS
p58IPK
Cyclin O
Cdk2Cyclin O
???

Figure 4. Two models to explain how Cyclin Oα interacts and activates the PERK pathway. (A) In standard conditions, $p58^{IPK}$ binds to PERK and negatively regulates its kinase activity. Upon ER stress conditions, Cyclin Oα binds to PERK indirectly, through its interaction with $p58^{IPK}$. Cyclin Oα inactivates the PERK's inhibitory function of $p58^{IPK}$. **(B)** Upon ER stress conditions, Cyclin Oα binds to PERK directly. We can also find Cyclin Oα bound to $p58^{IPK}$ and Cyclin Oα bound to Cdk2 in the cytoplasm of the cells in both models.

8. A putative role of Cyclin Oα in oxidative stress

Cyclin O is expressed in different mouse and human epithelial tissues, such as the skin, the respiratory epithelium and the inner lining of the digestive tract (intestinal epithelium). The epithelial lining provides a barrier between the external environment and the organ it covers. The constitutive expression of Cyclin O in epithelia, suggests that the function of Cyclin O may not always be related to apoptosis regulation. One example of this non-apoptotic function of Cyclin O is found in the epidermis. The epidermis is a multi-stratified squamous epithelium in which keratinocytes progressively undergo terminal differentiation towards the skin surface. Interestingly, the expression of Cyclin O in skin follows the same pattern: increased expression in the upper layers. However, in squamous cells carcinomas of the skin, cells get dedifferentiated and loose Cyclin O expression (data not shown). These data suggest that Cyclin O may have a role in epidermal differentiation.

Cyclin Oα does not show a uniform distribution in colonies of the M6 cell line, having a higher expression in the cells of the periphery of the colony than in the centre (Figure 24 of the Results section). M6 cells are epithelial-like cells with a mucosecretor phenotype derived from the human colon adenocarcinoma cell line HT29[251]. These cells grow forming compact colonies. The peripheric distribution of Cyclin O observed in the colonies of M6 cells is not found in other non-epithelial cells such as MEFs. Furthermore, this peripheric distribution is also observed when staining active mitochondria with the Mitotracker-red dye and with and anti-p58^{IPK} antibody in the same cells. These findings suggest that Cyclin Oα and p58^{IPK} may be related to the function of active mitochondria. Mitotracker-red dye (Invitrogen) is a fluorescent dye that is retained by mitochondria depending on their membrane potential[252]. The mitochondrial transmembrane potential

(ΔΨm) is related to the oxidative status of the mitochondria, the higher the oxidative rate, and the higher ΔΨm and, as a consequence, higher retention of the dye. The fact that Cyclin Oα is localized in the periphery of these epithelial cells, where there is higher contact with the medium, higher mitotic index and higher mitochondrial activity, suggests that Cyclin Oα could be related to oxidative metabolism or oxidative stress. Moreover, Cyclin Oα colocalizes with mitochondrial markers, suggesting that it is physically close to the mitochondria. Mitochondrial oxidative phosphorylation is the major cellular source of ROS production. Cells with excess nutrient uptake that have not converted to aerobic glycolisis increase oxidative phosphorylation and, as a consequence, the ROS production[253]. Oxidative stress occurs when the amount of ROS exceeds the levels of neutralizing agents called antioxidants, causing damage to macromolecules such as DNA, proteins and lipids.

The relationships between oxidative stress and ER stress are not well understood. Haynes *et al.*[254] reported that prolonged activation of the UPR induces oxidative stress which finally can lead to apoptosis. It has also been demonstrated that UPR-deficient cells under sustained ER stress failed to accumulate ROS. On the other hand, a lot of evidences suggest that the activation of the UPR occurs on the exposure to oxidative stress which it is believed that is an adaptive mechanism to preserve cell function and survival[255].

Cancer cells take up glucose at higher rates than normal tissue but use a smaller fraction of this glucose for oxidative phosphorylation. This effect is known as aerobic glycolisis or the Warburg effect[256]. Hypoxia in the tumour microenvironment is a common feature of solid tumours. As a tumour grows, it rapidly outgrows its blood supply, leaving portions of the tumour with regions where the oxygen concentration is significantly lower. The lack

of oxygen delivery results in local ischemia and hypoxia of the tumour[257]. Recent articles described that hypoxia is known to stimulate mitochondria to release ROS. The increased ROS production in response to hypoxia can promote cancer cell survival and tumour growth through activating Hypoxia Inducible Factor 1α (HIF-1α)[258]. Initially it was believed that one explanation for the Warburg effect was that tumour hypoxia selects cells dependent on anaerobic metabolism[259]. However, it was observed that cancer cells use glycolytic metabolism prior to the exposure to hypoxic conditions[260]. Thus, tumour hypoxia is a late-occurring event that may not be a major contributor in the switch to aerobic glycolisis by cancer cells[256]. Observations of our laboratory show that Cyclin O is expressed in a wide variety of tumour types. It is also demonstrated that these tumour tissues are resistant to apoptosis. One possible explanation could be that the hypoxic microenvironment of the tumour increases the release of ROS from the mitochondria. Then, ROS production induces the expression of Cyclin O, perhaps as a consequence of the activation of the ER stress pathway or through the induction of DNA damage and participation of the DNA damaging response, which then binds to $p58^{IPK}$. The binding of $p58^{IPK}$ to Cyclin O avoids the formation of Cyclin O/Cdk1/2 complexes, thus escaping apoptosis induction (Figure 5).

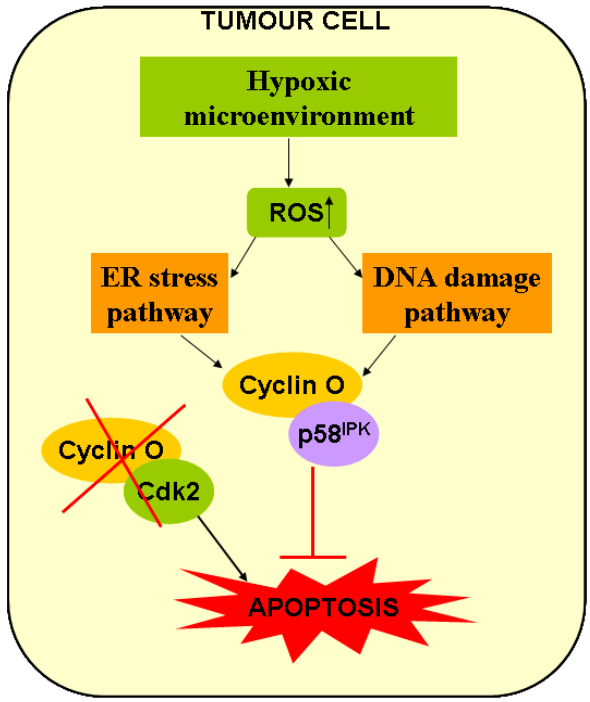

Figure 5. Cyclin O activation in tumour cells. Hypoxic microenvironment of the tumour cells increases the release of ROS which induces the expression of Cyclin O as a consequence of the activation of the ER stress and/or the DNA damage pathways. Then, Cyclin O binds to $p58^{IPK}$ avoiding the formation of Cyclin O/Cdk1/2 complexes and escaping apoptosis induction.

9. Participation of Cyclin O in the activation of the eIF2α kinases

The phosphorylation of eIF2α is mediated by four distinct protein kinases: HRI, GCN2, PKR and PERK. The term "integrated stress response" refers to the process mediated by the four eIF2α kinases that responds to different stress signals and converges in the phosphorylation of eIF2α, which activates a common set of target genes[116]. We have demonstrated that Cyclin O, in addition to activate the PERK kinase, participates in the activation of other eIF2α kinases by two different approaches. First, we observed that when Cyclin O is downregulated, the phosphorylation of eIF2α is decreased upon exposure of the cells to different environmental stresses such as UV irradiation and sodium arsenite treatment (Figure 25 of the Results section). Second, we have demonstrated by confocal microscopy that Cyclin O colocalizes with PERK, PKR and HRI kinases (Figures 26, 27, 28 of the Results section). Cyclin Oα expression can induce apoptosis both in PERK wt and in PERK knockout MEFs (data not shown). These results can be explained by compensation of the loss of PERK by the other eIF2α kinases. It has been demonstrated that mice that have lost the regulation by all eIF2α kinases, by introducing a Serine to Alanine point mutation in Ser51 of the eIF2α gene, develop a more severe β-cell defect dysfunction prior to birth compared to PERK knockout mice. This more severe phenotype in the Ser51Ala eIF2α mutant mice indicates that other eIF2α kinases may partially compensate for eIF2α phosphorylation in the absence of PERK[261]. PERK knockout mice develop diabetes because of excessive ER stress in their β-cells causing β-cell apoptosis[161]. Mutant mice carrying a heterozygous mutation in the phosphorylation site of eIF2α become obese and, because of β-cell dysfunction, diabetic when fed a high-fat diet[262]. Additionally, p58^{IPK} knockout mice show a gradual onset of glusosuria and hyperglycemia

associated with increased apoptosis of islet cells[263]. Thus, PERK, eIF2α and p58^{IPK} are involved in the pathogenesis of diabetes. Lack of p58^{IPK} had no apparent effect on the functional integrity of viable β-cells[263]. The less severe diabetic phenotype of p58^{IPK} knockout mice compare to the PERK or Ser51Ala phenotype may be related to the fact that p58^{IPK} is not directly involved in controlling protein translation, whereas PERK and eIF2α are key players in this vital process.

The oxidative stress may also be involved in the activation of PKR, HRI or GCN2 kinases. UV irradiation induces NOS activation and NO$^{\cdot}$ production, which leads to PERK and GCN2 activation[80]. Arsenite increases the levels of NOS and induces HRI activation[83]. Oxidative stress also activates PKR kinase by the activation of the cytokine IFN-γ[88]. We propose that Cyclin O may be involved in the activation of all the eIF2α kinases and its function may be related to its localization in the mitochondria. We believe that the production of ROS activates Cyclin O, which in turn activates the eIF2α kinases. We have observed that in PERK knockout cells Cyclin O can still interact with p58^{IPK} (data not shown), suggesting that this interaction is not exclusive of the PERK kinase. Although it is known that p58^{IPK} interacts directly with PKR and inhibits its kinase activity[98], the interaction of p58^{IPK} with the HRI or GCN2 kinases has not been reported. Whether or not the interaction of p58^{IPK} with Cyclin O alone or in complex with Cdk2 is necessary for the activation of the eIF2α kinases has also to be investigated (Figure 6).

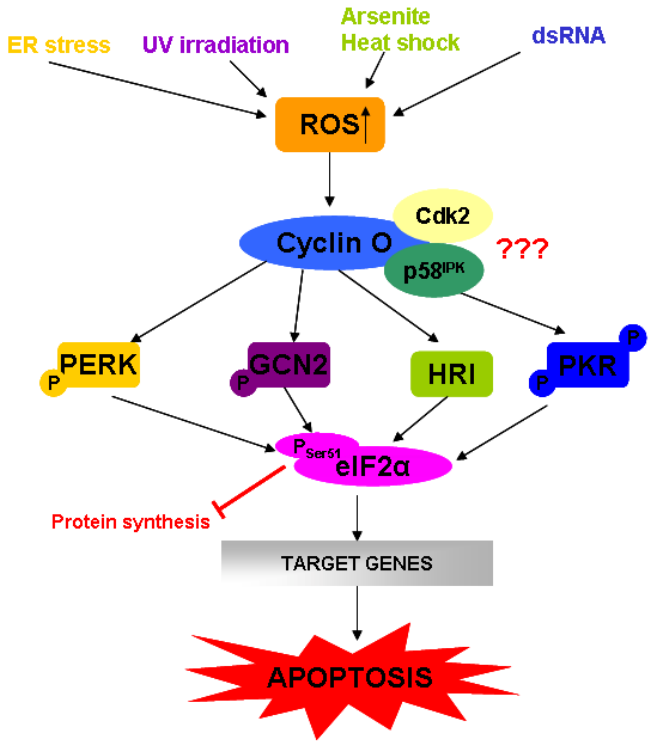

Figure 6. Cyclin O activates all the eIF2α kinases. Different environmental stresses induce the production of ROS which activate the expression of Cyclin O. Cyclin O activates the PERK, GCN2, HRI and PKR kinases, which converge in the phosphorylation of eIF2α which leads to apoptosis.

10. Concluding remarks

Oxidative stress causes damage to all components of the cell, including proteins, lipids and DNA and takes place when the production of ROS exceeds the natural antioxidant defence mechanisms. The ROS include superoxide ($O_2^{\cdot-}$), hydrogen peroxide (H_2O_2), hydroxyl radicals ($OH^{\cdot}$) and singlet oxygen ($^1O_2$) and they can oxidize DNA, which can lead to several types of DNA damage, including oxidized bases and single- and double-strand breaks. DNA damage produced by ROS is the most frequently occurring damage[264]. From previous experiments done in our laboratory we known that Cyclin O is induced after DNA damage[218]. Although the pathways activated by genotoxic agents are complex, the transcriptional response associated to DNA damage is mediated basically by p53[265]. The data published by Roig *et al.*[218], Granes *et al.*[217] and unpublished experiments of our group performed in p53 knockout MEFs propose that DNA damage induces Cyclin O expression through the p53 transcription factor. Then, Cyclin O binds and activates Cdk2 and induces the activation of the apical Caspase-8 in a process that requires *de novo* gene transcription and translation. Caspase-8 cleaves Bid and then activates the mitochondrial pathway that leads to apoptosis. In this thesis for the first time, we have identified genes positioned downstream of the expression of Cyclin O. We have also demonstrated the existence of a specific interaction between Cyclin Oα and $p58^{IPK}$ that could help us to better understand the mechanism of action of the Cyclin O and how connects with the stress pathways. Finally, we have shown the colocalization of Cyclin Oα with different mitochondrial markers, suggesting that the localization of Cyclin O in the mitochondria may be important for its function. Although we have demonstrated that Cyclin O binds and activates Cdk2 in response to intrinsic apoptotic stimuli such as glucocorticoids or DNA damaging agents[218], we still do not know whether activation of Cdk2 is necessary for Cyclin O to activate the different eIF2α

kinases. On the other hand, although we have demonstrated that both alpha and beta isoforms of Cyclin O can induce apoptosis and it seems that both are involved in the ER stress pathway, we still do not know whether they have the same mechanism of action.

Another question to be resolved is the localization of Cyclin O in the SGs upon environmental stresses. SGs are dense aggregations in the cytoplasm composed of proteins and RNAs that appear when the cell is under stress. One function of the SGs is protecting RNAs from harmful conditions. Upon environmental stresses, Cyclin O activates the eIF2α kinases which induce the phosphorylation of eIF2α. It is known that the phosphorylation of eIF2α is critical for the assembly of SGs[60]. One possibility is that once Cyclin O activates the eIF2α kinases and as a consequence of the phosphorylation of eIF2α, it goes to the SGs and remains there until the harmful conditions disappear.

We propose an integrated model based on the findings described in this thesis, showing the involvement of Cyclin O in the DNA damage pathway and in the integrated stress response activation (Figure 7). Different environmental stresses, such as ER stress, UV irradiation, arsenite treatment or viral infection, induce the production of ROS. When the amount of ROS exceeds the levels of neutralizing agents oxidative stress occurs, which causes DNA damage. In response to DNA damage, Cyclin O is induced through the p53 transcription factor. Then, Cyclin O activates PERK, GCN2, HRI and PKR kinases, which converge in the phosphorylation of eIF2α. The phosphorylation of eIF2α reduces protein synthesis and induces the formation of SGs containing stalled transcripts. Although the translation of most mRNAs is attenuated, genes carrying certain regulatory sequences in their 5' unstranslated regions can bypass the eIF2α-dependent translational block and they finally can induce apoptosis.

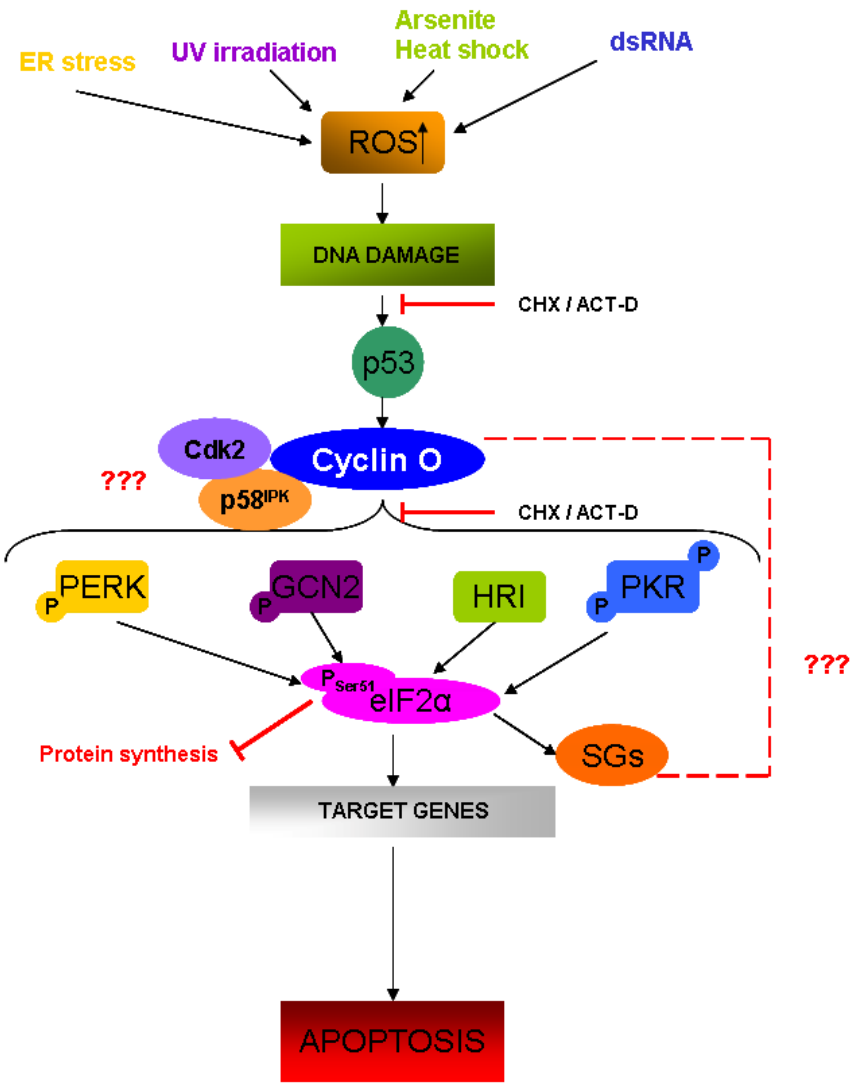

Figure 7. Integrated model showing the involvement of Cyclin O in the DNA damage pathway and in the activation of the integrated stress response. Different environmental stresses induce the production of ROS. When the amount of ROS exceeds the levels of neutralizing agents oxidative stress occurs, which causes DNA damage. In response to DNA damage, Cyclin O is induced through the p53 transcription factor. Then, Cyclin O activates the eIF2α kinases, which converge in the phosphorylation of eIF2α. The phosphorylation of eIF2α reduces protein synthesis and induces the formation of SGs. Although the translation of most mRNAs is attenuated, some genes are induced which ultimately will induce apoptosis. CHX: Cycloheximide; ACT-D: Actinomycin D.

CONCLUSIONS

1. Cyclin O protein is expressed constitutively in some human and mouse tissues and cell lines showing a cytoplasmic punctate pattern.
2. Endogenous Cyclin Oα is expressed at higher levels than Cyclin Oβ.
3. The LTALDL amino acid sequence of the N-terminal part of Cyclin Oα (LxxLxL motif) does not correspond to a Nuclear Export Signal.
4. In stressed cells, Cyclin Oα localizes in cytoplasmic granules compatible with being Stress Granules.
5. The L3A mutant and the β isoform of Cyclin O are constitutively localized to cytoplasmic granules compatible with being Stress Granules.
6. Cyclin Oα is partially located in the mitochondria and in the endoplasmic reticulum.
7. Cyclin Oα and Cyclin Oβ are upregulated by ER stress at the mRNA level.
8. Downregulation of Cyclin O abrogates ER stress-induced apoptosis.
9. Cyclin Oα and Cyclin Oβ are proapoptotic, but only Cyclin Oα can bind and activate Cdk2.
10. Cyclin O overexpression leads to the PERK pathway activation but not to the activation of the IRE1 or the ATF6 pathways.
11. Cyclin Oα interacts with PERK, BiP and $p58^{IPK}$ *in vitro*.
12. Cyclin Oα colocalizes with $p58^{IPK}$.
13. Downregulation of Cyclin O decreases the levels of phosphorylation of eIF2α after ER stress, arsenite treatment or UV irradiation.
14. Cyclin Oα colocalizes with PERK, PKR and HRI kinases.

BIBLIOGRAPHY

1. Melino,G. The Sirens' song. *Nature* 412, 23 (2001).

2. Kerr,J.F., Wyllie,A.H. & Currie,A.R. Apoptosis: a basic biological phenomenon with wide-ranging implications in tissue kinetics. *Br. J. Cancer* 26, 239-257 (1972).

3. Roach,H.I. & Clarke,N.M. Physiological cell death of chondrocytes in vivo is not confined to apoptosis. New observations on the mammalian growth plate. *J. Bone Joint Surg. Br.* 82, 601-613 (2000).

4. Kroemer,G. *et al.* Classification of cell death: recommendations of the Nomenclature Committee on Cell Death 2009. *Cell Death. Differ.* 16, 3-11 (2009).

5. Galluzzi,L. *et al.* To die or not to die: that is the autophagic question. *Curr. Mol. Med.* 8, 78-91 (2008).

6. Golstein,P. & Kroemer,G. Cell death by necrosis: towards a molecular definition. *Trends Biochem. Sci.* 32, 37-43 (2007).

7. Festjens,N., Vanden Berghe,T. & Vandenabeele,P. Necrosis, a well-orchestrated form of cell demise: signalling cascades, important mediators and concomitant immune response. *Biochim. Biophys. Acta* 1757, 1371-1387 (2006).

8. Danial,N.N. & Korsmeyer,S.J. Cell death: critical control points. *Cell* 116, 205-219 (2004).

9. Hanahan,D. & Weinberg,R.A. The hallmarks of cancer. *Cell* 100, 57-70 (2000).

10. Thompson,C.B. Apoptosis in the pathogenesis and treatment of disease. *Science* 267, 1456-1462 (1995).

11. Bouillet,P. *et al.* BH3-only Bcl-2 family member Bim is required for apoptosis of autoreactive thymocytes. *Nature* 415, 922-926 (2002).

12. Youle,R.J. & Strasser,A. The BCL-2 protein family: opposing activities that mediate cell death. *Nat. Rev. Mol. Cell Biol.* 9, 47-59 (2008).

13. Mattson,M.P. Apoptosis in neurodegenerative disorders. *Nat. Rev Mol. Cell Biol.* 1, 120-129 (2000).

14. Roshal,M., Zhu,Y. & Planelles,V. Apoptosis in AIDS. *Apoptosis.* 6, 103-116 (2001).

15. Ellis,H.M. & Horvitz,H.R. Genetic control of programmed cell death in the nematode C. elegans. *Cell* 44, 817-829 (1986).

16. Thornberry,N.A. *et al.* A novel heterodimeric cysteine protease is required for interleukin-1 beta processing in monocytes. *Nature* 356, 768-774 (1992).

17. Yuan,J., Shaham,S., Ledoux,S., Ellis,H.M. & Horvitz,H.R. The C. elegans cell death gene ced-3 encodes a protein similar to mammalian interleukin-1 beta-converting enzyme. *Cell* 75, 641-652 (1993).

18. Kumar,S. Caspase function in programmed cell death. 2. *Cell Death Differ.* 14, 32-43 (2007).

19. Martinon,F. & Tschopp,J. Inflammatory caspases: linking an intracellular innate immune system to autoinflammatory diseases. *Cell* 117, 561-574 (2004).

20. Schmitz,J. *et al.* IL-33, an interleukin-1-like cytokine that signals via the IL-1 receptor-related protein ST2 and induces T helper type 2-associated cytokines. *Immunity.* 23, 479-490 (2005).

21. Saleh,M. *et al.* Enhanced bacterial clearance and sepsis resistance in caspase-12-deficient mice. *Nature* 440, 1064-1068 (2006).

22. Martinon,F. & Tschopp,J. Inflammatory caspases and inflammasomes: master switches of inflammation. *Cell Death. Differ.* 14, 10-22 (2007).

23. Degterev,A., Boyce,M. & Yuan,J. A decade of caspases. *Oncogene* 22, 8543-8567 (2003).

24. Peter,M.E. & Krammer,P.H. The CD95(APO-1/Fas) DISC and beyond. *Cell Death. Differ.* 10, 26-35 (2003).

25. Tinel,A. & Tschopp,J. The PIDDosome, a protein complex implicated in activation of caspase-2 in response to genotoxic stress. *Science* 304, 843-846 (2004).

26. Cain,K., Bratton,S.B. & Cohen,G.M. The Apaf-1 apoptosome: a large caspase-activating complex. *Biochimie* 84, 203-214 (2002).

27. Eckhart,L., Ban,J., Fischer,H. & Tschachler,E. Caspase-14: analysis of gene structure and mRNA expression during keratinocyte differentiation. *Biochem. Biophys. Res. Commun.* 277, 655-659 (2000).

28. Jin,Z. & El Deiry,W.S. Overview of cell death signaling pathways. *Cancer Biol. Ther.* 4, 139-163 (2005).

29. Bump,N.J. *et al.* Inhibition of ICE family proteases by baculovirus antiapoptotic protein p35. *Science* 269, 1885-1888 (1995).

30. Salvesen,G.S. & Duckett,C.S. IAP proteins: blocking the road to death's door. *Nat. Rev Mol. Cell Biol.* 3, 401-410 (2002).

31. Vaux,D.L., Cory,S. & Adams,J.M. Bcl-2 gene promotes haemopoietic cell survival and cooperates with c- myc to immortalize pre-B cells. *Nature* 335, 440-442 (1988).

32. Brunelle,J.K. & Letai,A. Control of mitochondrial apoptosis by the Bcl-2 family. *J. Cell Sci.* 122, 437-441 (2009).

33. Roset,R., Ortet,L. & Gil-Gomez,G. Role of Bcl-2 family members on apoptosis: what we have learned from knock-out mice. 1. *Front Biosci.* 12, 4722-4730 (2007).

34. Kuwana,T. *et al.* BH3 domains of BH3-only proteins differentially regulate Bax-mediated mitochondrial membrane permeabilization both directly and indirectly. *Mol. Cell* 17, 525-535 (2005).

35. Saelens,X. *et al.* Toxic proteins released from mitochondria in cell death. *Oncogene* 23, 2861-2874 (2004).

36. Fulda,S. & Debatin,K.M. Extrinsic versus intrinsic apoptosis pathways in anticancer chemotherapy. *Oncogene* 25, 4798-4811 (2006).

37. Chinnaiyan,A.M., O'Rourke,K., Tewari,M. & Dixit,V.M. FADD, a novel death domain-containing protein, interacts with the death domain of Fas and initiates apoptosis. *Cell* 81, 505-512 (1995).

38. Hsu,H., Xiong,J. & Goeddel,D.V. The TNF receptor 1-associated protein TRADD signals cell death and NF-kappa B activation. *Cell* 81, 495-504 (1995).

39. Chaudhary,P.M. *et al.* Death receptor 5, a new member of the TNFR family, and DR4 induce FADD- dependent apoptosis and activate the NF-kappaB pathway. *Immunity.* 7, 821-830 (1997).

40. Schneider,P. *et al.* TRAIL receptors 1 (DR4) and 2 (DR5) signal FADD-dependent apoptosis and activate NF-kappaB. *Immunity.* 7, 831-836 (1997).

41. Chinnaiyan,A.M. *et al.* Signal transduction by DR3, a death domain-containing receptor related to TNFR-1 and CD95. *Science* 274, 990-992 (1996).

42. Pan,G. *et al.* Identification and functional characterization of DR6, a novel death domain-containing TNF receptor. *FEBS Lett.* 431, 351-356 (1998).

43. Kischkel,F.C. *et al.* Cytotoxicity-dependent APO-1 (Fas/CD95)-associated proteins form a death-inducing signaling complex (DISC) with the receptor. *EMBO J.* 14, 5579-5588 (1995).

44. Medema,J.P. *et al.* FLICE is activated by association with the CD95 death-inducing signaling complex (DISC). *EMBO J.* 16, 2794-2804 (1997).

45. Scaffidi,C. *et al.* Two CD95 (APO-1/Fas) signaling pathways. *EMBO J.* 17, 1675-1687 (1998).

46. Li,H., Zhu,H., Xu,C.J. & Yuan,J. Cleavage of BID by caspase 8 mediates the mitochondrial damage in the Fas pathway of apoptosis. *Cell* 94, 491-501 (1998).

47. Luo,X., Budihardjo,I., Zou,H., Slaughter,C. & Wang,X. Bid, a Bcl2 interacting protein, mediates cytochrome c release from mitochondria in response to activation of cell surface death receptors. *Cell* 94, 481-490 (1998).

48. Irmler,M. *et al.* Inhibition of death receptor signals by cellular FLIP. *Nature* 388, 190-195 (1997).

49. Kataoka,T. The caspase-8 modulator c-FLIP. *Crit Rev. Immunol.* 25, 31-58 (2005).

50. Chang,D.W. *et al.* c-FLIP(L) is a dual function regulator for caspase-8 activation and CD95-mediated apoptosis. *EMBO J* 21, 3704-3714 (2002).

51. Yeh,W.C. *et al.* Requirement for Casper (c-FLIP) in regulation of death receptor-induced apoptosis and embryonic development. *Immunity.* 12, 633-642 (2000).

52. Thorburn,A. Death receptor-induced cell killing. *Cell Signal.* 16, 139-144 (2004).

53. Zhang,N., Hartig,H., Dzhagalov,I., Draper,D. & He,Y.W. The role of apoptosis in the development and function of T lymphocytes. *Cell Res.* 15, 749-769 (2005).

54. Schisa,J.A., Pitt,J.N. & Priess,J.R. Analysis of RNA associated with P granules in germ cells of C. elegans adults. *Development* 128, 1287-1298 (2001).

55. Anderson,P. & Kedersha,N. RNA granules. *Journal of Cell Biology* 172, 803-808 (2006).

56. Krichevsky,A.M. & Kosik,K.S. Neuronal RNA granules: a link between RNA localization and stimulation-dependent translation. *Neuron* 32, 683-696 (2001).

57. Nover,L., Scharf,K.D. & Neumann,D. Cytoplasmic heat shock granules are formed from precursor particles and are associated with a specific set of mRNAs. *Mol. Cell Biol.* 9, 1298-1308 (1989).

58. Anderson,P. & Kedersha,N. Stressful initiations. *J. Cell Sci.* 115, 3227-3234 (2002).

59. Kim,W.J., Back,S.H., Kim,V., Ryu,I. & Jang,S.K. Sequestration of TRAF2 into stress granules interrupts tumor necrosis factor signaling under stress conditions. *Mol. Cell Biol.* 25, 2450-2462 (2005).

60. Anderson,P. & Kedersha,N. Stress granules. *Curr. Biol.* 19, R397-R398 (2009).

61. Kedersha,N. *et al.* Dynamic shuttling of TIA-1 accompanies the recruitment of mRNA to mammalian stress granules. *J. Cell Biol.* 151, 1257-1268 (2000).

62. Forch,P. *et al.* The apoptosis-promoting factor TIA-1 is a regulator of alternative pre-mRNA splicing. *Mol. Cell* 6, 1089-1098 (2000).

63. Le Guiner,C. *et al.* TIA-1 and TIAR activate splicing of alternative exons with weak 5' splice sites followed by a U-rich stretch on their own pre-mRNAs. *J. Biol. Chem.* 276, 40638-40646 (2001).

64. Piecyk,M. *et al.* TIA-1 is a translational silencer that selectively regulates the expression of TNF-alpha. *EMBO J.* 19, 4154-4163 (2000).

65. Dixon,D.A. *et al.* Regulation of cyclooxygenase-2 expression by the translational silencer TIA-1. *J. Exp. Med.* 198, 475-481 (2003).

66. Anderson,P. & Kedersha,N. Visibly stressed: the role of eIF2, TIA-1, and stress granules in protein translation.3238. *Cell Stress. Chaperones.* 7, 213-221 (2002).

67. Kulkarni,M., Ozgur,S. & Stoecklin,G. On track with P-bodies. *Biochem. Soc. Trans.* 38, 242-251 (2010).

68. Franks,T.M. & Lykke-Andersen,J. TTP and BRF proteins nucleate processing body formation to silence mRNAs with AU-rich elements. *Genes Dev.* 21, 719-735 (2007).

69. Liu,J., Valencia-Sanchez,M.A., Hannon,G.J. & Parker,R. MicroRNA-dependent localization of targeted mRNAs to mammalian P-bodies. *Nat. Cell Biol.* 7, 719-723 (2005).

70. Kedersha,N. *et al.* Stress granules and processing bodies are dynamically linked sites of mRNP remodeling. *J. Cell Biol.* 169, 871-884 (2005).

71. Jackson,R.J., Hellen,C.U. & Pestova,T.V. The mechanism of eukaryotic translation initiation and principles of its regulation. *Nat. Rev. Mol. Cell Biol.* 11, 113-127 (2010).

72. Holcik,M. & Sonenberg,N. Translational control in stress and apoptosis. *Nat. Rev. Mol. Cell Biol.* 6, 318-327 (2005).

73. Klann,E. & Dever,T.E. Biochemical mechanisms for translational regulation in synaptic plasticity. *Nat. Rev. Neurosci.* 5, 931-942 (2004).

74. Hinnebusch,A.G. Translational regulation of GCN4 and the general amino acid control of yeast. *Annu. Rev. Microbiol.* 59, 407-450 (2005).

75. Clemens,M.J. Targets and mechanisms for the regulation of translation in malignant transformation. *Oncogene* 23, 3180-3188 (2004).

76. Krishnamoorthy,T., Pavitt,G.D., Zhang,F., Dever,T.E. & Hinnebusch,A.G. Tight binding of the phosphorylated alpha subunit of initiation factor 2 (eIF2alpha) to the regulatory subunits of

guanine nucleotide exchange factor eIF2B is required for inhibition of translation initiation. *Mol. Cell Biol.* 21, 5018-5030 (2001).

77. Zhu,S. & Wek,R.C. Ribosome-binding domain of eukaryotic initiation factor-2 kinase GCN2 facilitates translation control. *J. Biol. Chem.* 273, 1808-1814 (1998).

78. Deng,J. *et al.* Activation of GCN2 in UV-irradiated cells inhibits translation. *Curr. Biol.* 12, 1279-1286 (2002).

79. Jiang,H.Y. & Wek,R.C. GCN2 phosphorylation of eIF2alpha activates NF-kappaB in response to UV irradiation. *Biochem. J.* 385, 371-380 (2005).

80. Lu,W., Laszlo,C.F., Miao,Z., Chen,H. & Wu,S. The role of nitric-oxide synthase in the regulation of UVB light-induced phosphorylation of the alpha subunit of eukaryotic initiation factor 2. *J. Biol. Chem.* 284, 24281-24288 (2009).

81. Rafie-Kolpin,M. *et al.* Two heme-binding domains of heme-regulated eukaryotic initiation factor-2alpha kinase. N terminus and kinase insertion. *J. Biol. Chem.* 275, 5171-5178 (2000).

82. Uma,S., Hartson,S.D., Chen,J.J. & Matts,R.L. Hsp90 is obligatory for the heme-regulated eIF-2alpha kinase to acquire and maintain an activable conformation. *J. Biol. Chem.* 272, 11648-11656 (1997).

83. Gurr,J.R. *et al.* Nitric oxide production by arsenite. *Mutat. Res.* 533, 173-182 (2003).

84. Lu,L., Han,A.P. & Chen,J.J. Translation initiation control by heme-regulated eukaryotic initiation factor 2alpha kinase in erythroid cells under cytoplasmic stresses.1. *Mol. Cell Biol.* 21, 7971-7980 (2001).

85. Garcia,M.A. *et al.* Impact of protein kinase PKR in cell biology: from antiviral to antiproliferative action. *Microbiol. Mol. Biol. Rev.* 70, 1032-1060 (2006).

86. Onuki,R. *et al.* An RNA-dependent protein kinase is involved in tunicamycin-induced apoptosis and Alzheimer's disease. *EMBO J.* 23, 959-968 (2004).

87. Bennasser,Y., Badou,A., Tkaczuk,J. & Bahraoui,E. Signaling pathways triggered by HIV-1 Tat in human monocytes to induce TNF-alpha. *Virology* 303, 174-180 (2002).

88. Pyo,C.W., Lee,S.H. & Choi,S.Y. Oxidative stress induces PKR-dependent apoptosis via IFN-gamma activation signaling in Jurkat T cells. *Biochem. Biophys. Res. Commun.* 377, 1001-1006 (2008).

89. Patel,R.C. & Sen,G.C. PACT, a protein activator of the interferon-induced protein kinase, PKR. *EMBO J.* 17, 4379-4390 (1998).

90. Kumar,A., Haque,J., Lacoste,J., Hiscott,J. & Williams,B.R. Double-stranded RNA-dependent protein kinase activates transcription factor NF-kappa B by phosphorylating I kappa B. *Proc. Natl. Acad. Sci. U. S. A* 91, 6288-6292 (1994).

91. Gil,J. *et al.* TRAF family proteins link PKR with NF-kappa B activation. *Mol. Cell Biol.* 24, 4502-4512 (2004).

92. Goh,K.C., deVeer,M.J. & Williams,B.R. The protein kinase PKR is required for p38 MAPK activation and the innate immune response to bacterial endotoxin. *EMBO J.* 19, 4292-4297 (2000).

93. Garcia,M.A. *et al.* Impact of protein kinase PKR in cell biology: from antiviral to antiproliferative action. *Microbiol. Mol. Biol. Rev.* 70, 1032-1060 (2006).

94. Gil,J. & Esteban,M. The interferon-induced protein kinase (PKR), triggers apoptosis through FADD-mediated activation of caspase 8 in a manner independent of Fas and TNF-alpha receptors. *Oncogene* 19, 3665-3674 (2000).

95. Meurs,E.F., Galabru,J., Barber,G.N., Katze,M.G. & Hovanessian,A.G. Tumor suppressor function of the interferon-induced double-stranded RNA-activated protein kinase. *Proc. Natl. Acad. Sci. U. S. A* 90, 232-236 (1993).

96. Abraham,N. *et al.* Characterization of transgenic mice with targeted disruption of the catalytic domain of the double-stranded RNA-dependent protein kinase, PKR. *J. Biol. Chem.* 274, 5953-5962 (1999).

97. Kumar,A. *et al.* Deficient cytokine signaling in mouse embryo fibroblasts with a targeted deletion in the PKR gene: role of IRF-1 and NF-kappaB. *EMBO J.* 16, 406-416 (1997).

98. Tan,S.L., Gale,M.J., Jr. & Katze,M.G. Double-stranded RNA-independent dimerization of interferon-induced protein kinase PKR and inhibition of dimerization by the cellular P58IPK inhibitor. *Mol. Cell Biol.* 18, 2431-2443 (1998).

99. Donze,O., Abbas-Terki,T. & Picard,D. The Hsp90 chaperone complex is both a facilitator and a repressor of the dsRNA-dependent kinase PKR. *EMBO J.* 20, 3771-3780 (2001).

100. Ron,D. Translational control in the endoplasmic reticulum stress response. *J. Clin. Invest* 110, 1383-1388 (2002).

101. Vattem,K.M. & Wek,R.C. Reinitiation involving upstream ORFs regulates ATF4 mRNA translation in mammalian cells. *Proc. Natl. Acad. Sci. U. S. A* 101, 11269-11274 (2004).

102. Ron,D. & Walter,P. Signal integration in the endoplasmic reticulum unfolded protein response. *Nat. Rev. Mol. Cell Biol.* 8, 519-529 (2007).

103. Cullinan,S.B. *et al.* Nrf2 is a direct PERK substrate and effector of PERK-dependent cell survival. *Mol. Cell Biol.* 23, 7198-7209 (2003).

104. Cullinan,S.B. & Diehl,J.A. Coordination of ER and oxidative stress signaling: the PERK/Nrf2 signaling pathway.1. *Int. J. Biochem. Cell Biol.* 38, 317-332 (2006).

105. Sitia,R. & Braakman,I. Quality control in the endoplasmic reticulum protein factory. *Nature* 426, 891-894 (2003).

106. Ellgaard,L. & Helenius,A. Quality control in the endoplasmic reticulum. *Nat. Rev. Mol. Cell Biol.* 4, 181-191 (2003).

107. Garcia-Mata,R., Gao,Y.S. & Sztul,E. Hassles with taking out the garbage: aggravating aggresomes. *Traffic.* 3, 388-396 (2002).

108. Kopito,R.R. Aggresomes, inclusion bodies and protein aggregation. *Trends Cell Biol.* 10, 524-530 (2000).

109. Schroder,M. & Kaufman,R.J. The mammalian unfolded protein response. *Annu. Rev. Biochem.* 74, 739-789 (2005).

110. Ellgaard,L. & Ruddock,L.W. The human protein disulphide isomerase family: substrate interactions and functional properties. *EMBO Rep.* 6, 28-32 (2005).

111. Hebert,D.N. & Molinari,M. In and out of the ER: protein folding, quality control, degradation, and related human diseases. *Physiol Rev.* 87, 1377-1408 (2007).

112. Oliver,J.D., Roderick,H.L., Llewellyn,D.H. & High,S. ERp57 functions as a subunit of specific complexes formed with the ER lectins calreticulin and calnexin. *Mol. Biol. Cell* 10, 2573-2582 (1999).

113. Shaw,P.E. Peptidyl-prolyl isomerases: a new twist to transcription. *EMBO Rep.* 3, 521-526 (2002).

114. Kaufman,R.J. Orchestrating the unfolded protein response in health and disease. *J. Clin. Invest* 110, 1389-1398 (2002).

115. Kaufman,R.J. Stress signaling from the lumen of the endoplasmic reticulum: coordination of gene transcriptional and translational controls. *Genes Dev.* 13, 1211-1233 (1999).

116. Harding,H.P. *et al.* An integrated stress response regulates amino acid metabolism and resistance to oxidative stress. *Mol. Cell* 11, 619-633 (2003).

117. Harding,H.P., Calfon,M., Urano,F., Novoa,I. & Ron,D. Transcriptional and translational control in the Mammalian unfolded protein response. *Annu. Rev. Cell Dev. Biol.* 18, 575-599 (2002).

118. Hampton,R.Y. ER stress response: getting the UPR hand on misfolded proteins. *Curr. Biol.* 10, R518-R521 (2000).

119. Xu,C., Bailly-Maitre,B. & Reed,J.C. Endoplasmic reticulum stress: cell life and death decisions. *J. Clin. Invest* 115, 2656-2664 (2005).

120. Urano,F., Bertolotti,A. & Ron,D. IRE1 and efferent signaling from the endoplasmic reticulum. *J. Cell Sci.* 113 Pt 21, 3697-3702 (2000).

121. Szegezdi,E., Logue,S.E., Gorman,A.M. & Samali,A. Mediators of endoplasmic reticulum stress-induced apoptosis. *EMBO Rep.* 7, 880-885 (2006).

122. Cox,J.S., Shamu,C.E. & Walter,P. Transcriptional induction of genes encoding endoplasmic reticulum resident proteins requires a transmembrane protein kinase. *Cell* 73, 1197-1206 (1993).

123. Harding,H.P., Zhang,Y. & Ron,D. Protein translation and folding are coupled by an endoplasmic-reticulum-resident kinase. *Nature* 397, 271-274 (1999).

124. Wang,Y. *et al.* Activation of ATF6 and an ATF6 DNA binding site by the endoplasmic reticulum stress response. *J. Biol. Chem.* 275, 27013-27020 (2000).

125. Zhang,K. & Kaufman,R.J. The unfolded protein response: a stress signaling pathway critical for health and disease. *Neurology* 66, S102-S109 (2006).

126. Scheuner,D. *et al.* Translational control is required for the unfolded protein response and in vivo glucose homeostasis. *Mol. Cell* 7, 1165-1176 (2001).

127. Iwakoshi,N.N. *et al.* Plasma cell differentiation and the unfolded protein response intersect at the transcription factor XBP-1. *Nat. Immunol.* 4, 321-329 (2003).

128. Hoozemans,J.J. *et al.* The unfolded protein response is activated in Alzheimer's disease. *Acta Neuropathol.* 110, 165-172 (2005).

129. Delepine,M. *et al.* EIF2AK3, encoding translation initiation factor 2-alpha kinase 3, is mutated in patients with Wolcott-Rallison syndrome. *Nat. Genet.* 25, 406-409 (2000).

130. Ma,Y. & Hendershot,L.M. The role of the unfolded protein response in tumour development: friend or foe? *Nat. Rev. Cancer* 4, 966-977 (2004).

131. Koritzinsky,M. *et al.* Gene expression during acute and prolonged hypoxia is regulated by distinct mechanisms of translational control. *EMBO J.* 25, 1114-1125 (2006).

132. Blais,J.D. *et al.* Activating transcription factor 4 is translationally regulated by hypoxic stress. *Mol. Cell Biol.* 24, 7469-7482 (2004).

133. Oikawa,D., Kimata,Y., Kohno,K. & Iwawaki,T. Activation of mammalian IRE1alpha upon ER stress depends on dissociation of BiP rather than on direct interaction with unfolded proteins. *Exp. Cell Res.* 315, 2496-2504 (2009).

134. Tirasophon,W., Welihinda,A.A. & Kaufman,R.J. A stress response pathway from the endoplasmic reticulum to the nucleus requires a novel bifunctional protein kinase/endoribonuclease (Ire1p) in mammalian cells. *Genes Dev.* 12, 1812-1824 (1998).

135. Wang,X.Z. *et al.* Cloning of mammalian Ire1 reveals diversity in the ER stress responses. *EMBO J.* 17, 5708-5717 (1998).

136. Bertolotti,A. *et al.* Increased sensitivity to dextran sodium sulfate colitis in IRE1beta-deficient mice. *J. Clin. Invest* 107, 585-593 (2001).

137. Nikawa,J., Akiyoshi,M., Hirata,S. & Fukuda,T. Saccharomyces cerevisiae IRE2/HAC1 is involved in IRE1-mediated KAR2 expression. *Nucleic Acids Res.* 24, 4222-4226 (1996).

138. Calfon,M. *et al.* IRE1 couples endoplasmic reticulum load to secretory capacity by processing the XBP-1 mRNA. *Nature* 415, 92-96 (2002).

139. Ruegsegger,U., Leber,J.H. & Walter,P. Block of HAC1 mRNA translation by long-range base pairing is released by cytoplasmic splicing upon induction of the unfolded protein response. *Cell* 107, 103-114 (2001).

140. Sidrauski,C. & Walter,P. The transmembrane kinase Ire1p is a site-specific endonuclease that initiates mRNA splicing in the unfolded protein response. *Cell* 90, 1031-1039 (1997).

141. Yoshida,H., Oku,M., Suzuki,M. & Mori,K. pXBP1(U) encoded in XBP1 pre-mRNA negatively regulates unfolded protein response activator pXBP1(S) in mammalian ER stress response. *J. Cell Biol.* 172, 565-575 (2006).

142. Acosta-Alvear,D. *et al.* XBP1 controls diverse cell type- and condition-specific transcriptional regulatory networks. *Mol. Cell* 27, 53-66 (2007).

143. Lee,A.H., Iwakoshi,N.N. & Glimcher,L.H. XBP-1 regulates a subset of endoplasmic reticulum resident chaperone genes in the unfolded protein response. *Mol. Cell Biol.* 23, 7448-7459 (2003).

144. Reimold,A.M. *et al.* Plasma cell differentiation requires the transcription factor XBP-1. *Nature* 412, 300-307 (2001).

145. Reimold,A.M. *et al.* An essential role in liver development for transcription factor XBP-1. *Genes Dev.* 14, 152-157 (2000).

146. Urano,F. *et al.* Coupling of stress in the ER to activation of JNK protein kinases by transmembrane protein kinase IRE1. *Science* 287, 664-666 (2000).

147. Nguyen,D.T. *et al.* Nck-dependent activation of extracellular signal-regulated kinase-1 and regulation of cell survival during endoplasmic reticulum stress. *Mol. Biol. Cell* 15, 4248-4260 (2004).

148. Hu,P., Han,Z., Couvillon,A.D., Kaufman,R.J. & Exton,J.H. Autocrine tumor necrosis factor alpha links endoplasmic reticulum

stress to the membrane death receptor pathway through IRE1alpha-mediated NF-kappaB activation and down-regulation of TRAF2 expression. *Mol. Cell Biol.* 26, 3071-3084 (2006).

149. Bertolotti,A., Zhang,Y., Hendershot,L.M., Harding,H.P. & Ron,D. Dynamic interaction of BiP and ER stress transducers in the unfolded-protein response. *Nat. Cell Biol.* 2, 326-332 (2000).

150. Jousse,C. *et al.* Inhibition of a constitutive translation initiation factor 2alpha phosphatase, CReP, promotes survival of stressed cells. *J. Cell Biol.* 163, 767-775 (2003).

151. Novoa,I., Zeng,H., Harding,H.P. & Ron,D. Feedback inhibition of the unfolded protein response by GADD34-mediated dephosphorylation of eIF2alpha. *J. Cell Biol.* 153, 1011-1022 (2001).

152. Yan,W. *et al.* Control of PERK eIF2alpha kinase activity by the endoplasmic reticulum stress-induced molecular chaperone P58IPK. *Proc. Natl. Acad. Sci. U. S. A* 99, 15920-15925 (2002).

153. van Huizen,R., Martindale,J.L., Gorospe,M. & Holbrook,N.J. P58IPK, a novel endoplasmic reticulum stress-inducible protein and potential negative regulator of eIF2alpha signaling. *J. Biol. Chem.* 278, 15558-15564 (2003).

154. Tan,S.L., Gale,M.J., Jr. & Katze,M.G. Double-stranded RNA-independent dimerization of interferon-induced protein kinase PKR and inhibition of dimerization by the cellular P58IPK inhibitor. *Mol. Cell Biol.* 18, 2431-2443 (1998).

155. Petrova,K., Oyadomari,S., Hendershot,L.M. & Ron,D. Regulated association of misfolded endoplasmic reticulum lumenal proteins with P58/DNAJc3. *EMBO J.* 27, 2862-2872 (2008).

156. Oyadomari,S. *et al.* Cotranslocational degradation protects the stressed endoplasmic reticulum from protein overload. *Cell* 126, 727-739 (2006).

157. Rutkowski,D.T. *et al.* The role of p58IPK in protecting the stressed endoplasmic reticulum. *Mol. Biol. Cell* 18, 3681-3691 (2007).

158. Harding,H.P., Zhang,Y., Bertolotti,A., Zeng,H. & Ron,D. Perk is essential for translational regulation and cell survival during the unfolded protein response. *Mol. Cell* 5, 897-904 (2000).

159. Zinszner,H. *et al.* CHOP is implicated in programmed cell death in response to impaired function of the endoplasmic reticulum. *Genes Dev.* 12, 982-995 (1998).

160. Lange,P.S. *et al.* ATF4 is an oxidative stress-inducible, prodeath transcription factor in neurons in vitro and in vivo. *J. Exp. Med.* 205, 1227-1242 (2008).

161. Harding,H.P. *et al.* Diabetes mellitus and exocrine pancreatic dysfunction in perk-/- mice reveals a role for translational control in secretory cell survival. *Mol. Cell* 7, 1153-1163 (2001).

162. Zhang,P. *et al.* The PERK eukaryotic initiation factor 2 alpha kinase is required for the development of the skeletal system, postnatal growth, and the function and viability of the pancreas. *Mol. Cell Biol.* 22, 3864-3874 (2002).

163. Deng,J. *et al.* Translational repression mediates activation of nuclear factor kappa B by phosphorylated translation initiation factor 2. *Mol. Cell Biol.* 24, 10161-10168 (2004).

164. Oyadomari,S. *et al.* Targeted disruption of the Chop gene delays endoplasmic reticulum stress-mediated diabetes. *J. Clin. Invest* 109, 525-532 (2002).

165. Ohoka,N., Yoshii,S., Hattori,T., Onozaki,K. & Hayashi,H. TRB3, a novel ER stress-inducible gene, is induced via ATF4-CHOP pathway and is involved in cell death. *EMBO J.* 24, 1243-1255 (2005).

166. Donati,G., Imbriano,C. & Mantovani,R. Dynamic recruitment of transcription factors and epigenetic changes on the ER stress response gene promoters. *Nucleic Acids Res.* 34, 3116-3127 (2006).

167. Ma,Y., Brewer,J.W., Diehl,J.A. & Hendershot,L.M. Two distinct stress signaling pathways converge upon the CHOP promoter during the mammalian unfolded protein response. *J. Mol. Biol.* 318, 1351-1365 (2002).

168. Wang,X.Z. & Ron,D. Stress-induced phosphorylation and activation of the transcription factor CHOP (GADD153) by p38 MAP Kinase. *Science* 272, 1347-1349 (1996).

169. Scheuner,D. *et al.* Translational control is required for the unfolded protein response and in vivo glucose homeostasis. *Mol. Cell* 7, 1165-1176 (2001).

170. Sok,J. *et al.* CHOP-Dependent stress-inducible expression of a novel form of carbonic anhydrase VI. *Mol. Cell Biol.* 19, 495-504 (1999).

171. Wang,Y. *et al.* Activation of ATF6 and an ATF6 DNA binding site by the endoplasmic reticulum stress response. *J. Biol. Chem.* 275, 27013-27020 (2000).

172. Shen,J., Chen,X., Hendershot,L. & Prywes,R. ER stress regulation of ATF6 localization by dissociation of BiP/GRP78 binding and unmasking of Golgi localization signals. *Dev. Cell* 3, 99-111 (2002).

173. Schroder,M. The unfolded protein response. *Mol. Biotechnol.* 34, 279-290 (2006).

174. Yoshida,H. *et al.* ATF6 activated by proteolysis binds in the presence of NF-Y (CBF) directly to the cis-acting element responsible for the mammalian unfolded protein response. *Mol. Cell Biol.* 20, 6755-6767 (2000).

175. Haze,K. *et al.* Identification of the G13 (cAMP-response-element-binding protein-related protein) gene product related to activating transcription factor 6 as a transcriptional activator of the mammalian unfolded protein response. *Biochem. J.* 355, 19-28 (2001).

176. Thuerauf,D.J., Morrison,L. & Glembotski,C.C. Opposing roles for ATF6alpha and ATF6beta in endoplasmic reticulum stress response gene induction. *J. Biol. Chem.* 279, 21078-21084 (2004).

177. Yamamoto,K. *et al.* Transcriptional induction of mammalian ER quality control proteins is mediated by single or combined action of ATF6alpha and XBP1. *Dev. Cell* 13, 365-376 (2007).

178. Wu,J. *et al.* ATF6alpha optimizes long-term endoplasmic reticulum function to protect cells from chronic stress. *Dev. Cell* 13, 351-364 (2007).

179. Kondo,S. *et al.* OASIS, a CREB/ATF-family member, modulates UPR signalling in astrocytes. *Nat. Cell Biol.* 7, 186-194 (2005).

180. Zhang,K. *et al.* Endoplasmic reticulum stress activates cleavage of CREBH to induce a systemic inflammatory response. *Cell* 124, 587-599 (2006).

181. Lin,J.H. *et al.* IRE1 signaling affects cell fate during the unfolded protein response. *Science* 318, 944-949 (2007).

182. Lin,J.H., Li,H., Zhang,Y., Ron,D. & Walter,P. Divergent effects of PERK and IRE1 signaling on cell viability. *PLoS. One.* 4, e4170 (2009).

183. Szegezdi,E., Fitzgerald,U. & Samali,A. Caspase-12 and ER-stress-mediated apoptosis: the story so far. *Ann. N. Y. Acad. Sci.* 1010, 186-194 (2003).

184. Fischer,H., Koenig,U., Eckhart,L. & Tschachler,E. Human caspase 12 has acquired deleterious mutations. *Biochem. Biophys. Res. Commun.* 293, 722-726 (2002).

185. Rao,R.V. *et al.* Coupling endoplasmic reticulum stress to the cell death program. Mechanism of caspase activation. *J. Biol. Chem.* 276, 33869-33874 (2001).

186. Marciniak,S.J. *et al.* CHOP induces death by promoting protein synthesis and oxidation in the stressed endoplasmic reticulum. *Genes Dev.* 18, 3066-3077 (2004).

187. McCullough,K.D., Martindale,J.L., Klotz,L.O., Aw,T.Y. & Holbrook,N.J. Gadd153 sensitizes cells to endoplasmic reticulum stress by down-regulating Bcl2 and perturbing the cellular redox state. *Mol. Cell Biol.* 21, 1249-1259 (2001).

188. Puthalakath,H. *et al.* ER stress triggers apoptosis by activating BH3-only protein Bim. *Cell* 129, 1337-1349 (2007).

189. Wei,M.C. *et al.* Proapoptotic BAX and BAK: a requisite gateway to mitochondrial dysfunction and death. *Science* 292, 727-730 (2001).

190. Scorrano,L. *et al.* BAX and BAK regulation of endoplasmic reticulum Ca2+: a control point for apoptosis. *Science* 300, 135-139 (2003).

191. Hetz,C. *et al.* Proapoptotic BAX and BAK modulate the unfolded protein response by a direct interaction with IRE1alpha. *Science* 312, 572-576 (2006).

192. Upton,J.P. *et al.* Caspase-2 cleavage of BID is a critical apoptotic signal downstream of endoplasmic reticulum stress. *Mol. Cell Biol.* 28, 3943-3951 (2008).

193. Li,J., Lee,B. & Lee,A.S. Endoplasmic reticulum stress-induced apoptosis: multiple pathways and activation of p53-up-regulated

modulator of apoptosis (PUMA) and NOXA by p53. *J. Biol. Chem.* 281, 7260-7270 (2006).

194. Szegezdi,E., Macdonald,D.C., Ni,C.T., Gupta,S. & Samali,A. Bcl-2 family on guard at the ER. *Am. J. Physiol Cell Physiol* 296, C941-C953 (2009).

195. Yamamoto,K., Ichijo,H. & Korsmeyer,S.J. BCL-2 is phosphorylated and inactivated by an ASK1/Jun N-terminal protein kinase pathway normally activated at G(2)/M. *Mol. Cell Biol.* 19, 8469-8478 (1999).

196. Yoneda,T. *et al.* Activation of caspase-12, an endoplastic reticulum (ER) resident caspase, through tumor necrosis factor receptor-associated factor 2-dependent mechanism in response to the ER stress. *J. Biol. Chem.* 276, 13935-13940 (2001).

197. Malumbres,M. & Barbacid,M. Mammalian cyclin-dependent kinases 2. *Trends in Biochemical Sciences* 30, 630-641 (2005).

198. Zhang,J. *et al.* Nuclear localization of Cdk5 is a key determinant in the postmitotic state of neurons. *Proc. Natl. Acad. Sci. U. S. A* 105, 8772-8777 (2008).

199. Malumbres,M. *et al.* Cyclin-dependent kinases: a family portrait. *Nat. Cell Biol.* 11, 1275-1276 (2009).

200. Sherr,C.J. & Roberts,J.M. CDK inhibitors: positive and negative regulators of G1-phase progression. *Genes Dev.* 13, 1501-1512 (1999).

201. Pavletich,N.P. Mechanisms of cyclin-dependent kinase regulation: structures of Cdks, their cyclin activators, and Cip and INK4 inhibitors. *J. Mol. Biol.* 287, 821-828 (1999).

202. Fisher,R.P. Secrets of a double agent: CDK7 in cell-cycle control and transcription. *J. Cell Sci.* 118, 5171-5180 (2005).

203. Satyanarayana,A. & Kaldis,P. Mammalian cell-cycle regulation: several Cdks, numerous cyclins and diverse compensatory mechanisms. *Oncogene* 28, 2925-2939 (2009).

204. Akoulitchev,S., Chuikov,S. & Reinberg,D. TFIIH is negatively regulated by cdk8-containing mediator complexes. *Nature* 407, 102-106 (2000).

205. Sano,M. & Schneider,M.D. Cyclins that don't cycle--cyclin T/cyclin-dependent kinase-9 determines cardiac muscle cell size. *Cell Cycle* 2, 99-104 (2003).

206. Wang,S. & Fischer,P.M. Cyclin-dependent kinase 9: a key transcriptional regulator and potential drug target in oncology, virology and cardiology. *Trends Pharmacol. Sci.* 29, 302-313 (2008).

207. Chen,X. Cyclin G: a regulator of the p53-Mdm2 network. *Dev. Cell* 2, 518-519 (2002).

208. Edelheit,S. & Meiri,N. Cyclin S: a new member of the cyclin family plays a role in long-term memory. *Eur. J. Neurosci.* 19, 365-375 (2004).

209. Botz,J. *et al.* Cell cycle regulation of the murine cyclin E gene depends on an E2F binding site in the promoter. *Mol. Cell Biol.* 16, 3401-3409 (1996).

210. Morgan,D.O. Principles of CDK regulation. *Nature* 374, 131-134 (1995).

211. Margalit,A., Vlcek,S., Gruenbaum,Y. & Foisner,R. Breaking and making of the nuclear envelope. *J. Cell Biochem.* 95, 454-465 (2005).

212. Golsteyn,R.M. Cdk1 and Cdk2 complexes (cyclin dependent kinases) in apoptosis: a role beyond the cell cycle.2. *Cancer Letters* 217, 129-138 (2005).

213. Kranenburg,O., vanderEb,A. & Zantema,A. Cyclin D1 is an essential mediator of apoptotic neuronal cell death.4. *Embo Journal* 15, 46-54 (1996).

214. Brady,H.J., Gil-Gomez,G., Kirberg,J. & Berns,A.J. Bax alpha perturbs T cell development and affects cell cycle entry of T cells. *EMBO J.* 15, 6991-7001 (1996).

215. Williams,O., Gil-Gomez,G., Norton,T., Kioussis,D. & Brady,H.J. Activation of Cdk2 is a requirement for antigen-mediated thymic negative selection. *Eur. J. Immunol.* 30, 709-713 (2000).

216. Gil-Gomez,G., Berns,A. & Brady,H.J. A link between cell cycle and cell death: Bax and Bcl-2 modulate Cdk2 activation during thymocyte apoptosis. *EMBO J.* 17, 7209-7218 (1998).

217. Granes,F., Roig,M.B., Brady,H.J.M. & Gil-Gomez,G. Cdk2 activation acts upstream of the mitochondrion during glucocorticoid induced thymocyte apoptosis.1. *European Journal of Immunology* 34, 2781-2790 (2004).

218. Roig,M.B. *et al.* Identification of a novel cyclin required for the intrinsic apoptosis pathway in lymphoid cells. *Cell Death Differ.* 16, 230-243 (2009).

219. Adams,P.D. *et al.* Identification of a cyclin-cdk2 recognition motif present in substrates and p21-like cyclin-dependent kinase inhibitors. *Mol. Cell Biol.* 16, 6623-6633 (1996).

220. Bonet,J. *et al.* The role of residue stability in transient protein-protein interactions involved in enzymatic phosphate hydrolysis. A computational study. *Proteins* 63, 65-77 (2006).

221. Jeffrey,P.D. *et al.* Mechanism of CDK activation revealed by the structure of a cyclinA-CDK2 complex. *Nature* 376, 313-320 (1995).

222. Zwijsen,R.M., Buckle,R.S., Hijmans,E.M., Loomans,C.J. & Bernards,R. Ligand-independent recruitment of steroid receptor coactivators to estrogen receptor by cyclin D1. *Genes Dev.* 12, 3488-3498 (1998).

223. Zhang,B. *et al.* The significance of controlled conditions in lentiviral vector titration and in the use of multiplicity of infection (MOI) for predicting gene transfer events. *Genet. Vaccines. Ther.* 2, 6 (2004).

224. Sambrook,J., Fritsch,E. & Maniatis,T. Molecular Cloning. A Laboratory Manual. Cold Spring Harbor Laboratory Press, Cold Spring Harbor, New York, USA (1989).

225. Campbell,R.E. *et al.* A monomeric red fluorescent protein. *Proc. Natl. Acad. Sci. U. S. A* 99, 7877-7882 (2002).

226. Lachmanovich,E. *et al.* Co-localization analysis of complex formation among membrane proteins by computerized fluorescence microscopy: application to immunofluorescence co-patching studies. *J. Microsc.* 212, 122-131 (2003).

227. Li,Q. *et al.* A syntaxin 1, Galpha(o), and N-type calcium channel complex at a presynaptic nerve terminal: analysis by quantitative immunocolocalization. *J. Neurosci.* 24, 4070-4081 (2004).

228. Spector,D.L. SnapShot: Cellular bodies. *Cell* 127, 1071 (2006).

229. Kimball,S.R. Regulation of global and specific mRNA translation by amino acids. *J. Nutr.* 132, 883-886 (2002).

230. Jiang,H.Y. & Wek,R.C. GCN2 phosphorylation of eIF2alpha activates NF-kappaB in response to UV irradiation. *Biochem. J.* 385, 371-380 (2005).

231. Srivastava,S.P., Kumar,K.U. & Kaufman,R.J. Phosphorylation of eukaryotic translation initiation factor 2 mediates apoptosis in response to activation of the double-stranded RNA-dependent protein kinase. *J. Biol. Chem.* 273, 2416-2423 (1998).

232. Cuevas,I.C., Frasch,A.C. & D'Orso,I. Insights into a CRM1-mediated RNA-nuclear export pathway in Trypanosoma cruzi. *Mol. Biochem. Parasitol.* 139, 15-24 (2005).

233. Dingwall,C., Robbins,J., Dilworth,S.M., Roberts,B. & Richardson,W.D. The nucleoplasmin nuclear location sequence is larger and more complex than that of SV-40 large T antigen. *J. Cell Biol.* 107, 841-849 (1988).

234. Ikuta,T., Eguchi,H., Tachibana,T., Yoneda,Y. & Kawajiri,K. Nuclear localization and export signals of the human aryl hydrocarbon receptor. *J. Biol. Chem.* 273, 2895-2904 (1998).

235. la Cour,T. *et al.* NESbase version 1.0: a database of nuclear export signals. *Nucleic Acids Res.* 31, 393-396 (2003).

236. Doble,B.W. & Woodgett,J.R. GSK-3: tricks of the trade for a multi-tasking kinase. *J. Cell Sci.* 116, 1175-1186 (2003).

237. Cardozo,T. & Pagano,M. The SCF ubiquitin ligase: insights into a molecular machine. *Nat. Rev. Mol. Cell Biol.* 5, 739-751 (2004).

238. Moshe,Y., Boulaire,J., Pagano,M. & Hershko,A. Role of Polo-like kinase in the degradation of early mitotic inhibitor 1, a regulator of the anaphase promoting complex/cyclosome. *Proc. Natl. Acad. Sci. U. S. A* 101, 7937-7942 (2004).

239. Zhou,B.P. *et al.* Dual regulation of Snail by GSK-3beta-mediated phosphorylation in control of epithelial-mesenchymal transition. *Nat. Cell Biol.* 6, 931-940 (2004).

240. Kanemori,Y., Uto,K. & Sagata,N. beta-TrCP recognizes a previously undescribed nonphosphorylated destruction motif in Cdc25A and

Cdc25B phosphatases. *Proceedings of the National Academy of Sciences of the United States of America* 102, 6279-6284 (2005).

241. Kedersha,N. & Anderson,P. Mammalian stress granules and processing bodies. *Methods Enzymol.* 431, 61-81 (2007).

242. Samali,A., Fitzgerald,U., Deegan,S. & Gupta,S. Methods for monitoring endoplasmic reticulum stress and the unfolded protein response. *Int. J. Cell Biol.* 2010, 830307 (2010).

243. Zinszner,H. *et al.* CHOP is implicated in programmed cell death in response to impaired function of the endoplasmic reticulum. *Genes Dev.* 12, 982-995 (1998).

244. Yamaguchi,H. & Wang,H.G. CHOP is involved in endoplasmic reticulum stress-induced apoptosis by enhancing DR5 expression in human carcinoma cells. *J. Biol. Chem.* 279, 45495-45502 (2004).

245. Collison,A., Foster,P.S. & Mattes,J. Emerging role of tumour necrosis factor-related apoptosis-inducing ligand (TRAIL) as a key regulator of inflammatory responses. *Clin. Exp. Pharmacol. Physiol* 36, 1049-1053 (2009).

246. Upton,J.P. *et al.* Caspase-2 cleavage of BID is a critical apoptotic signal downstream of endoplasmic reticulum stress. *Mol. Cell Biol.* 28, 3943-3951 (2008).

247. Fornace,A.J., Jr. *et al.* DNA-damage-inducible genes in mammalian cells. *Prog. Clin. Biol. Res.* 340A, 315-325 (1990).

248. Kohno,K. Stress-sensing mechanisms in the unfolded protein response: similarities and differences between yeast and mammals. *J. Biochem.* 147, 27-33 (2010).

249. Nickel,W. & Seedorf,M. Unconventional mechanisms of protein transport to the cell surface of eukaryotic cells. *Annu. Rev. Cell Dev. Biol.* 24, 287-308 (2008).

250. Gale,M., Jr. *et al.* P52rIPK regulates the molecular cochaperone P58IPK to mediate control of the RNA-dependent protein kinase in response to cytoplasmic stress. *Biochemistry* 41, 11878-11887 (2002).

251. Lesuffleur,T., Barbat,A., Dussaulx,E. & Zweibaum,A. Growth adaptation to methotrexate of HT-29 human colon carcinoma cells is associated with their ability to differentiate into columnar

absorptive and mucus-secreting cells. *Cancer Res.* 50, 6334-6343 (1990).

252. Davy,C.E. *et al.* Human papillomavirus type 16 E1 E4-induced G2 arrest is associated with cytoplasmic retention of active Cdk1/cyclin B1 complexes. *J. Virol.* 79, 3998-4011 (2005).

253. Poyton,R.O., Ball,K.A. & Castello,P.R. Mitochondrial generation of free radicals and hypoxic signaling. *Trends Endocrinol. Metab* 20, 332-340 (2009).

254. Haynes,C.M., Titus,E.A. & Cooper,A.A. Degradation of misfolded proteins prevents ER-derived oxidative stress and cell death. *Mol. Cell* 15, 767-776 (2004).

255. Kitamura,M. & Hiramatsu,N. The oxidative stress: endoplasmic reticulum stress axis in cadmium toxicity. *Biometals* (2010).

256. Vander Heiden,M.G., Cantley,L.C. & Thompson,C.B. Understanding the Warburg effect: the metabolic requirements of cell proliferation. *Science* 324, 1029-1033 (2009).

257. Vaupel,P. & Mayer,A. Hypoxia in cancer: significance and impact on clinical outcome. *Cancer Metastasis Rev.* 26, 225-239 (2007).

258. Fruehauf,J.P. & Meyskens,F.L., Jr. Reactive oxygen species: a breath of life or death? *Clin. Cancer Res.* 13, 789-794 (2007).

259. Gatenby,R.A. & Gillies,R.J. Why do cancers have high aerobic glycolysis? *Nat. Rev. Cancer* 4, 891-899 (2004).

260. Elstrom,R.L. *et al.* Akt stimulates aerobic glycolysis in cancer cells. *Cancer Res.* 64, 3892-3899 (2004).

261. Wu,J. & Kaufman,R.J. From acute ER stress to physiological roles of the Unfolded Protein Response. *Cell Death. Differ.* 13, 374-384 (2006).

262. Scheuner,D. *et al.* Control of mRNA translation preserves endoplasmic reticulum function in beta cells and maintains glucose homeostasis. *Nat. Med.* 11, 757-764 (2005).

263. Ladiges,W.C. *et al.* Pancreatic beta-cell failure and diabetes in mice with a deletion mutation of the endoplasmic reticulum molecular chaperone gene P58IPK. *Diabetes* 54, 1074-1081 (2005).

264. De Bont,R. & van Larebeke,N. Endogenous DNA damage in humans: a review of quantitative data. *Mutagenesis* 19, 169-185 (2004).

265. Stoklsa,T. & Golab,J. Prospects for p53-based cancer therapy. *Acta Biochim. Pol.* 52, 321-328 (2005).

ANNEX

Roig MB, Roset R, Ortet L, Balsiger NA, Anfosso A, Cabellos L, et al. Identification of a novel cyclin required for the intrinsic apoptosis pathway in lymphoid cells. Cell Death Differ. 2009; 16(2): 230-43.

Roset R, Ortet L, Gil-Gómez G. Role of Bcl-2 family members on apoptosis: what we have learned from knock-out mice. Front Biosci. 2007; 12: 4722-30.